



UNCLASSIFIED

~~OFFICIAL USE ONLY~~

BNWL-321

2-

AEC
RESEARCH
and
DEVELOPMENT
REPORT

**PACIFIC NORTHWEST LABORATORY
MONTHLY ACTIVITIES REPORT
FOR AUGUST 1966**

DIVISION
OF
REACTOR DEVELOPMENT AND TECHNOLOGY PROGRAMS

SEPTEMBER, 1966

Op for	60013-271-4	DEC 5 1966	REV DATE
A Hasler	63006	Feb	
Site Rept	63006	Feb	12-7-66
A Hasler			



BATTELLE-NORTHWEST

BATTELLE MEMORIAL INSTITUTE / PACIFIC NORTHWEST LABORATORY

UNCLASSIFIED

~~OFFICIAL USE ONLY~~

LEGAL NOTICE

This report was prepared as an account of Government sponsored work. Neither the United States, nor the Commission, nor any person acting on behalf of the Commission:

A. Makes any warranty or representation, expressed or implied, with respect to the accuracy, completeness, or usefulness of the information contained in this report, or that the use of any information, apparatus, method, or process disclosed in this report may not infringe privately owned rights; or

B. Assumes any liabilities with respect to the use of, or for damages resulting from the use of any information, apparatus, method, or process disclosed in this report.

As used in the above, "person acting on behalf of the Commission" includes any employee or contractor of the Commission, or employee of such contractor, to the extent that such employee or contractor of the Commission, or employee of such contractor prepares, disseminates, or provides access to, any information pursuant to his employment or contract with the Commission, or his employment with such contractor.

PACIFIC NORTHWEST LABORATORY

RICHLAND, WASHINGTON

operated by

BATTELLE MEMORIAL INSTITUTE

for the

UNITED STATES ATOMIC ENERGY COMMISSION UNDER CONTRACT AT(45-1)-1830

PRINTED BY/FOR THE U. S. ATOMIC ENERGY COMMISSION

UNCLASSIFIED

3 3679 00060 3003

BNWL-321

C-44a,b,c
Nuclear Technology
(Special Distribution)

PACIFIC NORTHWEST LABORATORY
MONTHLY ACTIVITIES REPORT
FOR AUGUST 1966

AEC DIVISION OF
REACTOR DEVELOPMENT AND TECHNOLOGY PROGRAMS

S. L. Fawcett - Director
F. W. Albaugh - Associate Director
R. S. Paul - Associate Director

D. C. Worlton	Manager, Applied Physics and Electronics
H. A. Kornberg	Manager, Biology
M. T. Walling	Manager, Chemistry
H. Harty	Manager, Engineering Development
W. D. Richmond	Manager, Engineering Services
A. R. Keene	Manager, Environmental Health and Engineering
J. J. Fuquay	Manager, Environmental and Radiological Sciences
E. R. Astley	Manager, FFTF Project
D. R. de Halas	Manager, Materials
C. A. Bennett	Manager, Mathematics
J. J. Cadwell	Manager, Metallurgy
F. G. Dawson	Manager, Reactor Physics

September 1966

NOTICE: PRELIMINARY REPORT

This report contains information of a preliminary nature prepared in the course of work under Atomic Energy Commission Contract AT(45-1)-1830. This information is subject to correction or modification upon the collection and evaluation of additional data.

PACIFIC NORTHWEST LABORATORY
RICHLAND, WASHINGTON

UNCLASSIFIED

TABLE OF CONTENTS

	<u>Page</u>
SUMMARY	4
CIVILIAN POWER REACTORS	
Nuclear Systems Concepts Analysis	15
Conceptual Reactor Design Studies	18
USAEC-AECL Cooperative Program	18
APPLIED AND REACTOR PHYSICS	
Plutonium Criticality Studies	21
Phoenix Fuel Reactor Program	23
High Temperature Reactor Lattice Physics Studies	26
REACTOR FUELS AND MATERIALS	
Basic Swelling Studies	30
Nondestructive Testing	31
Nuclear Ceramics	33
Nuclear Graphite	36
Irradiation Damage to Reactor Metals	42
ATR Gas Loop Operation and Maintenance	54
Metallic Fuels Development	56
ENGINEERING DEVELOPMENT	
Neutron Flux Monitors	58
Microwave and Infrared Detection of Coolant Impurities and Measurement of In-Reactor Temperatures	59
PLUTONIUM RECYCLE PROGRAM	
Fuels Development	60
EBWR Demonstration Program	62
Reactor Physics	63
Fuel Cycle Analysis	71
Reactor Engineering Development	72
Materials Development	73
Test Reactor Operation	74
NUCLEAR SAFETY	
Containment Systems Experiment	78
Pressure Vessel Crack Monitoring	80
Reactor Safety Analysis and Evaluation	81
Columbia River Sedimentation Studies	81
Waste Solidification Condensate Treatment	81
Fission Product Aerosol Containment	82
Disposal of Reactor Off-Gas Into Soil Systems	84
Radioactive Residue Process Development	84

CUSTOMER

Assistance to General Atomic	86
U. S. Naval Research Laboratory	87

SUMMARYCIVILIAN POWER REACTORSCONCEPTUAL REACTOR DESIGN STUDIES

A draft report on the plant cost versus siting study was completed and forwarded to the AEC for comment.

Participation in the current AEC Civilian Power Reactor Evaluation included attending two organizational meetings at AEC Headquarters.

USAEC-AECL COOPERATIVE PROGRAM

Experiments to study two-phase mixing in rod bundle fuel elements were performed on an electrically heated test section which simulates flow channels formed by fuel pins in a square pitch array located adjacent to pins on a triangular pitch array (as in a 19-rod bundle). For an inlet temperature of 165°C (330°F) and mass velocities of 2.0 and 3.0 x 10⁶ lb/hr-ft² at 900 psi system pressure, severe flow oscillations were observed as bulk boiling began in the smaller channel.

Heat treatments appear to have little or no effect on the nil ductility transition temperature for Zr - 2.5 wt% Nb alloy tubing with 30% CW, but noticeable effect on the 60% CW material.

In the development of the apparatus for measuring pressure tube creep in-reactor, the effect of coolant flow rate on diameter measurements was evaluated. These tests show the diameter measurement noise is independent of coolant flow rate. This noise level equivalent to 0.0003-inch diameter change is still too high.

The entire set of equations describing nuclear and thermal hydraulic operating characteristics of the BLW-250 have been programmed on the analog computer, and debugging is complete.

Etched specimens of five zirconium alloys exposed in-flux in the G-7 loop in pH-10 NH₄OH, <0.05 ppm O₂ did not undergo accelerated oxidation in 37 days.

Specimens of six zirconium alloys were placed out-of-flux in the G-7 loop at water transport times ~1 sec and ~1 min from the flux. Weight gains were similar at the two out-of-flux positions.

APPLIED AND REACTOR PHYSICSPLUTONIUM CRITICALITY STUDIES

Measurements were completed in the first of several experiments on the fundamental behavior of neutrons in plutonium assemblies. Foil activations were made with Pu, In, and Cu foils for determining flux distribution and intracellular distribution of ²³⁹Pu fission rate in a hydrogen moderated heterogeneous Pu assembly with an H/Pu ratio of 35.

Pulsed neutron source, reactor noise, and P_k variance-to-mean type measurements were also made on the heterogeneous Pu assembly.

Comparisons with critical data on homogeneous hydrogen-moderated Pu assemblies show transport theory calculations to agree better with experiment if GAMTEC-II cross section data are used in place of the 16-group Hansen-Roach cross section set.

PHOENIX FUEL REACTOR PROGRAM

The water-reflected CAF experiments have been completed. Preparations for the PRCF experiments are continuing with scope drawings complete and preliminary safeguards calculations under way.

Additional high exposure Pu was committed to the fabrication of Al - 20 wt% Pu alloy fuel plates for the PRCF experiment.

A document describing preliminary 3-D design calculations for the MTR-Phoenix experiment is in preparation.

HIGH TEMPERATURE REACTOR PHYSICS STUDIES

Most of the construction work which was halted by the strike at Hanford was resumed by the end of the month.

A purchase order has been placed for the independent safety channels.

The control rod fuel pieces have surface defects which are larger than specified but which may not impair their strength and integrity at high temperature.

The digital control valves are to be delivered three months later than scheduled.

Fabrication of the two sample oscillators are 40% complete compared to a scheduled 75%.

The heating and cooling requirements are being translated into functions which relate control device position, sensor feedback signal, and sensor set-points. Digital programs are being written to control the heating and cooling operations as well as to provide information on valve operation.

Various programs are being written to record the state of process variables and other information.

Training of the reactor operations personnel continued.

Process Specifications and Operating Procedures are being written.

Small quantities of fuel material can be obtained from ORNL in the form of microspheres. The major portion of the experimental fuel will be in the form of dense but irregular particles.

The startup and calibration experiments are described in a document under review. The remaining lattice components and experimental pieces are being designed for fabrication.

An experiment which apparently measures the neutron lifetime in a reactor is being analyzed for use in calibration of reactor periods.

REACTOR FUELS AND MATERIALS

BASIC SWELLING STUDIES

Three capsules continue to operate successfully at control temperatures of 450°C (1000 psi), 450°C (~30 psi), and 525°C (~30 psi) toward burnups of 0.75 at.% BU, 0.3 at.% BU, and 0.4 at.% BU, respectively.

Metallographic examinations of uranium and uranium alloy specimens irradiated to 0.16 at.% BU at 500 psi over the temperature range of 500 - 625°C corroborate the strong influence of pressure, carbon and Fe-Al additions in reducing the amount of swelling without drastically altering the mode by which it occurs.

Density measurements made on uranium and uranium alloy specimens irradiated to 0.1 and 0.2 at.% BU, respectively, over the temperature range 610 - 705°C indicate that swelling is quite small, independent of temperature, independent of composition, and is linear with burnup.

NONDESTRUCTIVE TESTING

Significant improvements were obtained in the ability of the multi-parameter eddy current tester to eliminate signals due to various extraneous parameters. The coil driving circuitry has been completed, and work is progressing on the flaw propagation portion of the instrument. The background noise present in the thermal wave testing system has been substantially reduced.

NUCLEAR CERAMICS

A phase study of the Pu-U-O system was initiated. Samples were prepared by pelletizing and sintering mixed powder compacts consisting of UO₂ and PuO₂ with the PuO₂ content varying in intervals from zero to 100%.

Two especially designed test cans, each containing UO₂ samples of micronized, ceramic grade, and fused -325-mesh powders, and pre-sintered ceramic-grade pellets, were pneumatically impacted at 1100°C and 240,000 psi to produce specimens for studies of recovery and recrystallization effects.

Samples of the pre-sintered material are being annealed at a series of temperatures between 300 and 1600°C and subsequently observed for x-ray diffraction line broadening, microhardness, and microstructural changes.

Mechanically rotated assemblies were designed for performing irradiation tests on (U,Pu)O₂ in the 100-K Snout Facility. These movable assemblies will subject each of several UO₂ - PuO₂ specimens to identical neutron fluxes in a cyclical fashion and will eliminate the major problem associated with in-pile experimentation, i.e., unpredictable time and spacial flux variation.

Flow test dummies were fabricated and delivered to K-Reactor for hydraulic testing. Six UO₂ - PuO₂ irradiations, each comprising six specimens, are planned. Parameters to be investigated are oxide stoichiometry, heterogeneity of the mixture, and heat rating.

Selected-area optical and electron microscopy on several impacted specimens indicated that UO₂ single crystals undergo marked crystallographic

reorientation during impactation. Evidence for both ordinary slip and deformation twinning was found.

An inert-gas fusion apparatus for analyses of nitrogen and oxygen content of metals and compounds was partially installed in a glove box.

Metallography of nonstoichiometric UO_{2+x} fuels was completed for $UO_{1.90}$, $UO_{1.99}$, $UO_{2.02}$, $UO_{2.05}$, $UO_{2.15}$, and five $UO_{2.00}$ fuel rods which had experienced substantial center melting during irradiation. Migration of the excess component to the central, molten region was apparent for all compositions.

A study to determine the nature of eutectic melting in the $PuO_2 - UO_2 - BeO$ ternary system was begun. Fourteen samples covering the composition range from 4 - 36 mole% PuO_2 , 4 - 36 mole% UO_2 , and 60 - 90 mole% BeO were prepared.

Initial success was achieved in chemically thinning UO_2 to electron transparency.

UO_2 single-crystal specimens were sent to Argonne National Laboratory for use in vapor-pressure experiments. Specimens were supplied as part of the materials and information exchange program.

NUCLEAR GRAPHITE

A potential energy function for graphite interplanar interaction has been refined. The calculated cohesive energy from the improved function is -1.15 kcal/mole compared to the previous calculated value of -1.29 kcal/mole and experimental value of -1.01 kcal/mole.

The Sutton & Howard equations relating bulk thermal expansion of polycrystalline graphite to single-crystal properties contain two pairs of accommodation coefficients. Using a model for graphite which ascribes accommodation to the presence of basal-plane microcracks, relationships among the accommodation coefficients can be derived. These relationships modify the form of the equation to a form proposed empirically by Simmons. The newly derived accommodation factors permit a significantly closer fit to experimental data than the old model.

Graphite irradiations are planned in the Fermi Reactor starting in early 1967. Approximately 300 samples, 1/4-inch diameter and 1-3/4-inch long, will be irradiated in fluxes ranging from 2 to 8×10^{14} n/cm²-sec ($E > 0.18$ MeV) and at temperatures from approximately 400 to 700°C.

The ETR high-temperature capsule (GEH-13-12) is estimated to operate at a maximum temperature of 1400°C rather than 1600°C because the gamma heating values are now estimated at 12 watts/g rather than 16 watts/g.

The first discharge of irradiated graphite from EBR-II is scheduled for mid-August at a maximum exposure of 3×10^{21} nvt, $E > 0.18$ MeV.

The irradiation of ²³⁸dimensionally stable²³⁸ graphites in the GETR has been delayed by premature discharge of capsule H-3-23. Sample temperatures could not be duplicated after core configuration changes were made. Since capsule

redesign and modification are required for 50 Mw operation of the GETR beginning next cycle, the modified capsule will be used to continue these irradiations.

The long-term irradiation capsule GEH-3-13 continues to operate satisfactorily.

The discrepancy between the rate of graphite loss from boronated graphite oxidized in helium containing 1% O₂ as determined by weight measurement and the rate calculated from the concentration of CO₂ in the effluent gas stream has been investigated further. Although hydrolysis of B₄C is thermodynamically feasible, the rate is slow and cannot account for the discrepancy. The accuracy of the CO₂ analyses will be checked on two different chromatographs.

Specimens of TSX graphite were prepared for transmission electron microscopy. Three types of structures were observed: (1) delicate lace-like networks, (2) translucent web-type foils between opaque edges, and (3) translucent saw-tooth protrusions into open areas. The web-type foils appeared to be regions of greater structural regularity and the saw-tooth protrusions appeared to be the (100) or so-called "zig-zag" faces of graphite crystallites.

Irradiated graphite samples heated in contact with sodium for 100 hours at 537°C expanded from 1.1 to 2.4%. Unirradiated graphite samples containing carbon black were extensively cracked by treatment with sodium.

IRRADIATION DAMAGE TO REACTOR METALS

Procurement of 316 stainless steel plate, sheet, rod, and tube rounds will be completed by the end of August. Orders are placed for similar shapes of Incoloy 800 and Inconel 625.

Pacific Northwest Laboratory will obtain from GE-APO assorted, nickel-base alloys, irradiated at elevated temperatures, for tensile testing.

A test series on irradiated and control samples of nickel alloy PDRL-120 has been completed. Tensile data and metallography are being evaluated.

An in-reactor creep capsule containing an annealed 304 stainless steel specimen was constructed to replace a previous capsule in which a heater failed prior to testing at 840°C, 5000 psi. The high temperature creep capsule, under development for nickel-base alloy studies, is completed to the last step of welding on the outer shell.

Transmission electron microscopy examinations have been made on AISI 348 stainless steel irradiated at 60°C to 1.0×10^{20} fast fluence. Thin foils were examined in the as-irradiated condition and after postirradiation anneals at 450, 500, and 600°C. Very little recovery of displacement-type defects was observed at the lower annealing temperature, but complete recovery was observed after annealing at 600°C. A significant portion of the defects were removed by the one-hour anneal at 500°C. Additional thin foils of AISI 304 stainless steel irradiated at 650°C to approximately 1.0×10^{20} fast fluence were examined in the as-irradiated condition and after postirradiation anneals at 900, 1000, and 1200°C. No evidence of gas agglomeration was noted in any of

the unstressed sections examined to date. The examination of thin foils from the stressed section of AISI 304 stainless steel tested in creep in-pile at 525, 650, and 750°C is in progress. Stressed and unstressed sections will be compared to detect the presence or absence of gas agglomerates.

The current series of tensile tests on irradiated and unirradiated specimens of Inconel 600 and Inconel X-750 have been completed.

Examination of all the tensile and microstructural data available to date on the three program alloys, Hastelloy X-280, Inconel 600, and Inconel X-750, has led to a postulation of the mechanisms by which certain experimental treatments have resulted in improved postirradiation properties: (1) increased ductility of areas adjacent to grain boundaries, and (2) reduced irradiation-induced grain boundary area embrittlement due to traps for irradiation defects in the matrix.

A stress-rupture test series on 11 unirradiated Hastelloy X-280 specimens are continuing at Battelle-Columbus. Fifteen irradiated Inconel 600 and Inconel X-750 specimens have been shipped to Columbus for the next test series.

A mathematical model and computer program have been established to evaluate the compliance and calibration constants of the Double Cantilever Beam (DCB) specimen. Evaluation of the compliances of specimens from which experimental data had previously been determined indicated agreement within 1.3% between experimental-determined and calculated values.

A series of irradiation experiments in the EBR-II and Fermi reactors are planned for determining the combined effects of fast neutron irradiation and environment on the mechanical and physical properties of selected reactor structural materials. Over 50% of the mechanical test specimens scheduled for irradiation on this program have been fabricated. Characterization of the mechanical properties of the alloys selected is currently being performed at test temperatures between room temperature and 800°C. The microstructure is being characterized by conventional electron and optical microscopy. Final plans and schedules for the Fermi irradiation program were discussed in Washington, D.C., on August 31, 1966, with all participating laboratory representatives and members of cognizant USAEC offices.

An experimental program aimed at defining the effects of fast reactor irradiation on the mechanical behavior of candidate FFTF cladding alloys is being formulated. The most important parameter to be studied is the elevated temperature loss in creep ductility after fast reactor irradiation. Post-irradiation biaxial stress-rupture tests in sodium are to be performed in the temperature range 800 to 1400°F (425 to 760°C) to provide data on creep-rupture strength and ductility in a simulated FFTF environment. The stress-rupture studies emphasize 304 and 316 stainless steel; however, post-irradiation tensile screening studies will be conducted to evaluate various other alloys and heat treatments. The cladding program will stress mechanical tests in flowing sodium, thermal cycling effects, aging effects, and evaluation of fuel element cladding after irradiation.

General facilities layout of the 321-A Building has been determined, and a cost estimate produced. Equipment has been transferred into Building 321-A for assembly of one of each type of test rig. Preliminary assembly of these rigs will substantially expedite final assembly of the balance of the rigs.

The SAND I computer code has been adapted for use in the UNIVAC 1107. The function of this program is to perform calculations required in the analysis of neutron spectra from the activation of foils. A sample calculation has been made to illustrate one useful function of this code, namely, the determination of the activation and energy sensitivity limits of selected foil detectors.

ATR GAS LOOP OPERATION AND MAINTENANCE

Review of vendor data submittals for the ATR gas loop continued. A meeting was held with Johnson Service Company to present comments on the main instrument panel submittal.

Investigation of filter shielding problems indicates that it would be advantageous to insulate the Hastelloy pipe to reduce the temperature requirements of the shielding material, thus allowing a wider selection of candidate shielding materials.

Examination of the Struther-Wells heater has shown no evidence of contamination of the molybdenum heating elements by the helium atmosphere. The molybdenum is, in part, recrystallized. Tensile specimens of standard molybdenum recrystallized at 2500°F (1370°C) retain good ductility at room temperature.

A sample holder arrangement has been designed which should provide sufficient support to hold refractory metal and superalloy corrosion coupons in the test section of the ATR model gas loop. Construction of this holder and exposure of the test coupons in the loop to provide additional ATR corrosion support data is the immediate goal.

METALLIC FUELS DEVELOPMENT

The irradiation of tubular thorium-base fuel elements under water cooled power reactor conditions continued successfully in the ETR pressurized water loops. The maximum exposure element has currently achieved 5.3×10^{20} fissions/cc (15,200 MWd/ton).

Examination of one element irradiated to 1.4 at.% burnup (11,850 MWd/ton) shows no evidence of porosity or dimensional instability of the element as a result of irradiation. Isotopic uranium analyses and cesium fission product analyses confirm the 1.4 at.% burnup computed from reactor data.

ENGINEERING DEVELOPMENT

NEUTRON FLUX MONITORS

Laboratory tests, conducted at the 1.8×10^5 Ci gamma facility (Co^{60}), verified that a balanced gamma response characteristic was achieved between the two electrode elements of the new, dual-chamber, boron-11, beta current

generator detector, which will be used for reactor, in-core, thermal neutron flux measurements.

MICROWAVE AND INFRARED DETECTION OF COOLANT IMPURITIES AND MEASUREMENT OF IN-REACTOR TEMPERATURES

Using microwave resonant cavity techniques and employing a standing wave ratio meter as a tuned voltmeter, successful laboratory measurements demonstrated detection of 400 parts per million change of water vapor in helium gas at a nominal frequency of 30 GHz.

PLUTONIUM RECYCLE PROGRAM

FUELS DEVELOPMENT

A paper, entitled "Transient Meltdown Irradiations of Vibrationally Compacted UO₂ Fuel Rods in TREAT," by R.C. Liimatainen, M.D. Freshley, and F.J. Testa, describes the results of a joint BNW-ANL program on the transient irradiation behavior of Zircaloy clad, vibrationally compacted UO₂ fuel rods in the Transient Reactor Test Facility.

With the exception of one thoria filled test element, all fuel and test elements for the Batch Core Experiment in the PRTR have been shipped.

Three instrumented UO₂ - 2 wt% PuO₂ fuel rods were charged in PRTR. Each rod is equipped with a thermocouple and a pressure sensor to indicate the temperature and pressure in the gas plenum during reactor operation.

All fuel elements for the Batch Core Experiment have been delivered to the PRTR site. Plans have been initiated for the fabrication of replacement elements.

Fifty-three fuel rods containing pelleted UO₂ - PuO₂ fuel fabricated by General Electric Company will be shipped to Battelle-Northwest this month.

The determination of the low energy gammas and x-rays emitted by the three Shippingport plutonium samples has continued during this reporting period with limited success.

Three capsules, containing short pieces of EBWR UO₂ - 1.5 wt% PuO₂ fuel rods, have attained an estimated maximum burnup of 25,100 MWd/tonne of fuel (6.23×10^{20} fissions/cm³). Thirty-three production-run EBWR fuel rods are in reactors.

REACTOR PHYSICS

The scope of a study to theoretically predict lattice parameters was extended to include a 7-inch and 9-inch lattice.

Calculations have continued to determine the effectiveness of gamma rays in producing photoneutrons in deuterium using transport theory methods.

Fuel loading and critical testing have begun with the High Power Density Core (HPDC) in the PRTR.

A paper summarizing the analytical and experimental results of the HPDC experiment conducted in the PRCF has been accepted by the American Nuclear Society for presentation at the November meeting.

Critical experiments have continued in the PRCF using H₂O moderator and 1/2-inch diameter, 2 wt% PuO₂ - UO₂ fuel rods containing plutonium which has 24 wt% Pu²⁴⁰. Calculations have been performed using the series of computer codes THERMOS, HRG, and HFN to obtain analytical results which can be compared with the results of the critical experiments which involve fuel elements containing various concentrations of Pu²⁴⁰.

A series of k_{∞} measurements are being made for square graphite lattices containing 0.5-inch diameter fuel rods at spacings of 2.0 inches, 4.0 inches, and 5.0 inches. The experimental phase of the 4.0-inch lattice is in progress now.

Reactor experiments are planned to study the reactivity effect of lumping PuO₂ in various sized particles. The experiments will be conducted with both graphite and light water moderator. The first delivery of fuel rods is in preparation and should be received next month.

Work has continued of the analysis and interpretation of previously obtained scattering law results for H₂O (20°C and 95°C), D₂O, and ice.

Most of the effort on combining individual measurement runs to final cross-section values has been completed for previously obtained MeV total cross section data.

The draft of an article describing a method of high-resolution monochromatization of slow neutrons has been completed.

Attention is called to a revised value of $\alpha(2200 \text{ m/s}) = 0.356 \pm 0.017$ for Pu²⁴¹ from reactor irradiation measurements at Harwell which is significantly lower than that recommended from most evaluations.

New cross section data and descriptions for the plutonium isotopes are included now on the BNW Master Library.

Comparisons of RBU with other codes are being made to evaluate the RBU code.

REACTOR ENGINEERING DEVELOPMENT

A method to analyze water-moderated commercial power reactor core designs within specified thermal and hydraulic limits has been developed. Checking the method against results from the Connecticut Yankee Reactor is continuing.

MATERIALS DEVELOPMENT

One analysis of the metal near the mark on the taper of tube 5696 indicated a zirconium hydride concentration of 27 ppm.

Monitoring the PRTR moderator system water activity during the recent critical tests has shown that a marked Co⁶⁰ concentration increase has occurred. The Co⁶⁰ concentration increased from 0.08 $\mu\text{Ci/ml}$ to $4.1 \times 10^{-3} \mu\text{Ci/ml}$ after the addition of 24 ppm boron over a three-week period.

A total solids analysis for borated water is being investigated which will measure material other than boric acid present in the water sample.

Use of highly concentrated H_3PO_4 at $200^\circ C$ gave improved dissolution of sintered PuO_2 . During August, familiarization work was begun with sodium metal-ammonia solution so that a study can be made of the efficiency of this technique for reducing ceramic fuel oxides.

TEST REACTOR OPERATION

The batch core critical tests were completed in August. Work directed toward the start of the power tests included completion of the reflector conversion to light water, completion of the boron shim system and miscellaneous repair activities.

NUCLEAR SAFETY

CONTAINMENT SYSTEMS EXPERIMENT

Continuation of the strike prevented progress on construction. Scope designs for cost estimating purposes were completed on a 1000 cfm air cleaning system and on potential modifications of the high temperature loop.

Runs were made in the aerosol development facility to examine the effect of air velocity on airborne concentration versus time for I_2 in dry air. Two runs with xenon were made to evaluate mixing effects and to test xenon sampling equipment.

Nine blowdown tests were run on the SM-2 vessel with 8-inch rupture discs and water conditions of $250^\circ F$ and 200 psig.

Low removal efficiencies were obtained with vapor phase cleaning experiments on iodine contaminated painted surfaces. Decontamination factors were two or less.

Testing was continued on alumina insulated electrodes for use as capacitance probes in CSE vessels.

PRESSURE VESSEL CRACK MONITORING

The design of a prototype monitoring instrumentation system for full scale application to pressure piping surveillance by acoustic emission methods has been initiated. Increased amplification of the signals obtained from a high sensitivity accelerometer shows that considerable acoustic emission signals are generated during the extension of a preformed crack.

REACTOR SAFETY ANALYSIS AND EVALUATION

Two subsize steel vessels irradiated in the ETR reactor for two reactor cycles were burst at $56^\circ C$ and $72^\circ C$, respectively. Each specimen contained a one-inch long flaw. The NDT temperature was estimated to lie just above the higher temperature or approximately $73^\circ C$.

RADIOACTIVE RESIDUE PROCESS DEVELOPMENT

Excessive corrosion caused failure of a pot in a rising level glass run using a modified PW-1 flowsheet. However, moderately high feed rates, self-cleaning of the off-gas lines, and separate addition of melt making additive to the pot were successfully demonstrated.

The GE-412 computer operated during the WSE pot calcination run and has been programmed for a spray calciner run. Modifications to improve the program are being made.

Corrosion studies to date have not explained the failure of the 310 stainless steel receiver pot during the recent WSEP rising level glass run (RLG-B).

WASTE SOLIDIFICATION CONDENSATE TREATMENT

Experiments on the two-step scavenging treatment of glass melter condensates were continued with selection of an optimum concentration of ammonium phosphotungstate. The decontamination performance of procedures was evaluated statistically.

The efficiency of sprays containing hydrazine for removing airborne methyl iodide was determined for three hydrazine concentrations.

The physical chemistry study of reactions in the heterogeneous system, hydrazine, water, methyl iodide, and sodium hydroxide, continued with the objectives of determining the rate-controlling step and characterizing the reaction mechanism. Variables included hydrazine concentration, temperature, and liquid surface area effect.

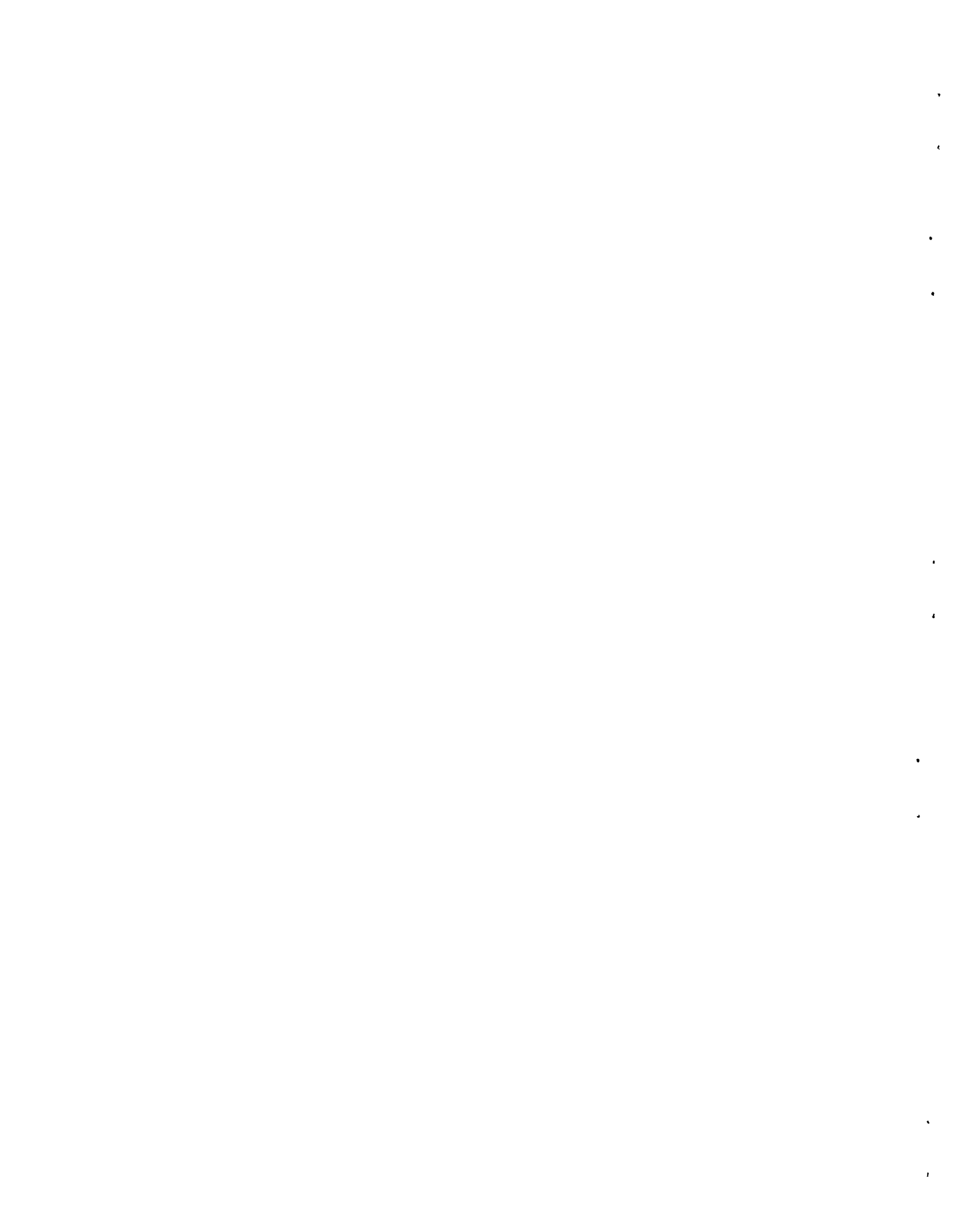
The seismic exploration program performed for IDO-AEC at NRTS in connection with the LOFT program was completed, and results were transmitted to the Waste Management Branch.

CUSTOMER

Several candidate designs of blood heaters to be installed in the abdominal aortas of living swine were analyzed to determine the uniformity of the heat flux and surface temperature at the heated surfaces. Design alternatives were found that would assure heat flux uniformity within 5% over the entire heat transfer surface.

Four sets of PuO₂ - graphite compacts were prepared. Welding problems occurred with the final closure; several techniques to overcome them are being investigated.

The fast-neutron spectra and the iron damaging rate have been calculated at the pressure vessel inner edge of the Organic Moderated Reactor Experiment (OMRE) and the Yankee reactors.



DIVISION OF REACTOR DEVELOPMENT AND TECHNOLOGY PROGRAMS (F. W. Albaugh)CIVILIAN POWER REACTORSNUCLEAR SYSTEMS CONCEPTS ANALYSIS (E. A. Eschbach)Fuel Utilization Studies

Previously reported calculations of uranium requirements in the expanding nuclear power industry projected for the United States showed an insensitivity to the thermal reactor type assumed as a basis in the projection. However, the reactors used in these calculations were characterized with considerably higher specific powers than current reactor designs indicate. In order to determine whether specific power effects were masking differences between reactor types, several calculations were redone with a range of specific powers. The results are summarized in the accompanying table. The table indicates that the specific power effect is masking the differences between reactors, but that the differences are not as great as might be expected because the amount of plutonium produced for export for breeder reactor inventory requirements per unit of electricity produced is nearly identical for all reactors. After a long period of time, the bulk of the uranium will have been used for burnup rather than inventory, and the effect of specific power or uranium requirements will then be less important than during the next several years.

Plutonium Values for the HWO CR

Plutonium values have been calculated for a UC fueled heavy water - organic cooled reactor (HWO CR). This design is described in AI-CE-MEMO-6. Several economic conditions have been examined besides the one reported previously* and are shown in the accompanying table along with the plutonium value results calculated by the PUV E code. In general, the economic parameterization covered three interest rates for one uranium price, one variation of the price of uranium feed, and an incremental cost variation representing a zoned 10% fabrication penalty which minimizes the number of elements containing plutonium.

*See December 1965, Monthly Report, Physics and Instruments Department.

URANIUM REQUIREMENTS FOR VARIOUS THERMAL REACTORS AND SPECIFIC POWERS

<u>Reactor</u>	<u>Specific Power</u> kwt/kg	<u>10³ T Natural U Used by</u>				<u>Maximum</u> <u>Separative</u> <u>Work</u> <u>10⁶ kg/yr</u>
		<u>1981</u>	<u>1999</u>	<u>2020</u>	<u>2041</u>	
<u>Original Calculations Optimized at all Plutonium Recycle Percentages</u>						
HWR	110	48.8	411	755	1062	5.91
PWR	63	67.6	479	852	1207	19.67
HWO CR	40	51.2	390	707	984	4.62

Reduced Specific Power with no Reoptimizations of Operating Conditions

HWR	31	58.8	442	784	1094	6.23
PWR	25	98.9	585	957	1304	23.17
HWO CR	25	54.9	407	724	1001	4.69

Reduced Specific Power Optimized at Full and no Plutonium Recycle Only
(Corresponds to each reactor operating either with uranium only or plutonium)

HWR	55	55.2	426	768	1099	7.96
PWR	45	93.0	586	1019	1392	22.70
HWO CR	25	54.9	366	636	853	4.21
HWR	25	61.3	453	813	1168	8.25
PWR	25	95.5	549	927	1284	20.56

Reduced Specific Power Optimized at Full, Partial, and No Plutonium Recycle

HWR	55	60.7	470	842	1203	8.36
PWR	45	84.2	543	954	1334	21.97
HWO CR	25	53.2	390	692	953	3.98
HWR	25	70.1	494	835	1193	8.38
PWR	25	104.1	596	995	1364	22.70

PLUTONIUM VALUES IN AN HWO CR

Economic Variables				Plutonium Values*, \$/g Total/\$/g Fissile					
Interest Rates, %		Uranium	Plutonium	Cycle No.					
Fuel	Fuel	Feed	Fabrication						
Cycle	Inventory	Price,	Penalty,	1	2	3	4	5	
		\$/kg	\$/kg						
(1)	10	10	23.10	0	6.03/9.06	4.49/7.92	3.48/6.67	2.63/5.32	1.84/3.87
(2)	10	10	17.30	0	5.19/7.81	3.89/6.89	2.97/5.73	2.25/4.59	1.57/3.34
(3)	12	12	23.50	0	5.99/8.97	4.52/7.95	3.53/6.76	2.67/5.39	1.93/4.05
(4)	10	10	23.50	2.63	5.59/8.40	4.18/7.40	3.26/6.29	2.50/5.08	1.78/3.76
(5)	8	8	23.50	0	5.81/8.79	4.27/7.59	3.25/6.29	2.41/4.92	1.63/3.45

17

*The fissile content is little affected by these parameterizations so that the comparisons are on at about equal exposures and compositions in each cycle.

CONCEPTUAL REACTOR DESIGN STUDIES (J. C. Fox)Nuclear Electric Plant Capital Costs vs. Site Location

A draft report on the plant cost versus siting study was completed and forwarded to the AEC for comment. Additional data on cooling tower cost as influenced by design considerations are being reviewed, and this section of the report will be revised prior to publication. In addition, some cost information on sea water versus fresh water condenser installations is being sought.

Civilian Power Reactor Evaluations

As part of the Pacific Northwest Laboratory's participation in the current AEC power reactor review, J. C. Fox will serve on a study group for alternate cooled fast breeder reactors. Two organizational meetings at AEC Headquarters were attended, and the further details of our participation will be worked out with ORNL.

USAEC-AECL COOPERATIVE PROGRAM (J. J. Cadwell)Cross-Flow Mixing Between Parallel Flow Channels During Boiling

The experimental portion of the program to determine values of cross-channel mixing during two-phase flow in rod bundle fuel elements was continued. The basic purpose of this program is to obtain a method to predict local flow and enthalpy conditions in each subchannel of rod bundle fuel elements. This information will help provide a more accurate means to predict boiling burnout conditions.

Experiments were performed on an electrically heated test section which simulates a flow channel formed by fuel pins in a square pitch rod array located adjacent to a channel formed by pins on a triangular pitch array (as in a 19-rod bundle). Isothermal runs to measure system heat losses and to enable thermocouple calibration were completed.

Runs with heat generation are now being performed using a 0.080-inch simulated rod spacing in the test section. Data were taken at an inlet temperature of 330°F with mass velocities of 1.0, 2.0, and 3.0 x 10⁶ lb/hr-ft² at 900 psia system pressure. The maximum heat fluxes considered for these flow rates and inlet temperatures ranged from about 0.3 to 0.7 x 10⁶ Btu/hr-ft². These are about 30% below the burnout heat flux based upon previous 19-rod bundle burnout data. For all these conditions, power was increased until significant boiling occurred in the smaller flow channel of the test section. For coolant mass velocities of 2.0 and 3.0 x 10⁶ lb/hr-ft², significant inlet flow oscillations occurred during boiling in the smaller channel; however, when the larger channel entered boiling, as test section power was gradually increased, a severe inlet flow reduction was observed. The inlet flow reduction was followed by a rapid increase in test section temperatures.

During this time, system water temperature oscillations (approximately 15°F at 180 degrees) were observed at the outlet of the counter-flow heat exchangers which were used to cool the outlet of the test section from 500°F to 180°F. Water at 70 psig was being used on the shell side of the heat

exchangers with flows as small as 0.1 lb/hr-ft² (Reynolds number = 10,000). Since there was a possibility that film boiling was occurring in the heat exchangers, a 60 gpm pump was used to pressurize the shell side to 500 psig. A decrease in oscillations was noted though some fluctuations persisted. Additional improvement may be realized if parallel flow is used since the difference in outlet temperatures of both streams will be reduced to about 50°F rather than 300°F. Higher heat exchanger flows will also provide better mixing at the temperature measuring point.

Data were also taken with an inlet temperature of 510°F and mass velocities of 2.0 and 3.0 x 10⁶ lb/hr-ft² at 900 psia. The maximum heat flux considered for these conditions was about 0.45 x 10⁶ Btu/hr-ft². For all runs at this higher inlet temperature, no significant flow oscillations were observed during boiling of either channel.

Evaluation of Zr - 2.5 wt% Nb Pressure Tubing

The general objective of this program is to evaluate Zr - 2.5 wt% Nb alloy tubing as a pressure tube material with reference to tests and reactor experience that has been obtained on Zr-2 pressure tubes.

A series of heat treated test specimens have been prepared with milled slots for crack propagation tests. The heat treatment for these test specimens consists of a solution heat treatment at about 880°C and a water quench. After quenching, these specimens were aged in vacuum for eight hours at 500°C.

Drop weight tests to determine the nil ductility transition (NDT) for heat treated Zr - 2.5 wt% Nb have been done. Tests were made on specimens which had been solution heat treated and water quenched only, and also on specimens which were aged after the solution heat treatment and water quenching. After these heat treatments, there was still observed a significant difference in the NDT temperature for the 30% CW and 60% CW material source. For the solution heat treatment and water quenched only condition, the test specimens taken from the 30% CW source material showed an NDT at room temperature or slightly above, while for specimens obtained from the 60% CW source the NDT was about 35°F. For the heat treatments which included aging, the NDT for specimens obtained from the 30% CW source was again room temperature or slightly above, while for specimens obtained from the 60% CW source the NDT was between -40°F and -43°F. Metallographic examinations have not yet been done. So far these test results indicate that heat treatments alone have little influence on the nil ductility transition temperature of the 30% CW source material but appear to have some effect on the 60% CW source material.

In the 350°C creep loop a series of flow tests have been completed. In this test series the flow through the measuring venturis was varied in steps from about 15 gpm through 30 gpm to measure the effect of turbulent flow noise on pressure drop fluctuations. In these tests where the pressure drop varied with varying flow rates from about 25 inches of water to 100 inches of water, the error signal was relatively constant at about 2 inches of water, with pressure snubbers in all pressure sensing lines. Two inches of water would represent about 0.0003-inch change in diameter

of the pressure tube creep specimen. Without snubbers the fluctuation in pressure drop was about 10 inches of water. These fluctuations are random and do not appear to be attributable to pressurizing or circulating pump action. Flow in the test assembly is entirely turbulent, and these random pressure fluctuations appear to be attributable to turbulence. The test assembly has been shut down and will remain so until some adequate means of averaging the ΔP fluctuations is found.

Hydraulic and Nuclear Stability in Parallel Flow Channel Systems

The entire set of equations describing nuclear and thermal-hydraulic operating behavior of the BLW-250 have been programmed on the analog computer, and debugging is complete. An initial test case has been run using control functions simulating base load operation. The parametric study of hydraulic and nuclear stability will begin early in September.

The present representation employs a two-node nuclear kinetics model based on coupled reactor theory. This model was programmed and debugged during the month and replaces the original four-region nuclear model.

In-Flux and Out-of-Flux Oxidation of Zirconium Alloys in the G-7 Loop

Etched specimens of five zirconium alloys were exposed in the ETR G-7 loop (quadrant 218). Materials irradiated under the USAEC-DRD&T Irradiation Damage to Reactor Materials Program (IDRM) were included in the same quadrant. The quadrant was exposed 37 days at 270 to 280°C bulk water temperature in pH-10 NH_4OH , <0.05 ppm oxygen. The fast neutron flux (>1 Mev) was $\sim 5 \times 10^{13}$ nv. Average weight gains for the five alloys from the USAEC-AECL program are shown below.

Alloy	Weight Gain mg/dm ²
Zircaloy-2	12.5
Zircaloy-4	14.3
VALLOY (Zr-1.2 Cr-0.08 Fe)	9.4
VALLOY-S (Zr-1.2 Cu-0.3 Fe)*	20.0
Zr-2.5 Nb, quenched, 20% cold work	7.3
Zr-2.5 Nb, annealed, 20% cold work	8.9

*This alloy also undergoes accelerated oxidation out-of-flux in the G-7 loop coolant.

The weight gains indicate that in-flux oxidation was not accelerated in the pH-10 NH_4OH system. Several samples from the set will be sectioned to confirm the result metallographically. By contrast, specimens of Zircaloy-2, Zircaloy-4, and Zr-3Nb-1Sn irradiated under the IDRM program in the same loop in pH-10 LiOH at ~ 0.1 and ~ 1 ppm oxygen underwent accelerated oxidation. There was no evidence of accelerated corrosion of samples of the IDRM materials also exposed in quadrant 218 to the NH_4OH environment.

APPLIED AND REACTOR PHYSICS

PLUTONIUM CRITICALITY STUDIES (E. D. Clayton)

Neutron Spectra Experiments

Measurements were completed in the first of several experiments on the fundamental behavior of neutrons in plutonium fueled assemblies. Experiments are currently planned on three geometrically similar critical assemblies having different H/Pu atomic ratios. The first of these rectangular parallelepiped assemblies was reflected on two sides with 1-inch of Lucite and consisted of alternate 2-inch (nominal) rows of PuO₂-polystyrene compacts and Lucite, giving an H/Pu atomic ratio of 35. The base geometry was held fixed at 6 rows by 7 rows (four PuO₂-polystyrene and three Lucite). Delayed criticality was achieved by increasing the height to 6.92 layers. The approximate over-all dimensions of the clean critical assembly were 12.08 x 14.10 x 13.94 inches.

Foil activation measurements were made to determine the flux distribution across one dimension of the assembly and to determine the intracellular distribution of the ²³⁹Pu fission rate, the ¹¹⁵In (n,γ) reaction, the ¹¹⁵In (n,n') ^{115m}In reaction, and the ⁶³Cu (n,γ) ⁶⁴Cu reaction.

Reduction of the experimental data and its comparison with calculations is in progress. Measurements are under way on the second assembly.

Pulsed Neutron Source Experiments and Analysis of Reactor Noise

Pulsed neutron source, reactor noise, and P_k variance-to-mean type measurements were made on the plutonium assembly comprised of 2-inch layers of fuel (PuO₂-polystyrene compacts with H/Pu of 15) and 2-inch layers of Lucite. This arrangement gave an average H/Pu ratio over the core of 35.

Preliminary analysis of the pulsed neutron data indicate a delayed critical decay constant (α) of 135 sec⁻¹ at a buckling of 0.019 cm⁻². This value may be compared with a geometrically similar checkerboard assembly comprised of alternate fuel bearing and Lucite cubes with the same H/Pu (35). This latter value was 275 sec⁻¹ at a buckling of 0.021 cm⁻². The results indicate the neutron lifetime ($\ell = \frac{\beta_{eff}}{\alpha}$) to be significantly increased in the assembly with alternate layer arrangement.

Theoretical Analysis of Homogeneous Plutonium Critical Assemblies

Previous calculations performed as a basis for nuclear criticality safety have frequently utilized the 16-group Hansen-Roach cross section set in conjunction with the S₄ approximation to the transport equation.

Experimental data on the criticality of homogeneous plutonium assemblies obtained at the Pacific Northwest Laboratory have been used as a test of computational methods and cross section sets used. Comparisons were made of critical eigenvalues computed by S₄ theory with the Hansen-Roach cross section set and the cross sections provided by the GAMTEC-II code with Sher (1962) normalized ²³⁹Pu data. Calculations were also made with 18-group diffusion theory utilizing the GAMTEC-II cross sections. The results are presented in the following table.

MEASURED AND COMPUTED CRITICALITY

PLUTONIUM NITRATE SOLUTIONS

(4.6% ²⁴⁰Pu)

Sphere Diameter (inches)	Reflector	Pu Conc. (g/l)	k_{eff}	
			Diffusion Theory (P_1)	Transport Theory (S_4)
			GAMTEC-II Sher (62)	GAMTEC-II Sher (62)
				Hansen-Roach
14.0	Water	33.0	0.999	1.015
14.0	Water	47.9	1.005	1.019
11.5	Water	73.0	1.001	1.021
11.5	Water	268.7	1.001	1.018
15.2	Water	24.4	1.000	1.014
15.2	Water	38.7	1.007	1.013
15.2	0.048" Stainless Steel	39.0	0.997	1.008
15.2	0.048" Stainless Steel	172.8	0.993	1.010

22

PuO₂-Polystyrene Assemblies (H/Pu = 15)

(2.2% ²⁴⁰Pu)

Infinite Slab Thickness (cm)	Reflector	k_{eff}
16.07	Bare	0.994
5.99	Plexiglas	0.991

BNWL-321

It is seen that better agreement is obtained between transport theory and experiment utilizing the GAMTEC-II cross sections than those of Hansen and Roach. It is also interesting to note that the Hansen-Roach set shows a larger discrepancy for higher Pu concentrations where the GAMTEC-II data agree rather well with experiment. However, for the data presented, diffusion theory provides better over-all agreement with experiment than does transport theory.

A paper summarizing the analyses of the experiments and calculations is being prepared.

PHOENIX FUEL REACTOR PROGRAM (P. L. Hofmann)

MTR-Phoenix Experiment

CAF-Phoenix Experiments

The second of a series of approach-to-critical experiments was completed in the CAF. The purpose of the experiment is to estimate the poison worth of a cadmium rod in the center of a 19-element Phoenix core. In addition to the approach-to-critical experiment, reactor noise recordings were made to obtain an independent measure of the subcriticality. The data are now being analyzed. The lattice support structures have been modified to accommodate a beryllium reflected lattice, which is now being prepared for a third experiment. The contents of the 19 fuel cans are being reduced from 145 fuel layers to 15 fuel layers.

PRCF-Phoenix Experiments

The experiment planned for the PRCF requires simulating the MTR core. It will be light water moderated, with a beryllium side reflector. MTR type fuel assemblies will be used. Present plans are to use the existing H₂O safety and control rod drives with new in-core components for control and safety functions. The core assembly and the safety and control hardware will be suspended from a new top plate for the PRCF reactor tank.

Three scope drawings, showing the proposed arrangement and significant details, were completed and circulated for comment. The comments have been received and are being incorporated.

To support the PRCF experimental phase of the Phoenix fuel program, a series of calculations was made to aid in the estimation of the void and temperature coefficient. These calculations were made using the TEMPEST-HRG-HFN computer programs. The systems that were investigated ranged in fuel temperature from 20°C to 600°C. The percent void in the fuel region was varied from 0% to 50%.

The following table lists the results of the calculation, in terms of calculated k_{eff} , for the cases considered.

An analog simulation of the PRCF-Phoenix experiment has been set on the MIDAS program to obtain preliminary safeguards information about the loading. Power excursions have been calculated for ramp reactivity additions using calculated fuel temperature, moderator density and void coefficients.

RESULTS FROM PRCF SAFEGUARDS CALCULATIONS

	<u>I</u>	<u>II</u>	<u>III</u>	<u>IV</u>	<u>V</u>	<u>VI</u>	<u>VII</u>	<u>VIII</u>
Reflector Temp (°C)	20	46	46	46	46	46	46	46
TEMPEST Fuel Temp. (°C)	20	46	100	100	100	100	100	100
HRG Fuel Temp. (°C)	20	46	100	100	200	600	100	100
% Void in Fuel	0	0	0	5	5	5	20	50
k _{eff}	1.20570	1.20282	1.18856	1.17057	1.17051	1.16876	1.10714	0.91907

In addition, transient heat transfer and steam generation equations were derived for the analog simulation of a postulated power excursion during the PRCF experiment. These equations include transient models for the fuel temperature, clad surface temperature, and void formation from boiling.

The equations were formulated in the same manner as presented in HW-69168 SUP, "Plutonium Recycle Critical Facility Final Safeguards Analysis Supplements," except for a case of flat plates instead of rods.

Fuel Fabrication for PRCF

Final dimensional sizing of the perimeter welds on the fuel plates is still delayed awaiting the availability of a precision press. This delay is not affecting the program completion date. A radiograph technique was developed to determine the weld quality. All the welded plates were radiographed. About 2% of the plates were rejected for weld quality, and these plates will be rewelded.

The usable scrap Al - 20 wt% Pu alloy, which was cast and extruded to sheet-bar stock, was not rolled because of the results from spectrochemical analyses. Further analyses proved the material to be acceptable. Therefore, the sheet-bar extrusions will be used to fabricate fuel plates. About 4.8 kg of high exposure PuO₂ were blended to 19 wt% Pu²⁴⁰. About 2.4 kg of this material was reduced and cast into Pu-Al alloy billets for extrusion. Upon receipt of the analytical results, fabrication of the fuel plates will be initiated.

Aluminum sheet stock for cladding and picture frames was ordered for September delivery.

Nuclear Design Calculations

A document describing some of the preliminary design calculations that were made on the full plutonium core using the two-group, three dimensional diffusion code WHIRLAWAY is now being written. This document will describe the geometry that was examined and the calculational methods employed.

The results of these preliminary calculations indicate that fairly severe power peaking will occur in the follower fuel just below the stationary fuel. The calculations also predict that the shutdown margin and the core lifetime may not be as great as previously estimated. However, these conclusions will be re-examined in the very near future when a new cross section library will be available. This new cross section library was compiled specifically for the Phoenix fuel study.

Phoenix Fuel Application Study

A brief report covering possible Phoenix fuel applications in compact thermal power reactors along with possible engineering and economic advantages has been submitted to the AEC in Washington, D.C., for review.

HIGH TEMPERATURE REACTOR LATTICE PHYSICS STUDIES (R. E. Heineman)Reactor Construction

No work was done on the reactor or the reactor shell during the month.

All craftwork was interrupted on all other parts of construction during the month due to the strike. Electrical work was gradually resumed, and by month-end both piping and electrical work were going ahead on a full schedule.

Reactor Equipment

The order for the independent safety channels was placed by the AEC with the low bidder. One meeting with the successful bidder has been held to discuss the specifications and to look at the actual installation site.

The electronic driver circuits for the PMACS display were returned to BNW. Although the display works, some features are still being questioned. The vendor has been informed that it is not acceptable.

Twenty-eight of the control rod fuel pieces have been shipped to BNW. The remainder have been fabricated but had surface defects larger than the specifications allowed. As an alternative BNW has proposed the substitution of strength tests as the criterion for acceptance. Testing on some pieces is now under way.

The vendor and architect-engineer layout drawings for the installation of the neutron generator are being reviewed.

The vendor who was to supply the seven valves, which are operated by digital motors and controlled by PMACS, has informed the AEC that delivery will be delayed from August 15 to November 15. This will delay the present schedule for completion of the gas system.

Additional EGCR graphite has been purchased which is suitable for the fabrication of up to 54 spare heater rods. This is in addition to the material on hand and provides material for a total of up to 107 spare heater rods.

Design Review

Additional information is being developed in order to establish the time interval that can be tolerated, without incurring significant damage to the reactor floor slab if cooling water is lost.

HTLTR Oscillators

The purchase order to fabricate the main structure subassembly for the oscillator mechanism has been placed.

The drive system layout and power transmission system has been redesigned due to the unavailability of precision gears with the required ratios. In the original design both the light duty and the heavy duty systems were identical, except for the gear reduction in the transmission. The new designs use a different power transmission approach for each oscillator. This results in the use of commercially available components and a more economical system.

An acceptable design for an inflatable seal has been found after an extensive investigation of available shapes, deliveries, costs, and performance parameters. A purchase requisition for these items has been written and requests for bids have been sent.

Fabrication status of subassemblies are as follows: Key, 78%; Carriage, 35%; Oscillator mechanism, 33%; Valves, 68%; and Drive, 18%. It is estimated that the project is 40% complete compared to a scheduled 75%.

A conceptual design for a coupling between the heavy duty oscillator and the various experimental samples has been completed. The present concept allows the oscillator to be connected to either of two adjacent cells, or to be used to push fuel trains back into the core, without repositioning the oscillator mechanism. Discussions are under way to determine whether this coupling fully meets the requirements.

Programmed Measurements and Control System (PMACS)

Installation

The interface between one of the mechanical oscillators and PMACS has been completed. The interface logic will allow either program or hardware control of the oscillator mechanism. The system logic wiring needs to be checked.

Control of Heating and Cooling Circuits

An analog model of the graphite stack using 10 nodes was simulated on the 1133 Computer. This simulation shows that the stack is stable with proportional feedback.

The approximate power required to overcome the gas losses has been calculated to be 16 kW at a total gas flow of 85 standard cubic feet per minute flow and at a stack temperature of 1800°F.

One of the two sets of time constants mentioned in the June report was negligible compared to the other and will be ignored. A program was then described for the control of the heater circuits. The heater control program calculates the required energy to raise the temperature to the set point. During this heatup phase, feedback is used to maintain the heater rods below, or at, the set point. After the pile reaches the set point, a regulator program is used to maintain the pile temperature using the top, bottom, and side heaters.

The cooling requirements are being studied in order to specify their control programs. A sampled-data controller was analyzed and will be simulated on the analog computer in order to gain a feel for proportional control on a process with transport lag. This will allow determining sampling rates for the different control loops in the cooling system.

Programming

A total of eight logging programs have been written and 90% debugged. Heading and dummy analog outputs have been printed on the operator's typewriter temporarily until the logging typewriter is installed. The programs will log all current analog input values in raw counts and engineering units,

gas system values temperatures, heater temperatures, graphite, heater power, gas system flow and pressure, valve positions, and rod positions.

Work has begun on a special Input-Output program which will cause the magnetic tape to serve as a buffer for all alarm messages in the event the TV display is filled. In addition, all log messages will be buffered and written out at the proper time. Finally, the program will store on tape the kind and time of occurrence of all alarms during any one run.

Work has started on the programming of a gas routine which is composed of the following cyclic sequence: Evacuate - Fill - Recirculate and Purge (optional). The purpose of this program is to set the proper valve positions for all nine valves in each state. There is an interplay between program and operator who must decide on manual or automatic control of specified valves.

A valve maintenance routine has been written but not debugged. This routine will record the actual number of pulses required to close and open the seven stepping valves.

Various other options are available; for example, the operator can request 0 through n pulses on each valve, thus the routine can be used later for routine maintenance checks as well as for required acceptance tests. In addition, valve characteristics and flow data can be used to determine constants used in the cooling program.

Reactor Operations

Training of the operations staff on programming for PMACS continued. As a concrete aid in their training, some maintenance and test subroutines were written, and the gas loop control and check program was started.

The first draft of operating procedures to be used for reactor startup and calibration experiments was completed.

Preparation of the process specifications was started.

All personnel in the High Temperature Reactor Physics Section moved into the 318 Building during the month. Room was made available on a temporary basis for three personnel from the Digital Equipment Development Unit and from the Mathematics Department to assist on the programming of PMACS functions.

Reactor Physics Program

Experimental Fuels

Small quantities (5 to 200 gm) of $U^{238}O_2$, $U^{235}O_2$, $Pu^{239}O_2$, and possibly other compounds, can be provided in microsphere form by Oak Ridge National Laboratory. These materials will be used in cross section studies and special lattice samples in the HTLTR. The larger amounts of $U^{233}O_2$ (8 kg) and ThO_2 (400 kg) for lattice experiments will be obtained as, or made into, small irregularly shaped particles for making up the various isotopic mixtures required. Quotes on the final cleanup of the U^{233} were requested from ORNL. Transfer of an additional 280 gms of U^{233} that is available elsewhere, and in a form immediately usable, was also requested. This latter amount would be enough to make a few elements for a preliminary lattice experiment in the PCTR.

Experimental Oscillators

The mechanical requirements were defined for the devices that are to connect the oscillator ram to various components in experimental lattices. Mainly the components would include a central lattice cell, a neighbor cell, the central fuel element, a poison strip along the central cell boundary, and a graphite slab also at the cell boundary. A design is required that can perform at 1000°C after a few preliminary low temperature runs.

Startup and Calibration Experiments

The core to be inserted into the HTLTR at the time of nuclear startup will be a 7-1/2" lattice containing 1.36" diameter natural uranium fuel. This lattice has been measured several times in the PCTR, in full-sized critical experiments, and the temperature coefficient at low temperature has been measured. The results from the HTLTR will be compared with the data available from these other experiments.

Since these experiments are the first to be done in the HTLTR, more extensive documentation of the operations to be performed will be needed. The rough draft of this document is now being reviewed.

The first test core still requires fabrication of the test cell region, the two movable cells, and the thermocouple adaptor sleeves. An attempt is being made to place the fabrication of these parts off-site. There has been no bid response as yet. The modified heater thermocouples for use with this test core are being fabricated by Engelhard Industries, a different vendor than the supplier of the other reactor thermocouples. No problems caused by this change are anticipated.

Measurement of Neutron Lifetime

The experiment of N. A. Hill in which the worth of a poison was measured at a number of control rod positions (see BNWL-193, page 24) was analyzed further. The previous conclusion that the experiment provides a fairly sensitive method of determining the neutron lifetime in a reactor but is very insensitive to the delayed neutron fraction, appears to be further strengthened by this analysis. Further theoretical analysis of the method in order to provide an explanation of these results would appear to be quite useful.

Buffer Fuel

The Maritime Administration requested three or four empty stainless steel tubes from the N. S. Savannah surplus fuel that was obtained for buffer fuel. When these tubes were emptied, the fuel pellets, 3.9% enriched UO₂, were found to be chipped and fractured, probably caused by rough handling.

Driver Fuel

Fabrication of graphite stock for the driver fuel elements is under way at the Great Lakes Carbon Corporation. Delivery is scheduled for about mid-September. Arrangements were completed with an off-site shop to machine the end closures.

REACTOR FUELS AND MATERIALS

BASIC SWELLING STUDIES (R. D. Leggett)

The purpose of this program is to characterize fissionable materials and understand their behavior during irradiation. The theories developed provide a basis for the engineering exploitation of metallic fuel materials in advanced reactor applications. Specimens under study at the present time include uranium with and without dilute alloy additions and thorium-uranium alloys.

Irradiation Program

A tandem assembly of two capsules, P-9 and 35, continues to operate successfully. Capsule P-9 is controlled at 450°C and 1000 psi towards a goal exposure of 0.75 at.% BU; capsule 35 is a low pressure (~30 psi) capsule controlled at 525°C toward a goal exposure of 0.4 at.% BU. Capsule 36 is a controlled temperature, low pressure (~30 psi) capsule controlled at 450°C toward a goal exposure of 0.3 at.% BU. These capsules will provide data needed to evaluate the effects of temperature, pressure, burnup rate, and minor alloying additives on the irradiation behavior of uranium.

Heat treatments and density measurements are being made on a number of high purity uranium and uranium-base alloy specimens. These specimens will be irradiated at temperatures of 450°C - 700°C at pressures in the range 500 - 5000 psi and to burnups in the range of 0.2 - 0.8 at.% BU.

A new high pressure control system is being installed to extend the control range to 6000 psi. Development work is continuing on additional and improved capsule control instrumentation which will be required to handle tandemization of future capsules.

Postirradiation Examination

The metallographic examination of specimens recovered from two capsules irradiated at 500 psi and 550°C and 625°C, respectively, to about 0.16 at.% BU is partially complete. The Fe-Al alloy (407 ppm Fe, 645 ppm Al, 85 ppm Si, 500 ppm C, and 23 ppm N) exhibited only the amount of swelling theoretically due to solid fission product atoms. No tearing or porosity was observed. One of the specimens of this alloy operated at 525°C and the other at 610°C. The grain structure was unchanged from the preirradiation structure. A specimen of Fe-Si alloy (140 ppm Fe, 25 ppm Al, 95 ppm Si, 400 ppm C, and 14 ppm N) exhibited aligned tearing but no grain distortion, consistent with the 565°C operating temperature and the measured 2.6% swelling. A high-purity, high-carbon uranium specimen (54 ppm Fe, 10 ppm Al, 34 ppm Si, 480 ppm C, and 24 ppm N) that operated at 500°C exhibited severe grain distortion on one end, slight grain distortion at the other, and both grain boundary tearing and aligned tearing. It appears for this alloy that 500°C is about the critical temperature above which "irradiation growth" is no longer observed. Another specimen of this alloy which operated at 550°C exhibited a few "aligned" type tears. A high-purity, low-carbon sample (64 ppm Fe, 5 ppm Al, 25 ppm Si, 6 ppm C, and 8 ppm N), which also operated at 550°C, showed profuse aligned tearing. These observations are consistent with the observed density decrease

of 24% for the low carbon material but only 3% for the high carbon material. Specimens of the two types of high purity uranium irradiated at 625°C have grain boundary tears or pores 0.2 to 0.5 μ in diameter and tiny matrix pores <0.1 μ in diameter. Metallographic examination is continuing on these specimens. The strong influence of pressure, carbon, and Fe-Al additions in reducing uranium swelling is quite obvious, but the mechanisms by which these benefits are desired remain to be clarified. In all cases swelling seems to be occurring by the same basic processes that were observed at low pressure (\sim 30 psi) in high-purity, low-carbon uranium.

Density measurements made on specimens recovered from two capsules controlled at 700°C (beta phase) and irradiated to 0.1 and 0.2 at.% BU, respectively, indicate that swelling is small ("R" values of \sim 15), independent of composition (high and low carbon, high purity uranium; Fe-Al alloy; and Fe-Si alloy), and linear with burnup. Because of longitudinal thermal gradients in the capsule, several of the specimens operated in the high alpha, but it was not possible to distinguish their swelling behavior from that of specimens which operated in the beta phase. In the range of temperatures covered in these two capsules (610 - 705°C), temperature was not an important variable. This is not too surprising when the entire swelling versus temperature curve is considered, for the curve goes through a minimum in this temperature range, increasing rapidly below 600°C due to mechanical processes and increasing above about 730°C due to fission gas swelling. Metallographic examination of these specimens is under way.

NONDESTRUCTIVE TESTING (J. C. Spanner)

Detection of Irradiation Induced Shift in Nil-Ductility-Transition Temperature

Critical angle ultrasonic methods have been demonstrated to be capable of distinguishing neutron irradiated carbon steel samples from nonirradiated samples although response anomalies were found to exist on both irradiated and nonirradiated samples. Experimental methods are being developed whereby the effects of anomalies will be minimized.

A hot cell facility in 324 Building was obtained for temporary use. Plans are being made to equip the facility for ultrasonic measurements on irradiated specimens. Mechanical design of a remote-operated tank-manipulator is continuing. Design concepts are being modified in an attempt to reduce the estimated cost to a figure commensurate with available funds.

Electromagnetic Testing Research

Circuits for providing timing signals for the signal sampling unit being evaluated for use in the multiparameter eddy current tester operated satisfactorily. A significant improvement was observed in the testers ability to eliminate signals due to various parameters when using the new circuits as compared to that obtained without the new signal sampling technique. However, further improvement in the ability to discriminate between signals caused by large flaws is desired. Other techniques to extend the range of operation of the tester are being investigated.

Operation of the newly fabricated computer section for use with the multiparameter eddy current tester was checked and it functioned as expected for linear signals. Adjustment of the new computer (or transformation section)

differs from the original unit in that needed adjustments are made to eliminate the signals due to the various parameters individually instead of simultaneously. This results in a more straightforward series of adjustments which can be made faster and easier. However, the system is not as flexible as the previous "simultaneous adjustment" system which may give slightly better results with nonlinear signal inputs. A choice between the two computer sections depends upon the outcome of further comparison tests and the results of the evaluation of other techniques to extend the range of operation of the tester to better handle large flaw signals.

Design of the solid state version of the multiparameter eddy current tester is continuing. The coil driving circuitry has been completed, and work is progressing on the flaw detection portion of the instrument.

The coil driving circuitry consists of a crystal controlled oscillator, a tripler, and a power driver. The balanced output level is approximately 15 volts peak-to-peak with an output impedance less than 50 ohms. The basic frequency is 100 kHz, and the output signal contains both 100 kHz and 300 kHz components. This circuitry is readily adaptable to other frequencies if desired since the tripler is the only stage using tuned circuits.

Some design and experimentation have been done on the amplifier stages in the detector stages. These amplifiers will be used to amplify the flaw signals to a usable level. Initially, wide band amplifiers were used to maintain the flexibility of operating frequencies. It was found that the amplifier noise level was too high to allow the use of wide band stages. Effort is now being concentrated on amplifiers using tuned feedback to narrow the passband and thereby reduce the noise level. Emphasis is being placed on simple feedback networks that can be easily changed if a frequency change is desirable for a specific test.

Infrared and Thermal Research

Development of a thermal wave instrument for rapidly measuring thermal properties and nondestructively testing samples is continuing. This instrument employs a noncontacting transducer which induces a thermal wave in the sample and senses the response of the sample to the wave. Application of the instrument to highly conductive samples requires an extremely high signal-to-noise ratio in the output of the transducer. Improvements made in the circuit and temperature sensor this month improved the signal-to-noise ratio by approximately a factor of five at a frequency of 0.0275 Hz. Apparently due to the nature of the noise that was eliminated, the accuracy of phase measurements at 0.0275 Hz was improved by a factor of about ten. The degree of improvement at higher and lower frequencies is being determined.

Tests with aluminum and copper samples showed that the input thermal impedance of the transducer differed by only about one degree in phase angle when placed near the surfaces of the two materials. Amplitude differences with these two materials were relatively much greater, but previous experiments showed that the amplitude is strongly lift-off. Hence, the small phase angle difference is the more reliable indication of sample thermal properties. Reproducibility of a single phase angle indication with the present system is

better than $\pm 0.1^\circ$ at 0.0275 Hz. It is believed that averaging a number of phase angle indications would improve the reproducibility to $\pm 0.01^\circ$.

One of the former noise sources in the system was the miniature solid state temperature sensor, having a noise equivalent temperature of about 0.015°C . The other noise source was contact resistance in a 0.17 ohm rheostat in the power regulation circuit for the transducer. This source caused a temperature variation of approximately 0.015°C at the transducer. The over-all noise equivalent temperature of the system then, before the improvements, was about 0.02°C .

The improved temperature sensor now being used is the smallest bead thermistor made by Fenwal. The time constant of this unit is about one second in free air, and it is thus limited to frequencies below about 0.1 Hz. The noise equivalent temperature attainable with this sensor is about 0.001°C .

Improvements made in the power control system consisted simply of replacing the rheostat with a fixed resistor fabricated from constantan foil. The over-all noise equivalent temperature at the transducer at 0.0275 Hz is now about 0.003°C , including temperature variations due to noise in the power regulating system.

As a result of the improvement in noise equivalent temperature, other smaller noise sources are becoming apparent. One source is the change in power lead resistance to the transducer with changes in temperature. Air blowing on the leads cause noticeable noise in the temperature at the transducer due to the change in power consumed in the leads. Some of the more obvious noise sources are being corrected. However, further experiment will be required to determine how important the present system noise will be as compared to other experimental variables. A series of measurements on various high conductivity samples is planned to obtain the answer to this question.

NUCLEAR CERAMICS (R. E. Nightingale)

Phase Studies in Pu-U-O System

A phase study of the Pu-U-O system was initiated. Samples were prepared by pelletizing and sintering mixed-powder compacts consisting of UO_2 and PuO_2 with the PuO_2 content varying in intervals from 0 to 100%. Solid solutions were obtained in the samples only after sintering in an argon - 8% H_2 atmosphere at 1600°C for greater than 16 hr. An intermediate grinding and re-pelletizing step was also required. X-ray diffraction patterns of the compacts after sintering indicated two phases in those samples containing more than 40 mole% PuO_2 . The second phase was of the C-type rare earth structure and is typical of sesquioxide $(\text{U},\text{Pu})_2\text{O}_3$. Weight-gain measurements after an oxidation-reduction treatment at 800°C indicated that all samples were hypostoichiometric, with the exception of pure UO_2 . The degree of hypostoichiometry increased with PuO_2 content to a maximum value corresponding to a calculated oxygen-to-metal ratio of 1.84 for 100% plutonium. After the oxidation-reduction treatment, only a single phase was observed in all samples, and the lattice parameters corresponded closely to expected stoichiometric solid-solution values. The calculated average plutonium valence was not constant but decreased in a nearly uniform fashion with increased plutonium content.

Recovery and Recrystallization in Pneumatically-Impacted Ceramics

Two especially designed test cans, each containing UO_2 samples of micronized, ceramic grade, and fused -325-mesh powders, and pre-sintered ceramic-grade pellets, were pneumatically impacted at $1100^\circ C$ and 240,000 psi to produce specimens for study of recovery and recrystallization effects.

All specimens except the pre-sintered pellets were highly laminated after impactation. Although some of the pre-sintered pellets contained cracks and no pellet-to-pellet bonding was induced in the stacked pellet arrangement, the pellets contained few laminations. Microstructure studies indicated that the highly densified materials experienced no marked grain growth. However, both ceramic-grade and pre-sintered materials showed small regions of grain growth. The -325-mesh materials also showed no obvious recrystallization of the large grains.

Samples of the pre-sintered material are being annealed at a series of temperatures between 500 and $1600^\circ C$ and subsequently observed for x-ray diffraction line broadening, microhardness, and microstructural changes. Further impactation studies at higher temperatures are being planned to produce lamination-free UO_2 .

The constant-temperature reaction calorimeter was modified to improve the precision and increase the temperature limit to $80^\circ C$. Preliminary ex-calorimeter reaction experiments using a variety of UO_2 particle sizes indicated that reaction times of greater than one hour are necessary for complete dissolution of UO_2 in 5 N HNO_3 at $80^\circ C$. The reaction time could be decreased to 45 minutes using aqua regia solutions.

An approximate minimum heat of reaction with HNO_3 of 133 cal/g UO_2 was calculated from several preliminary experiments. A comparison of this value with the expected stored energy content of 1 cal/g UO_2 indicates that a measurement precision of at least $\pm 0.5\%$ must be attained if stored energy is to be measured by difference calorimetry. Tests are continuing to determine whether or not the precision of the calorimeter can be increased to this level without major modification.

Effects of Stoichiometry on Irradiation Behavior of $(U,Pu)O_2$

Mechanically-rotated assemblies were designed for performing irradiation tests on $(U,Pu)O_2$ in the 100-K Snout Facility. These movable assemblies will subject each of several $UO_2 - PuO_2$ specimens to identical neutron fluxes in a cyclical fashion and will eliminate the major problem associated with in-pile experimentation, i.e., unpredictable time and spacial flux variation.

The apparatus consists of a cylindrical aluminum magazine (3" dia. x 15" long) which contains six longitudinal, full-length flow channels, each 0.750" in diameter. Use of this device permits simultaneous irradiation of six specimens under identical flux-time conditions.

Flow-test dummies were fabricated and delivered to K Reactor for hydraulic testing. Six $UO_2 - PuO_2$ irradiations, each comprising six specimens, are planned. Parameters to be investigated are oxide stoichiometry, heterogeneity of the mixture, and heat rating.

Several of the planned tests will contain central thermocouples. These provide the most precise thermal record achievable and may also yield dynamic heat-transfer data. If some flux asymmetry exists in the irradiation position, a hysteresis in thermal response to the flux peak will occur when a fuel specimen is moved through the peak. Average thermal diffusivity of the fuel can be deduced from the variation in phase angle between the flux maximum and the maximum in fuel center temperature as a function of rotation rate. Refractory-metal thermocouples were designed and detailed specifications were prepared. Thermocouples will be ordered after establishing the feasibility of performing these tests in Snout.

Mechanism of Pneumatic-Impaction Bonding

Selected-area optical and electron microscopy on several impacted specimens indicated that UO_2 single crystals undergo marked crystallographic reorientation during impaction. Evidence for both ordinary slip and deformation twinning was found. In specimens initially positioned with (111) planes normal to the impaction direction, prominent striations and wide bands were produced on planes parallel to the impaction direction; those specimens having (111) planes initially parallel to the impaction direction showed little similar structure. Laue x-ray patterns and diffractometer scans of the same surfaces (parallel to impaction direction) confirmed that a multitude of crystallographic orientations exist in each former single crystal, with a few preferred directions indicated. X-ray patterns also revealed that crystals stacked atop each other during impaction suffered appreciably more reorientation than those positioned side by side (the latter perhaps being more effectively cushioned by the surrounding Al_2O_3 matrix).

Powder x-ray diffraction analysis showed that the lattice distortion produced by impaction is roughly inversely proportional to initial particle diameter. This observation is consistent with the high density of dislocation etch pits occurring to a limited depth (about 50 microns) around the periphery of both 3 mm impacted cubes and 1/2 mm crystal particles. Annealing for two hours at 1200°C in vacuum produced nearly complete recovery of well-defined crystallinity for all specimens.

Quality of the bond between crystal cubes is difficult to evaluate because of the extensive interfacial fracturing which occurred. From micrographs it seems clear, however, that matrix and enclosure foil tended to penetrate the vertical interface between side-by-side crystals, prying them apart before "hydrostatic" pressure exerted effective lateral forces. This behavior is consistent with earlier tracer observations that very little lateral movement occurs in the powder matrix during impaction. The peripheral UO_2 fracture layer, reported previously, apparently resulted from very tight impaction bonding between the molybdenum foil enclosure and the UO_2 crystal and subsequent fracturing of the UO_2 at a uniform distance (about 50 microns) from the Mo - UO_2 bonded interface.

Nitride Capabilities Development

An inert-gas fusion apparatus for analyses of nitrogen and oxygen content of metals and compounds was partially installed in a glove box. The system is

running and is currently undergoing tests to identify (1) conditions of analysis for actinide metal nitrides, (2) precision and accuracy of the results, and (3) effect of remote mounting arrangements on performance of the system.

Stoichiometry Effects in Oxide Fuels

Metallography of nonstoichiometric UO_{2+x} fuels was completed. Mosaic strips (75X) and selected area, 250X and 500X photomicrographs were made for $UO_{1.90}$, $UO_{1.99}$, $UO_{2.02}$, $UO_{2.05}$, $UO_{2.15}$, and five $UO_{2.00}$ fuel rods which had experienced substantial center melting during irradiation. Migration of the excess component to the central, molten region was apparent for all compositions. This resulted in precipitation of uranium metal near the center of hypostoichiometric fuels and precipitation of as-yet unidentified phases in the once-molten region of hyperstoichiometric oxides.

Portions of the drilled samples used for determining radial stoichiometry variations were prepared for powder x-ray analyses. Results should reveal the identity of precipitated phases in the specimens with average compositions of $UO_{2.02}$, $UO_{2.05}$, and $UO_{2.15}$.

PuO₂-UO₂-BeO Phase Equilibria

A study to determine the nature of eutectic melting in the PuO_2 - UO_2 - BeO ternary system was begun. Fourteen samples covering the composition range from 4 - 36 mole% PuO_2 , 4 - 36 mole% UO_2 , and 60 - 90 mole% BeO were prepared. After sintering at 1600 - 1650°C for eight hours, melting point determinations will be made in an argon atmosphere. X-ray diffraction and metallographic analyses will be performed on both sintered and melted specimens.

Direct Transmission Electron Microscopy of Pneumatically-Impacted Uranium Dioxide

Initial success was achieved in chemically thinning UO_2 to electron transparency. To date, the thinned areas have been quite narrow and rather non-descript. No dislocations have been resolved. Work is continuing to expand the extent of the thinned areas.

Materials Exchange

UO_2 single-crystal specimens were prepared, characterized, and sent to the Reactor Physics Division, Argonne National Laboratory, as part of the materials and information exchange program. This material will reportedly be used as specimens for high-temperature ($T < 2700^\circ K$), vapor-pressure experiments.

Current requests for materials include: UO_2 crystals for ORNL, Northwestern University, and IBM Research Laboratory; and PuO_2 specimens for ANL, ORNL, Sandia, and Japan.

NUCLEAR GRAPHITE (R. E. Nightingale)

EBR-II Irradiations

The first of three graphite pins being irradiated in EBR-II is scheduled for discharge in mid-August after one month in the reactor. Expected maximum

exposure is about 3×10^{21} nvt, $E > 0.18$ MeV. Observations of melt wires installed in the capsule should give an indication of the operating temperature and provide a check on the heat-transfer calculations.

High-Temperature Irradiations

Capsule design for GEH-13-12 is essentially complete, and the sample loading has been determined for the first irradiation in the ETR. A revised gamma heating estimate of 12 watts/g as compared to the original estimate of 16 watts/g will reduce operating temperature to about 1400°C maximum, compared to the planned 1600°C . Unfortunately, no positions having greater heating rates are presently available in ETR.

Fermi Irradiations

As discussed earlier, an irradiation is being planned in the Fermi Reactor beginning early in 1967. Present plans call for four irradiation pins, containing a total of approximately 320 samples, 0.25-inch dia. by 1.75-inch long. Neutron flux intensities range from 2.0 to 8.0×10^{14} n/cm²-sec ($E > 0.18$ MeV), and temperatures are estimated to be from 400 to 700°C . The operating schedule of the reactor will be 28 days up and 28 days down. At present, the capsule design is firm and a data package has been sent to the reactor operator. Samples have been selected from the most dimensionally stable graphites from GETR and EBR-II irradiations and include samples for electron and optical microscopy.

Irradiations in Hanford Reactors

In an effort to expedite discharge and storing of the samples from the Hanford hot test holes, the following schedule will be employed. All samples will be discharged and stored without measurements except samples from the following sets:

1. DDR 117 - GLC Raw Coke Contract
2. DDR 164 - SCC Process Variables Contract
3. DDR 136)
DDR 118) - SCC Additives Contracts
4. Pechiney Calcination Series
5. Cold Test Hole Irradiations

The above listed samples will receive full property measurements. If data are required on other samples, they may be removed from storage and measured at a later time.

Fracture Mechanisms in Polycrystalline Graphite

A study has been initiated to analyze the mechanical stress-strain diagram of polycrystalline graphite. The main purpose will be to separate and define the elastic and inelastic parts of the deformation process. The results will aid in the interpretation of the micrographs taken previously of graphite under stress.

Thermal Expansion of Graphite

Sutton and Howard [J. Nucl. Materials, 7, 58 (1962)] have related the thermal-expansion coefficients of a polycrystalline aggregate to the expansion coefficients of the crystallites in the following manner:

$$\alpha_{\perp} = (1-K_{\perp})\gamma \alpha_c + K_{\perp} \beta_{\perp} \alpha_a \quad (1)$$

$$\alpha_{\parallel} = (1-K_{\parallel})\gamma_{\parallel} \alpha_c + K_{\parallel} \beta_{\parallel} \alpha_a \quad (2)$$

where α_{\perp} and α_{\parallel} are the thermal expansion coefficients of the aggregate transverse and parallel, respectively, to the direction of extrusion; K_{\perp} and K_{\parallel} are constants defined by the Bacon orientation function of the crystallites [J. Appl. Chem., 6, 477 (1956)]; γ_{\perp} , γ_{\parallel} , β_{\perp} , and β_{\parallel} are the "accommodation factors", defined as the fractions, γ , of the lattice c-change and, β , of the lattice a-changes which contribute to the linear dimensional changes of the aggregate in the two principal directions; and α_c and α_a are the lattice expansion coefficients in the c and a directions of a single crystal.

Sutton and Howard assumed, however, that $\gamma_{\perp} = \gamma_{\parallel}$ and $\beta_{\perp} = \beta_{\parallel}$; this assumption is both unnecessary and incorrect. A model for graphite has been described wherein the accommodation arises from basal-plane microcracks introduced during cooling from graphitization temperature. Using this model, one can derive the following relationships among the accommodation factors:

$$\beta_{\perp} = \gamma_{\perp} + (1-\gamma_{\perp})/K_{\perp} \quad (3)$$

$$\beta_{\parallel} = \gamma_{\parallel} + (1-\gamma_{\parallel})/K_{\parallel} \quad (4)$$

Equations 1 and 2 can therefore be rewritten as:

$$\alpha_{\perp} = (1-K_{\perp}) \gamma_{\perp} (\alpha_c - \alpha_a) + \alpha_a \quad (5)$$

$$\alpha_{\parallel} = (1-K_{\parallel}) \gamma_{\parallel} (\alpha_c - \alpha_a) + \alpha_a \quad (6)$$

The equations have been tested by calculation of the accommodation factors for two bars of PGA graphite from the data tabulated by Sutton and Howard. The following table compares the mean accommodation factors and standard deviations calculated at intervals of 50°C over the range 100 to 700°C.

	Block No. 7110	Block No. 7113
Sutton & Howard γ (av.)	0.0373 ±0.037	0.378 ±0.021
β (av.)	1.45 ±0.60	1.03 ±0.48
Eq. 3-6, incl. γ_{\perp}	0.353 ±0.011	0.385 ±0.015
γ_{\parallel}	0.321 ±0.018	0.397 ±0.013
β_{\perp}	1.426 ±0.007	1.417 ±0.010
β_{\parallel}	1.176 ±0.005	1.144 ±0.003

The derived accommodation factors exhibit substantially smaller standard deviations than the factors for the Sutton and Howard equations. A "t" test, comparing the mean accommodation factors in the principal directions, shows that for Block 7113 γ_{\perp} and γ_{\parallel} are significantly different at the 95% probability level; the other three sets of accommodation factors are significantly different at more than the 99% level. In addition, the calculated accommodation factors do not show any systematic variation with temperature, a behavior consistent with the proposed model. In contrast, if the accommodation factors resulted from alteration of the lattice expansion coefficients by internal stresses, the reduction of these stresses with increasing temperature would lead to a systematic increase in γ with temperature.

Equations 5 and 6 have the same mathematical form as Simmons' equation [Proc. 3rd Conf. on Carbon, (Pergamon Press, 1959) p. 559].

$$\alpha_x = A_x(\alpha_c - \alpha_a) + \alpha_a.$$

However, Simmons' A_x is an empirical constant, which does not have a physical meaning in terms of the graphite structure. The γ factors derived from the proposed model have physical meaning and are related to the microcrack system observed in electron micrographs.

Damage Fundamentals

In the investigation of the structures and properties of irradiation-induced damage centers in graphite, the potential energy function for the van der Waals interaction must be known. Various potential energy functions suggested for this interaction in graphite have given an unsatisfactorily wide range (-0.27 to -4.36 kcal/mole) for the calculated cohesive energy, compared with the experimental value of -1.01 kcal/mole. Since the cohesive energy of -1.29 kcal/mole calculated by Girifalco [J. Chem. Phys., 25, 693 (1956)] is in best agreement with the experimental value, the function used by Girifalco

$$U_{ij} = A \left(\frac{1}{2} r_0^{-6} r_{ij}^{-12} - r_{ij}^{-6} \right)$$

was selected for further development. This development was carried out by evaluating r_0 from the condition that at equilibrium

$$\frac{\delta}{\delta c} \left(\sum U_{ij} \right) = 0$$

where c is the interplanar spacing and by evaluating A from the Dienes theoretical relationship [J. Appl. Phys., 23, 1194 (1952)],

$$c_{33} = \frac{1}{2V_0} \left(\sum \frac{\delta^2 U_{ij}}{\delta \epsilon_z^2} \right) \epsilon_z = 0$$

where ϵ is the elastic strain, using a recently measured value for the elastic coefficient ($c_{33} = 3.6 \times 10^{11}$ dyne cm⁻²). The calculated cohesive energy of -1.15 kcal/mole establishes the adequacy of the newly developed potential energy function.

Irradiations of "Dimensionally-Stable" Graphite

The irradiation of the H-3-23 capsule in the GETR was terminated one reactor cycle early since satisfactory operating conditions could not be provided. Previous sample temperatures could not be attained even after replacing the nitrogen atmosphere with argon. Reactor physics personnel felt core-loading changes would not provide sufficient additional heating. The capsule will be disassembled and the samples returned. Irradiation will continue in the modified capsule design required for 50 Mw operation of the GETR.

Irradiation of Nuclear Graphite

The thirteenth capsule, H-3-13, in the series of long-term irradiations of nuclear graphites is operating successfully in a new position (E-6) of the GETR. The capsule design was modified to allow operation in the former D-7 position at a reactor power level approaching 50 Mw. The E-6 position provides nearly the same flux at 32.5 Mw as estimated for D-7 at 50 Mw, so that the capsule will be irradiated in E-6 for the present cycle. Sample temperatures duplicate previous operating conditions.

Oxidation of Boronated Graphite

The discrepancy between the rate of graphite lost from boronated graphite oxidized in helium containing 1% O₂ as determined by weight measurement and the rate calculated from the concentration of CO₂ in the effluent gas stream has been investigated further. In general, it was found previously that during initial measurements the rate calculated from the CO₂ concentration is greater than that obtained by weight measurements, as it should be because of the buildup of B₂O₃ in the sample. However, following the removal of the B₂O₃ by leaching, the rate obtained by weight measurements exceeds the rate obtained from CO₂ evolution.

In an attempt to find the reason for this result, additional rate measurements and calculations were performed. The results obtained are presented in the following table.

<u>Run No.</u>	<u>Apparent ΔW_c (g)</u>	<u>$\Delta W_{B_2O_3}$ (g)</u>	<u>Actual ΔW_c (g)</u>	<u>Calculated ΔW_c (g)</u>
1	-0.0104	+0.0045	-0.0135	-0.0132
2	-0.0178	+0.0069	-0.0226	-0.0184
3	-0.0240	+0.0089	-0.0301	-0.0183

In the table, the apparent ΔW_c is the measured weight loss of the sample, and $\Delta W_{B_2O_3}$ is the weight of B₂O₃ formed during the run as obtained by subsequent leaching. The actual ΔW_c is the weight of carbon lost by the sample as obtained by correcting the apparent loss for the amount of B₂O₃ formed, and the calculated ΔW_c is the weight loss calculated from the concentration of CO₂ in the effluent gas.

In the case of Run 1, it is seen that the agreement between the actual and calculated weight losses is excellent. For Runs 2 and 3, however, the agreement is poor. In Run 2, it could be assumed that the weight of B_2O_3 formed during the run should be only $(0.0184-0.0178) \frac{2MB_2O_3}{3MO_2} \approx 0.0009$ g,

and that the additional 0.0060 g was formed by hydrolysis of B_4C during the leaching process. It was found, however, in two separate instances by leaching samples which had not been previously oxidized that a weight loss amounting to only 0.0002 g occurred. Therefore, although hydrolysis of B_4C is thermodynamically feasible under the leaching conditions employed, the rate must be extremely slow, and hence this process cannot account for the discrepancy. In the case of Run 3, even the apparent weight loss is greater than that calculated, so that hydrolysis of B_4C cannot explain the results.

Because no gaseous products other than CO_2 have been found, the rate discrepancy may be related to the CO_2 concentration. Measurements will be performed on two different gas chromatographs to check this possibility.

Electron Microscopy of TSX Graphite

Several transmission microscopy specimens of TSX graphite have recently been prepared. The specimens were made in the process of developing preparation techniques using the mechanical, spark, and microwave methods described in earlier monthly reports. Specimens have the shape of a small circular disk approximately 3 mm in diameter and 1 mm thick. One side of the disk is flat, while the other side has a rounded conical depression. The conical depression intersects the flat side producing an opening in the central part of the disk. The graphite near the edges of this open area is now being examined with the electron microscope.

As a preliminary to the electron-microscopy examination, some of the specimens have been inspected by means of stereoptical microscopy. It has been found that the specimen hole area has a sponge-like texture with many complex delicate protrusions into the central opening. The complexity of the structure is still more evident when viewed with the electron microscope. Three types of structures have been observed from preliminary examinations: (1) delicate lace-like networks; (2) translucent web-type foils between opaque edges; and (3) translucent saw-tooth protrusions into open areas.

The delicate lace networks were found to be so fragile that they could be moved by concentrating the electron beam in a given area. These networks did not occur uniformly at the edge of the openings but only in certain areas where their presence might be related to local structural characteristics. The networks were sufficiently attached that they remained at the location where first observed. It appears that, in some way, they reflect the oxidation of a particular structural characteristic of nuclear graphite, perhaps a binder region or an area of highly defected structure. While carbon-oxygen polymers may be involved in producing these networks, it is somewhat surprising to find such polymers resulting from oxidation with microwave-excited oxygen in the flowing system used.

An attempt was made to determine whether impurities might be somehow related to the formation of the lace-network structures. One microscope specimen was examined, by means of an electron microprobe, to determine if

significant amounts of elements, other than carbon, were present. Only trace quantities of any foreign matter were detected, and these were not in the lace structures. This finding is consistent with the relatively high purity (less than 10 ppm total ash) characteristic of TSX graphite.

The translucent web-type foils which were seen in certain areas of the specimen appeared to be regions of greater structural regularity. Moiré patterns were clearly visible. Other structural features present have not yet been interpreted.

Saw-tooth protrusions could be seen at a magnification of 30,000X and higher at many locations along the edges of the openings in the specimen. These structures were clearly translucent when observed at higher magnification and had certain structural features not yet identified. It appears that these very regular protrusions are the (100) or so-called "zig-zag" faces of graphite crystallites such as might occur within a coke particle in a graphite body.

Compatibility of Sodium with Graphite

Seven irradiated graphite samples were heated in contact with sodium for 100 hours at 537°C. The samples had been previously irradiated at 600 - 700°C to exposures of 1.4×10^{21} to 2.7×10^{21} nvt ($E > 0.18$ MeV). The sample series consisted of the graphite types CSF, TSX, NC8, CSGBF, and TSGBF. The interaction of sodium with the graphite expanded the samples from 1.1 to 2.4%. Expansions of 3.9% have been reported (NAA-SR-11309) for type TSP graphite irradiated to 1.1×10^{21} nvt. The smaller expansions observed in the present studies may be due to the type of graphite or the low concentration of impurities in the sodium. An irradiated graphite sample will be heated in contact with impure sodium containing sodium oxide.

Five unirradiated graphite samples containing various amounts of carbon black were heated in sodium for 100 hours at 537°C. The samples were identical except for the carbon-black content which was 0, 20, 25, 33, and 50%. The samples were graphitized at 3000°C. The only sample which was not cracked after exposure to sodium contained 25% carbon black, and this sample expanded 1.4%. Although the results of this test were not conclusive, graphite containing carbon black is expected to be less stable in contact with sodium.

IRRADIATION DAMAGE TO REACTOR METALS (A. L. Bement)

Alloy Selection

Procurement of three new program alloys, 316 stainless steel, Incoloy 800, and Inconel 625, is proceeding on schedule. Fabrication of all items of the 316 SS order will be finished by the end of August. Shipment of rolled products to PNL has begun. The Incoloy 800 and Inconel 625 orders have been placed with Huntington Alloys, Inc., and fabrication of the Incoloy 800 tube blanks is under way.

Arrangements have been made with GE Advanced Products Operation (APO) to obtain irradiated and control tensile samples of nine nickel-base alloys

irradiated as a part of the General Electric superheat and fast reactor programs. Data from these alloys will complement current PNL irradiation effects programs on nickel-base alloys.

A series of tests conducted on irradiated and unirradiated PDRL-120 at room temperature, 300°C, and 650°C has been completed. This high-strength alloy is of interest for fast reactor applications.

In-Reactor Measurements of Mechanical Properties

An in-reactor creep capsule containing an annealed 304 stainless steel specimen is near completion. This capsule was constructed to replace a previous capsule in which a heater failed prior to starting the test. The proposed test condition of 840°C and 5000 psi will complete a series of creep and creep-rupture tests in the range of 500 to 840°C. Burnout of the heater was attributed to the breakdown of a potting compound used on the heater connections. The use of this potting compound will be eliminated on future capsules.

The high temperature creep capsule, under development for nickel-base alloy studies, is completed to the last step of welding of the outer shell. The capsule will be lab checked and ready for reactor charging next month.

Irradiation Effects in Structural Materials

Stainless Steels

The purpose of this phase of the program is to determine the combined effects of irradiation and environment on the mechanical properties of stainless steels. Radiation-induced property changes will be determined from irradiations and tests conducted at various temperatures on several alloys. Particular emphasis will be placed on determining the existence of metallurgical instabilities and the mechanisms by which they are enhanced in a nuclear environment.

Transmission electron microscopy examinations have been made of AISI 348 stainless steel irradiated at 60°C to 1.0×10^{20} fast fluence. Additional foils were obtained from AISI 304 stainless steel irradiated at 650°C to 1.0×10^{20} fast fluence and tested at room temperature before and after a postirradiation anneal at 1000°C. The thin foil of the buttonhead portion of the AISI 348 stainless steel specimen in the as-irradiated condition revealed a high density of irradiation-induced defects (vacancy and interstitial clusters). A post tensile test anneal at 450°C for one hour did not appear to remove a significant portion of the damage. After annealing for one hour at 500°C, the density of the defects was markedly reduced; but some damage still remained. The irradiation-induced microstructural damage was, however, completely removed after annealing at 600°C for one hour. These observations are consistent with mechanical property data previously reported.

The main purpose of examining the irradiated AISI 304 tensile specimens was to observe bubbles of helium generated from the thermal neutron burnout of boron. No evidence of helium in the microstructure was seen, even in the specimen that had been annealed at 1000°C for one hour prior to testing. It should be pointed out that only the unstressed sections of both specimens

were examined. A section from the AISI 304 stainless steel specimen that had not received the postirradiation anneal was annealed in a vacuum at 900°C for one hour after it was thinned for transmission microscopy. No helium agglomeration was observed after this treatment.

Thin sections have been obtained from three AISI 304 stainless steel creep specimens tested in-reactor under the following conditions during irradiation: (a) 525°C, 30,000 psi; (b) 650°C, 20,000 psi; and (c) 750°C, 10,000 psi. All specimens were tested to failure. These foils will be examined to determine the nature of radiation-induced defects, particularly helium agglomeration, in regions plastically deformed under irradiation.

Nickel-Base Alloys

The purpose of this program is to determine the effects of modified microstructures on the irradiation stability of nickel-base alloys. Microstructural modifications are made by preirradiation thermal or thermo-mechanical treatments and are evaluated by tensile tests, stress-rupture tests, and microstructural examinations.

The paper submitted to Trans. Met. Soc. AIME by I. S. Levy, J. L. Brimhall, and B. Mastel, correlating the unirradiated tensile properties and microstructure of Hastelloy X-280, has been accepted for publication.

The paper, "Postirradiation Mechanical Property Improvement in Hastelloy X-280 and Inconel 600," by I. S. Levy has been accepted for presentation at the Winter Meeting of the American Nuclear Society.

The current series of tensile tests at 1350°F (730°C) on specimens of Inconel 600 and Inconel X-750, which were irradiated at 540°F (280°C) to an exposure of approximately 1×10^{20} nvt (<1 Mev), have been completed. Control tests are also completed. The results show that preirradiation treatments that improve unirradiated ductility also improve postirradiated ductility.

Previously, a correlation between the unirradiated tensile properties and the respective microstructures was reported for both Inconel 600 and Inconel X-750. In light of this correlation, an examination was made of the previous work on Hastelloy X-280 to determine if a generalized mechanism would explain improved postirradiation properties for all three nickel-base alloys. Based on these examinations, the following mechanisms are postulated. Improved tensile ductility (as well as improved creep-rupture properties in Hastelloy X-280) result from the preirradiation treatments in two ways: (1) increased ductility of the areas adjacent to grain boundaries and (2) effective trapping of irradiation defects in the matrix. The increased ductility is accomplished by the formation of stable grain boundary carbides, during the preirradiation treatments, that remove hardening constituents from the adjacent matrix areas. The traps are provided by incipient nuclei or precipitates.

A comparative phase analysis of Inconel 600 is being conducted using chemical extraction, electron microscopy, microprobe analysis, and theoretical phase-equilibria computations.

The stress-rupture tests at Battelle-Columbus, which were interrupted due to grip deformation and furnace element problems, are again under way. Eleven unirradiated Hastelloy X-280 specimens are in this current test series. Fifteen specimens of Inconel 600 and Inconel X-750, irradiated at 540°F (280°C) to 1×10^{20} nvt (<1 Mev), have been shipped to Columbus for the next test series.

Fracture Mechanics

During the interim period, an analytical computer program was developed by the Mathematical Analysis Section for the purpose of evaluating the compliance characteristics of the Double Cantilever Beam (DCB) specimen. Previously, the compliance crack length relationship of DCB specimens of a given geometry had been determined by a time-consuming experimental process. Because of the necessity for using DCB specimens of different geometries, a computer approach was merited. Basically, the mathematical procedure, called boundary collocation, involves satisfying a stress function in the form of a Fourier series at a number of locations along the boundary of the specimen. The first coefficient in the series, which is proportional to the stress intensity, is evaluated from the resulting matrix. Using this computer program to evaluate compliances on specimens for which experimental data are available indicates an agreement of 1.3%.

The hydride platelet orientation in hydrogen-charged, Zircaloy-2, DCB specimens has been determined to correlate hydride effects with observed fracture behavior. Specimens charged with hydrogen at levels of 100 and 400 ppm both exhibited similar hydride distributions. In general, the hydride platelets were found at grain boundaries with the plane of the platelets lying generally in the rolling plane of the plate.

FFTF Supporting Studies

Irradiations of Reactor Structural Materials in Fast Neutron Spectrum

The purpose of this phase of the program is to conduct a series of irradiation experiments in the EBR-II and Fermi reactors to determine the combined effects of fast neutron irradiation and environment on the mechanical and physical properties of selected reactor structural materials. Long- and short-term irradiations and mechanical tests will be performed with the goal of obtaining adequate design criteria for specific reactor components. The study of reference alloys irradiated under typical FFTF design and operating conditions will be emphasized.

Over 1200 tensile, creep, and stress-rupture mechanical test specimens have been procured for use on this program. Test specimens have been fabricated from AISI 304, 316, 348, and 321 stainless steels for irradiation in both the EBR-II and Fermi reactors. Characterization of the mechanical properties of these materials in the as-fabricated condition is currently being performed at test temperatures between room temperature and 800°C. Characterization of their structure is also being accomplished by means of optical and electron microscopy.

Final plans and schedules for the Fermi irradiation program will be discussed by representatives from each participating laboratory at a meeting in Washington, D.C., on August 31, 1966. Because of the length of time required to design and build an elevated temperature subassembly to irradiate in sodium between 650 - 760°C, subassemblies will be unavailable for irradiations scheduled in Fermi. Alternatives will be discussed in light of the over-all Fermi irradiation schedule and program objectives. Additional efforts will be devoted to the EBR-II irradiations in hope of obtaining elevated temperature irradiations in sodium to supplement the Fermi irradiations. All long-term high-exposure irradiations are currently scheduled for the EBR-II.

Fuel Cladding Support Studies for the FFTF

The effects of fast reactor irradiation on the mechanical properties of candidate FFTF fuel cladding alloys need to be defined in order to select the optimum cladding material and to provide a description of mechanical behavior in the expected FFTF environment. An experimental program aimed at defining the important fast neutron irradiation effects is being formulated in detail in support of the FFTF project.

The major problem areas requiring investigation have been identified in collaboration with fuel development personnel. The most important problem area identified for study is the degradation of creep ductility attributed to transmutation damage and second-phase redistribution. The FFTF will operate at temperatures where this effect may impose a serious fuel design limitation. Also of considerable concern are the effects of flowing sodium on postirradiation creep properties and the effects of thermal cycling, thermal aging, and fatigue on mechanical integrity.

Initial emphasis is placed on biaxial stress-rupture tests in sodium of specimens irradiated in a fast reactor environment. Tubular specimens are to be irradiated in the Fermi reactor to exposures of about 1×10^{21} , 5×10^{21} , and 2×10^{22} fast fluence and subsequently tested in sodium at temperatures from 700 to 1400°F (370 to 760°C) at stresses sufficient to cause rupture in times ranging from 1 to 10^4 hrs. Ductility parameters are to be determined after testing. In addition to the postirradiation creep-rupture studies, a need for in-reactor stress-rupture data also exists, particularly at the lower FFTF operating temperatures; namely, between 800 and 1100°F (425 and 595°C). At these temperatures, radiation damage of the displacement type can accumulate and affect stress-rupture properties. Such a property change cannot be evaluated on a postirradiation basis since the displacement damage will anneal out during long-term creep testing. In addition, intergranular fracture may control rupture at low strain rates in this temperature range. An in-reactor, liquid-metal, stress-rupture capsule is being designed for this application.

The creep-rupture program will concentrate on 304 and 316 stainless steels. Screening studies utilizing postirradiation tensile tests on 348, FV548 (316 + 1% Nb), and other candidate alloys in various metallurgical conditions will also be performed.

Neutron Dosimetry

The SAND I (Spectrum Analysis Neutron Detector) computer code has been adapted for use in the UNIVAC 1107 and test cases performed to insure proper operation.

The SAND I program is designed to perform a variety of tasks involved in the determination of neutron spectra with foil activation detectors. It is primarily employed for: (1) printing spectrum tables, (2) calculating activities and sensitivity limits induced by a spectrum, and (3) using the activities induced in foils to determine the shape of an unknown spectrum.

A flux spectrum and cross section functions are the basic input to the program. The primary operation of SAND I is numerical integration by

Simpson's rule, calculating such integrals as $\int_0^{\infty} \phi(E)\sigma(E)dE$, where $\phi(E)$ is a flux form and $\sigma(E)$ is a cross-section function. When calculating an unknown spectrum, the preceding quantities are used in an iterative process to modify an initial input spectrum until activities are obtained which agree with a measured set of activation data.

The second of the three uses of SAND I has been investigated to determine the effect of different reactor spectra on the response function (activity) of foil monitors. Knowledge of the energy range over which the detectors will be sensitive will enable selection of the most appropriate foils for the determination of the reactor spectra. The usefulness of the SAND I program can be illustrated by selecting a number of activation monitors and determining the expected response in different reactor environments. Knowing the approximate spectral shape, an experimenter could then insert these data into SAND I and obtain information regarding the energy range over which the majority of the activations will occur. Three reactor spectra were chosen for this illustration: the Watt fission spectrum, the water-moderated Ground Test Reactor (thermal) spectrum, and the Fast Flux Test Facility (fast) spectrum. The following table lists the activation monitor reactions and the energy sensitivity limits calculated by SAND I. For the three spectra, 90% energy limits were chosen, that is, 90% of the activity induced in the foils is caused by neutrons with energies in the listed range.

90% Energy Sensitivity Limits in Three Reactor Spectra

<u>Reaction</u>	<u>Fission</u>		<u>GTR**</u>		<u>FFTF</u>	
	<u>E_L*</u> (Mev)	<u>E_u*</u> (Mev)	<u>E_L</u> (Mev)	<u>E_u</u> (Mev)	<u>E_L</u> (Mev)	<u>E_u</u> (Mev)
In ¹¹⁵ (n,n')	1.50	4.60	1.20	5.80	1.10	3.40
Fe ⁵⁴ (n,p)	2.40	6.70	2.10	8.20	1.90	6.10
Ni ⁵⁸ (n,p)	2.50	6.60	2.30	8.00	2.00	6.00
S ³² (n,p)	2.70	6.60	2.52	8.10	2.48	6.10
Al ²⁷ (n,α)	6.78	11.10	5.52	10.80	6.78	10.50
Cu ⁶³ (n,2n)	12.3	15.7	12.2	16.9	12.2	15.2

*E_L = lower energy limit; E_u = upper energy limit.

**Data obtained from W. N. McElroy, et al, "Neutron Flux Spectra Determination by Foil Activation, Vol. 1."

Creep and Creep-Rupture Testing Facility

The building (321-A) assigned for use in this program has been scoped for general physical layout. Worksheet drawings, based on this scope, have been issued, and a project proposal and cost estimate are being prepared. The prototype cell which was to be located in the 326 Building has been re-designed for location in the 321-A Building. Radiation protection afforded by the cell design has been reviewed by Environmental Health and Engineering Department in order to establish operating procedures. With the exception of tantalum, the materials to be tested after irradiation will not result in any time limitation for the cell operator. Development of parts for the creep test rigs to be used in the prototype cell is progressing on schedule. Final assembly and bench testing will follow receipt of parts being manufactured off-site. A selection of equipment has been transferred to the 321-A Building to complete the assembly of one of each type of creep rig to be installed. A conceptual drawing of radiological shielding for the sodium loop facility, for irradiated specimen testing, has been prepared. Detailed design will commence after receipt of the fabrication blueprints for the loop.

Damage Mechanisms

The objective of this program is to determine how interactions between irradiation-induced defects interact with moving dislocations to modify the mechanisms of plastic deformation in a metal. Radiation damage and the role of interstitial impurities in alpha iron are currently being investigated.

During this period, the effort has been directed toward completing and checking a high vacuum annealing system and writing a journal article on the thermally activated flow techniques used in this investigation. One additional test of the relations derived from this investigation on iron has been made. It was shown that the data from dislocation velocity measurements on Si-Fe performed by Stein and Low could be satisfactorily described by equations derived from our experiments and that tests conducted at different temperatures obeyed the predicted relationship. Such temperature terms were absent in the equations of Stein and Low.

ATR Gas Loop Supporting Studies

High Temperature Test Equipment

Preliminary estimates indicate that additional high-temperature creep and tensile equipment than presently available will be required for the experimental phase of the program.

Transfer Facility

Early completion of the transfer facility (five months prior to loop startup per our request) has been incorporated into the Fluor construction schedule. The current schedule lists completion of the transfer facility by November 1, 1967.

Critical Assembly

Design approval and delivery schedule for the critical assembly have not yet been received from INC.

Test Assembly

A second exposure, 52 additional hours at 1600°F (870°C), was obtained on the refractory test assembly in the vertical section of the model loop. A summary of the total exposure for this assembly is presented in the following table. After removal from the loop, dimension measurements showed evidence of additional small changes in the diameter of the outside containing rings of the holder. No tightening of specimens in the holder occurred during this exposure. The top retaining nut remained frozen.

Tensile tests at room temperature and 1400°F (760°C) were conducted on Hastelloy-X specimens of the tapered head design. Tests were conducted to a point beyond the ultimate tensile strength without specimen fracture, and the deformation characteristics of this design were analyzed by means of comparative tensile data with buttonhead samples and by pre-post dimension measurements. Results show that a significant portion of the machine cross-head extension (~10%) is due to deformation in the tapered head at 1400°F (760°C). A much smaller error (~1%) is seen at room temperature. These tests point to the need for additional extensometry to obtain accurate elevated temperature strain measurements with the tapered head specimen geometry.

Thermal-Hydraulic Analysis

The analytical thermal-hydraulic study of the test assembly has been initiated. A computer program based on the heat transfer characteristics of a single tensile specimen will be utilized to build up the thermal behavior of the entire test assembly for specified operating conditions.

The table contains the temperature distribution data obtained from the test assembly exposure in the model loop. These results show an axial temperature gradient along the periphery of the assembly which is opposite in sign to the anticipated gradient (i.e., the gradient was expected to have the same sign as the gradient along the centerline position). This temperature distribution may reflect the basic flow pattern in the loop test section rather than the flow characteristics around the assembly, since the gas flows from a reduced throat section (1.5-inch diam.) into the test section (3-inch diam.) with the assembly (3-inch diam.) resting directly over the throat. This configuration is not typical of the ATR gas loop test section, which does not have a reduced section. Observations of the oxidized tantalum specimens (see Specimen Surface Behavior) after the second exposure in the model loop appear to be of interest to the thermal-hydraulic analysis. Specimen oxidation in the contaminated gas stream is quite likely controlled by the rate of arrival of impurity atoms at the specimen surface, which may be related to boundary layers, and hence to heat transfer coefficients. Using this rather general, qualitative analogy, the observed oxidation pattern, which shows more oxidation of the tapered buttonheads than of the gage section, may be indicative of different heat transfer coefficients in these areas of the specimen.

Test Section Liner

A literature review has to date revealed only one study of irradiation effects in niobium or niobium alloys at elevated temperature. The limited study indicated a relatively small decrease (~15%) in in-reactor rupture life

History of Test Assembly Exposure in Model Gas Loop

First Exposure

Temperature (nominal) 1700°F (925°C)
 Time at Temperature 135 hours
 Pressure Drop 2 inches H₂O
 Temperature Gradients (typical)

<u>Tier</u>	<u>Center Line</u>	<u>Periphery</u>	<u>Radial ΔT</u>
C	1730°F (944°C)	1667°F (909°C)	+63°F (+35°C)
A	<u>1714°F (935°C)</u>	<u>1679°F (916°C)</u>	<u>+35°F (+19°C)</u>
Axial ΔT	+16°F (+9°C)	-12°F (-7°C)	

Number of Thermal Cycles 4
 Average Heating Time 5 hours
 Average Cooling Time 3 hours

Gas Purity at 1700°F (925°C) Operation

H₂O 1 ppm
 H₂ + N₂ 0.5 ppm

Second Exposure

Temperature (nominal) 1600°F (870°C)
 Time at Temperature 52 hours
 Pressure Drop 3.5 inches H₂O
 Temperature Gradients

<u>Tier</u>	<u>Center Line</u>	<u>Periphery</u>	<u>Radial ΔT</u>
C	1624°F (885°C)	1491°F (810°C)	+133°F (+75°C)
A	<u>1610°F (877°C)</u>	<u>1563°F (850°C)</u>	<u>+ 47°F (+27°C)</u>
Axial ΔT	+14°F (+8°C)	-72°F (-40°C)	

Number of Thermal Cycles 1
 Heating Time 5 hours
 Cooling Time ~3 hours

Gas Purity

<u>Time</u>	<u>Temperature</u>	<u>Impurity</u>	<u>Analysis</u>
0	~350°F (177°C)	H ₂ O	26 ppm
2 hrs	~1000°F (538°C)	H ₂ O	4 ppm
		H ₂	4 ppm
5 hrs	~1600°F (870°C)	H ₂ O	1.5 ppm
		H ₂	1.5 ppm
		CO	~0.5 ppm

of Nb - 1 Zr at 1800°F (980°C) and 2000°F (1090°C). Several studies of Nb irradiated at reactor ambient temperatures have been conducted, and those experiments which included postirradiation annealing will be of some value in understanding high temperature irradiation effects in Nb. Since interstitial element contamination can have significant effects on the properties of Nb and Nb alloys, studies of the effect of model loop exposures on the properties of Nb will be conducted.

ATR and Model Loop Corrosion Surveillance

Design of the specimen holder for insertion of corrosion samples into the model loop has been completed. This holder, constructed primarily of Mo, Mo-TZM, and stainless steel, will accommodate 21 samples (1.50-inch x 0.50-inch x 0.06-inch). The assembly will be placed in the heater discharge section of the loop where specimen temperatures of 1900 to 2100°F (1040 to 1150°C) can be obtained. Sample materials will include Hastelloy X-280, Haynes 25, niobium, molybdenum, and tungsten, and evaluation techniques will be based primarily on weight change measurements and metallographic studies.

Specimen Surface Behavior

In the second exposure (52 hours) of the test assembly in the model loop, the contamination level in the helium was quite high during the initial portion of the exposure (as shown in the previous table). Post-exposure examination revealed considerably greater specimen contamination in this test compared to the first exposure (135 hours). Molybdenum specimens at the inlet end exhibited a cloudy, glaze-like surface contamination which appeared to be considerably thicker than the thin film observed after the first exposure. Presumably this surface contamination is solidified oxides which were liquid at the test temperature. Molybdenum specimens in the second and third tiers of the assembly, away from the gas inlet, showed little or no evidence of contamination. Tantalum specimens throughout the assembly exhibited a purple surface film, presumably an oxide. This contamination was more severe at the gas inlet end. The degree of contamination also varied along the length of each specimen, being more severe on the buttonheads than on the gage length. Tungsten specimens, niobium specimens, and the niobium alloy (SCb 291) holder exhibited little or no visible contamination. However, the absence of a visible surface film does not mean that specimens were not contaminated. Transparent oxide films or the direct dissolution of oxygen rather than film formation would escape detection by visual inspection. There is also the possibility that "gettering" by the tantalum and molybdenum can affect contamination of other materials or at various positions.

Neutron Dosimetry and Gamma Heat Probes

The standard practice of using metal wire to measure reactor fluences has until recently only required that the material remain intact and recoverable after exposure to service temperatures up to approximately 1000°C. At high temperatures, problems can arise with metal monitors such as iron and nickel with melting points around 1500°C. At temperatures above 1000°C, the materials are subject to both corrosion and high-temperature reactions

with other materials which they may contact. The determination of fluence requires that the solid monitor be weighed and the activity of some particular isotope be measured. The activity of the wire is generally expressed as disintegrations per second per milligram of material counted. Since the purity of the metal or alloy determines the quality of this activity, any corrosion or contamination by other elements would cause error.

The ATR gas loop is being designed for a gas outlet temperature of 2000°F (1095°C). It can be shown that even higher specimen temperatures may be reached, depending on the heat-transfer characteristics of the specimen assembly. Flux monitors, if they are not thermally grounded, could reach temperatures that approach their melting points. In order to provide methods of measuring fluence at temperatures above the serviceable limits of present monitor materials, monitors must be developed that will not melt, corrode, or become easily contaminated by their environments.

One group of materials that lends itself to high-temperature service is the metallic oxides. Monitors prepared by mixing oxides of metals such as iron and nickel with aluminum oxide are presently being tested by the Dragon Project in England. The material is formed into small pellets that do not require a large irradiation space and are easily handled and counted. The art of mixing has not been developed to the point, however, where the same amount of metal is contained in each individual pellet. Calibration of each pellet is required and is accomplished by exposing the pellet to a reactor neutron flux for a short period of time, counting the induced activity, and calculating the amount of metal that each pellet contains.

We have obtained some of these pellets and have irradiated a portion of them for calibration. After calibration they will be used for low-temperature monitors along with the standard metal monitors to determine their usefulness. Attainment of a local source of supply and of improved mixing and forming methods is desired. Calibration of the monitors would then be reduced to lot sampling as is the case with metal monitors.

Fast Neutron Mechanisms

Preliminary testing and calibration of the mass spectrometer gas detection system for the hydrogen permeation apparatus has been completed. Hydrogen flows on the order of 1×10^{-7} atm cc/sec can be detected with the present equipment. This sensitivity is adequate for the initial higher temperature (>400°C), steady-state hydrogen permeation experiments that will be conducted on the relatively permeable iron and nickel-base alloys. In addition, the versatility of the present cycloidal-focussing spectrometer system is required for projected surface effect studies in order to identify hydrogen compounds formed by the reaction of effusing hydrogen with carbide, nitride, or oxide components of surface corrosion product layers.

A high sensitivity hydrogen leak detector will be required as the primary sensing element in the gas detection system for lower temperature permeation work, the more-demanding dynamic permeation experiments, and in-reactor permeation studies. These specialized mass spectrometers are capable of measuring hydrogen flows as low as 1×10^{-10} atm cc/sec.

Work is also progressing on the development of simple gas-metal analogue systems that can be used for ancillary investigations of helium bubble behavior and effects in fast reactor alloys. Bubble growth and mobility, bubble-defect interactions, and other basic aspects of normal bubble behavior are essentially independent of all but the P-V-T properties of the occluded gas, provided that the particular gaseous element or compound involved is neither appreciably soluble in nor reactive with the matrix over the temperature range of interest. Thus, internally precipitated water vapor bubbles can, for example, be used to simulate inert gas bubble behavior in iron, nickel, cobalt, copper, silver, lead, and many of their alloys.

The advantages of such an analogue approach are numerous. In many cases, one of the analogue gas reactants and a matrix component represent a solid-state system that is amenable to heat treatment. Hence, some control can often be exercised over both the size and the spatial distribution (including intergranular versus intragranular distribution) of the resultant bubbles. The internal bubble pressure can also be regulated in the case of hydrogenous analogue compounds by varying the fugacity of the hydrogen in the specimen environment.

An analogue approach is particularly valuable when possible vacancy effects are of concern. Since the diffusivities of the interstitial components of the normal analogue gases are not a function of either vacancy availability or mobility, it is possible to increase bubble pressure and thus induce swelling without involving or in any way perturbing the vacancy flux to the growing bubbles. The formation of strain centers in helium-metal systems under conditions of restricted vacancy supply can also be readily simulated inasmuch as interstitial elements are relatively mobile and can react at temperatures substantially less than those required for appreciable vacancy diffusion.

The initial experimental work in these areas is being conducted using a hydrogen-cuprous-oxide-water vapor analogue system. A special reaction cell with provision for the filamentary dissociation of molecular hydrogen has been constructed to facilitate hydrogen charging at low reaction temperatures.

High Pressure Studies

Two internal documents, "Ultra-High Pressure Research - Its Present Status and Capabilities" and "Effects of Pressure on Point Defects Present in Irradiated Solids," have been written and distributed. These papers are the first two in a series of six outlining the applications of ultra-high pressure in irradiation damage studies.

The irradiation-induced phase transformation in ZrO_2 has been investigated. It is known that the transformation from the monoclinic to the cubic form occurs after the solid experiences, at 1 atmosphere, 10^{16} fissions/cc from the uranium and thorium impurities in ZrO_2 . Zirconia has also been transformed from the monoclinic to the tetragonal (pseudo-cubic) form under the action of pressure alone. This raises the questions: what is the combined effect of irradiation and pressure on the phase transformation, and will

the transformation require a fewer number of fissions/cc under pressure than at 1 atmosphere. In an attempt to answer some of these questions, monoclinic ZrO_2 is being doped with small amounts of fissionable materials and subjected to various pressures under irradiation. The high pressure device, described previously, has been improved to conduct x-ray diffraction analysis of a material under pressure, before and after irradiation. In this manner, the required fission density for the transformation under isobaric conditions can be isolated. This information should verify the effectiveness of a 'fission spike' in promoting phase transformations at 1 atmosphere.

ATR GAS LOOP OPERATION AND MAINTENANCE (G. A. Last)

Evaluation of the Struther-Wellis Heater

The microstructure and hardness survey of the molybdenum heating elements has been completed and is summarized in the following table. These data show that some softening of the molybdenum occurred over the first four to five feet of the heater length, but the wrought structure is still maintained. In the last seven to eight feet of the heater, the molybdenum is completely recrystallized with only small variations in grain size. Metallographic examination revealed no indication of second phase particles resulting from contamination by the helium gas, although the material contains some large carbide particles which are typically found in commercial purity molybdenum.

Tensile specimens of standard molybdenum material were recrystallized at 2500°F (1370°C) in vacuum to provide a baseline for later tests on material from the recrystallized section of the heater. Results of the room temperature tensile tests are also presented below. The elongation values show that recrystallized standard material has a ductile-brittle transition below room temperature. Experiments in the electron beam tensile furnace have led to a specimen design for which acceptable temperature gradients can be maintained at 2500°F (1370°C). Specimens for elevated temperature testing are now being fabricated.

Shielded Filter

Several materials that would operate at 1600°F (870°C) without undue swelling or reactions with the Hastelloy pipe have been examined as possible substitutes for the iron beads specified for the shielded filter. Unfortunately, the materials selected are costly and hard to procure. Based on the data accumulated, it would be to our advantage to insulate the Hastelloy pipe to reduce the temperature of the shielding material. This concept permits the use of either lead or iron shot and would result in a considerable savings in shielding material. Insulating the Hastelloy pipe with approximately 3 inches of Min-K insulation reduces the shielding material temperature from 1600°F (870°C) to about 200°F (93°C). These recommendations have been transmitted to the Architect Engineer for his consideration.

Microstructure and Hardness of Molybdenum Heating Elements

<u>Sample</u>	<u>Distance from Inlet End, ft.</u>	<u>Structure</u>	<u>Micro- hardness DPH</u>	<u>ASTM Grain Size</u>
Standard heat- ing element				
Fin	-	Wrought	280	-
Weld	-	Large grained, two phase	177	-
Heater				
Fin 2	0	Wrought	291	-
	3	Wrought	240	-
	6	Recrystallized	182	8
	9	Recrystallized	182	8
	12	Recrystallized	177	7.5
Fin 8	0	Wrought	283	-
	3	Wrought	250	-
	6	Recrystallized	180	8
	9	Recrystallized	179	8
	12	Recrystallized	175	7.5
Fin 14	0	Wrought	282	-
	3	Wrought	253	-
	6	Recrystallized	182	8
	9	Recrystallized	-	8.5
	12	Recrystallized	-	-
Fin 23	0	Wrought	-	-
	3	Wrought	-	-
	6	Recrystallized	178	8.5
	9	Recrystallized	184	8.5
	12	Recrystallized	180	7.5
Weld	0	Large grained, two phase	171	-
	12	Large grained, two phase	177	-

Room Temperature Tensile Properties of Standard Molybdenum
Recrystallized at 2500°F (1370°C) in Vacuum

<u>Sample No.</u>	<u>Yield Strength, psi</u>	<u>Tensile Strength, psi</u>	<u>Elongation % in 1 in.</u>
2	81,000	84,100	32
8	71,000	83,000	37
10	83,000	83,000	36

Gas-Cooled Loop Vendor Data Review

Review of contract submittals for the ATR gas loop continued. Major efforts during the past month were devoted to a review of the gas purification system, main instrument panel, and the transmitter panel. A meeting was held at Johnson Service Company in Sausalito, California, on August 11, attended by PNL, INC, Fluor, IDO, and Ebasco Services to present comments on the main instrument panel submittals, and to assure that the vendor is aware of his responsibilities for the entire instrument system. A meeting of the cognizant agencies was held to make a complete review of the system and to resolve and consolidate the comments to be presented.

METALLIC FUELS DEVELOPMENT (G. A. Last)

Irradiation of Thorium-Uranium-Zirconium Fuel Elements

The irradiation of six tubular Zircaloy-2 clad, thorium - 2.5 wt% uranium, 1.0 wt% zirconium fuel elements continued successfully in the ETR-P7 and M3 loops. The current conditions for the six elements are summarized in the following table. The volume increase of 2.5% for the element having the highest exposure is only slightly greater than that required to accommodate the solid fission product atoms.

Irradiation Status of Th - 2.5 wt% U - 1.0 wt% Zr Fuel Elements

<u>Fuel No.</u>	<u>BU Fissions/cm³ (Mwd/ton)</u>	<u>Maximum Core Temp. °C</u>	<u>Surface Heat Flux cal/sec-cm² (Btu/hr-ft)</u>	<u>Specific Power watts/gram (KW ft)</u>	<u>Fuel Volume Increase %</u>
65	5.3x10 ²⁰ (15,200)	465	43 (5.7x10 ⁵)	40 (120)	2.5
64	3.6x10 ²⁰ (10,300)	420	35 (4.6x10 ⁵)	31 (95)	1.4
71	1.9x10 ²⁰ (5,500)	495	49 (6.6x10 ⁵)	45 (138)	0.6
72	1.0x10 ²⁰ (3,000)	490	46 (6.2x10 ⁵)	42 (129)	0.0
70	0.9x10 ²⁰ (2,700)	470	42 (5.6x10 ⁵)	39 (118)	0.1
85	0.5x10 ²⁰ (1,500)	445	37 (4.9x10 ⁵)	34 (103)	-0.5

Postirradiation Evaluation of Thorium-Uranium-Zirconium Fuel Element

Optical and electron metallography of a Th - 2.5 wt% U - 1 wt% Zr alloy fuel element irradiated to 1.4 at.% burnup (11,850 MWd/ton) in the ETR pressurized hot water loops is being compared with metallography of unirradiated fuel. Both unirradiated and irradiated specimens were etched by ion bombardment for 1/2, 1, and 2-hour periods. A superficial substructure has been observed in the grains of the irradiated sample that is not evident in the unirradiated sample. Additional metallographic examinations will be made to verify or refute the existence of the observed substructure and to provide additional data on the damage imparted to the fuel by its irradiation exposure. The accumulated irradiation exposure has not produced microporosity or dimensional instability in the fuel alloy.

Chemical burnup and uranium isotopic analyses have been made on a sample of the fuel material. The uranium isotopic analyses before and after the irradiation are as follows:

<u>Uranium Isotope</u>	<u>% Before</u>	<u>% After</u>
232	--	0.02
233	0.09	35.10
234	1.07	2.73
235	93.20	44.99
236	0.24	10.26
238	5.40	6.93
	<u>100.01</u>	<u>100.03</u>

Burnup by the cesium fission-product method is 1.3 at.% compared to 1.5 at.% calculated from the isotopic analyses. The accumulated ETR exposure data indicated a burnup of 1.4 at.%. These three independent estimates of the burnup are in good agreement and lend credence to the ETR exposure data.

High Exposure Uranium Irradiation Test

A fuel element irradiation test has been designed to operate uranium fuel rods at high temperatures to burnups greater than 10,000 MWd/ton. The variables to be studied include fuel composition, external restraint, and internal void volume. The combined effects of the uranium plasticity and the restraints from the cladding and system pressure are expected to cause the uranium swelling to be accommodated by a central hole. Two uranium compositions are being used: U + 350 ppm Fe + 800 ppm Al, and U + 150 ppm Fe + 100 ppm Si. Fuel rods 0.450-inch diameter were fabricated by coextrusion with either 0.025 or 0.050-inch thick Zr-2 cladding. Central voids ranging from 5 to 20% of the fuel volume will be provided. Fuel enrichment of 4.5% is being used to achieve the desired temperatures and burnup rate.

The fuel rods have been fabricated and beta heat treated. Metallographic examination of both as-extruded and heat treated sections has been made, indicating satisfactory quality and dimensions. The clad-to-core bonds are uniform, and no unusual conditions were observed in the beta treated uranium structure. Current work involves preparation of the central voids.

ENGINEERING DEVELOPMENT

NEUTRON FLUX MONITORS (W. G. Spear)

Regenerating Detectors

Arrangements were nearly completed for procurement of a new set of 0.25-inch diameter chambers for reactor in-core investigations to establish a more complete definition of operational characteristics useful in the commercial exploitation of the concept. This set will include detectors with a regenerative coating (approximately 90% U²³⁴ and 10% U²³⁵), with conventional U²³⁵ coating, and with no fissile material. This selection should provide valuable comparison data, adequate experimental control, and thorough investigation of regenerating detector constant sensitivity and relative gamma characteristics.

Because of the emphasis on fast flux reactors, investigations are in progress regarding candidate isotopes for application of the regenerating concept to in-core measurement of fast flux.

Beta Current Generator Detectors

Laboratory tests conducted at the 1.8×10^5 Ci gamma facility (Co⁶⁰) verified that a balanced gamma response characteristic was achieved between the two electrode elements of the new dual-chamber detector. The matched response is important to the achievement of gamma compensation, which will be obtained by subtraction of the carbon signal from the boron-11 signal. This dual-chamber detector concept for in-core reactor neutron flux measurement is being developed to provide fast response and long-life operational characteristics. The B¹¹ captures thermal neutrons and transmutes to B¹², which decays by the emission of a 13.4 MeV betas to C¹² with a relatively short half-life of about 20 milliseconds. The beta particle emission generates an electrical signal current proportional to the thermal neutron flux level.

Planned initial laboratory tests will determine the detector neutron characteristics at low flux levels (about 10^8 nv). When these tests are completed, high flux level in-core testing will be conducted to ascertain the operational characteristics.

Microwave Detectors

Change in the resonant frequency of a microwave cavity, due to the change in dielectric constant caused by neutron bombardment of an appropriate gas, can be used as a measure of the neutron flux density. The neutron (n,p) reaction and subsequent ionization of the gas by the resulting charged particles create, within the cavity, a plasma with an electron number density proportional to the neutron flux density, where the dielectric constant of the plasma is proportional to the electron density.

Inasmuch as the electric field within the cavity tends to concentrate within the walls of any capsule used to contain the gas, techniques are being sought to establish a gas-tight seal between the cavity and waveguide. It now appears that appropriate facilities are available for the brazing of the

required metalized ceramic seals, which have been ordered. Test cavities have been designed for use with the seals. Successful cavity sealing will permit acceleration of the planned reactor in-core experimentation. For future effect, attention is being given to application of the microwave techniques for fast flux measurements.

MICROWAVE AND INFRARED DETECTION OF COOLANT IMPURITIES AND MEASUREMENT OF IN-REACTOR TEMPERATURES (W. G. Spear)

Microwave Detection of Impurities in Coolant Gases

The dielectric constant of a gas is a function of the constituents of the gas. If a gas, such as helium, is mixed with water vapor, the dielectric constant of the mixture will depend upon the relative amounts of helium and water vapor. Since the resonant frequency of a microwave cavity is inversely proportional to the dielectric constant of the media contained within the cavity, the shift in frequency of the cavity can be utilized in measuring the amount of water vapor at a given pressure and temperature. For experimentation, a microwave generator is stabilized to the resonant frequency of the designed sample cavity through use of a reference cavity. The amount of detuning of the sample cavity is then measured in a simple fashion to give an indication of water vapor present.

Short-term tests are being performed using the developed variable pressure saturator to introduce controlled amounts of moisture into the helium gas stream. For these tests, a standing wave ratio meter is used as a tuned voltmeter to provide a measurement of moisture. A water vapor change of approximately 8000 ppm gave a full scale reading, with changes as low as 400 ppm being detected at levels of 1200 ppm, where the 1200 ppm level was the minimum operational level of the saturator. The actual value of the corresponding microwave frequency shift was not determined due to difficulties in measuring shifts of this magnitude. In planned experimental work, measurements at both lower and higher concentrations of moisture will be made along with determination of the frequency shift values, with future effort planned at higher temperatures and for long-term stability determinations.

High Temperature Measurements

Measurement of extremely high temperatures subjects the sensor and its associated lead-in wires to an environment in which limited accuracy and short life is expected. The requirement to monitor high temperatures in nuclear reactors in a reliable fashion with long-lived sensors dictates that new techniques be used.

A method to accurately monitor reactor in-core temperature as high as 1500°C (higher, using special metals) would be to measure the temperature-induced frequency shift of an inserted microwave cavity. By selecting the proper excitation mode and cavity geometry, the temperature may be related to one linear cavity dimension. A completed cavity design should permit achieving a sensitivity of about 360 kHz per degree Centigrade change in temperature (or about 3 parts in 10^5 frequency change per °C temperature change). This variation in frequency should be detectable using heterodyne techniques and phase sensitive detectors. Laboratory tests for the technique are not complex

and will permit verification of the linearity of temperature change with frequency shift over the extended range of temperature monitoring contemplated. For the initial step, fabrication of the high melting point cavities and waveguides has been resolved.

Infrared Technique

Calibration of equipment (variable pressure saturator) used to add controlled amounts of water vapor to a gas stream was completed. The equipment proved effective in producing dew points between 10°F and 60°F, where these dew points correspond to gas inlet pressures of 75 lb/in² and 8 lbs/in², respectively, above atmospheric pressure.

The Mark I hygrometer calibration data were obtained using the developed rotating filter wheel and several balancing wedge filters, where the best filter yielded a calibration extending, in a smooth fashion, from dew points of -50°F, with ±5°F sensitivity, to +55°F, with a resulting ±1°F sensitivity.

This hygrometer derives its signal from the 2.6 micron water vapor absorption band, which is very close to an absorption band at 2.7 microns for carbon dioxide. The instrument showed considerable sensitivity to carbon dioxide, a fault to be corrected by modification of the rotating filter wheel. Two other filter wheels peaking at 2.5 microns should provide the desired sensitivity to water vapor, while avoiding the carbon dioxide absorption band. In addition, a filter wheel is being assembled for operation at the 1.87-micron water vapor absorption band. Absorption strengths are less in this region, but there is no interference with absorption bands of other gases. Furthermore, lead sulphide detection sensitivity is more uniform in this region, and suitable optical materials for lenses and filters are fully available.

PLUTONIUM RECYCLE PROGRAM (F. G. Dawson)

FUELS DEVELOPMENT

The results of a joint BNW-ANL program on the transient irradiation behavior of Zircaloy clad, vibrationally compacted UO₂ fuel rods in the Transient Reactor Test Facility are described in a paper submitted for publication in Nuclear Applications. The paper, entitled "Transient Meltdown Irradiations of Vibrationally Compacted UO₂ Fuel Rods in TREAT," was authored by R. C. Liimatainen, M. D. Freshley, and F. J. Testa. In these transient experiments particular emphasis was placed on determining the extent of cladding-fuel-water reaction, the peak pressure produced during transient meltdown, the rate of pressure rise, and the particle size distribution for the fragmented fuel and cladding. These experiments provided data for a comparison between the transient irradiation behavior of vibrationally compacted UO₂ fuel rods and fuel rods containing UO₂ sintered pellets.

The PRTR irradiation program, which was outlined in the fiscal 1967 through fiscal 1970 Plutonium Utilization Document⁽¹⁾, has been presented

(1) BNWL-298, Program Analysis and Plans, Plutonium Utilization Program, FY-1967 through -1970, dated July 1966.

in detail in a topic report entitled "Plutonium Utilization Program: PRTR Irradiation Plans" by M. D. Freshley, R. E. Sharp, and R. E. Skavdahl. This report is currently being prepared by Technical Publications for distribution. The PRTR irradiation plan includes fuel element irradiation tests to be conducted in the Plutonium Recycle Test Reactor with the Batch Core Experiment and in the Fuel Element Rupture Test Facility. Individual fuel rod reactivity measurements will be made in the Plutonium Recycle Critical Facility. The Batch Core Experiment will provide statistically significant performance data on vibrationally compacted, mixed-oxide fuel elements operating at maximum fuel temperatures being considered for power reactors and to maximum fuel element burnups of 15,000 MWd/MT_{fuel}. These tests will provide needed information concerning the feasibility of operating full core loadings of plutonium-bearing fuels of specific powers to burnups of interest for commercial power reactor applications.

Irradiation testing of nondefected and deliberately defected fuel rods will be conducted in the FERTF at maximum rod powers to 28 kw/ft with fuel temperatures above melting. Because a commercial power reactor should be capable of accommodating in-core leaker fuel elements, a study of the defect behavior of oxide fuel rods constitutes an important part of the fuel element testing program. Another important objective of the program is to provide a direct comparison of irradiation behavior of pelleted and vibrationally compacted oxide fuel rods operating under high performance conditions, i.e., maximum linear rod powers in the range of 20 - 28 kw/ft and with significant fuel melting. The FERTF fuel testing program will be performed in three sets of experiments conducted at nominal maximum linear rod powers of 20, 24, and 28 kw/ft. Each set of experiments will be conducted in essentially the same way with the only significant difference being maximum rod power.

One thoria-filled, pressure test element is still being held by Plutonium Fuels Engineering. With this exception, all fuel and test elements for the Batch Core Experiment in the PRTR have been shipped. An inventory of hardware and fuel component items for replacement elements has been accomplished, and work is being initiated to procure needed material.

PRTR Fuel Rod Pressure Test

Three instrumented UO₂ - 2 wt% PuO₂ fuel rods were charged in PRTR. Each rod is equipped with a thermocouple and a pressure sensor to indicate the temperature and pressure in the gas plenum during reactor operation. Two of the rods located in one 19-rod cluster are positioned near the center of the reactor core. The other instrumented fuel rod is contained in a 19-rod cluster located near the periphery of the batch core.

Mark I-R Pellet Fuel Rods

The order placed with General Electric Company for design and fabrication of 77 Mark I-R high power density fuel rods containing pelleted UO₂ - PuO₂ fuel is progressing on schedule. These rods will be irradiated in the PRTR to provide a direct comparison of the irradiation behavior of pelleted and vibrationally compacted oxide fuel rods operating under high performance conditions.

Fifty-three fuel rods have been completed by General Electric Company and will be shipped to Battelle-Northwest Laboratories this month. The remaining 24 fuel rods are scheduled for delivery in September.

Plutonium Characterization Studies

The determination of the low energy gammas and x-rays emitted by the three Shippingport plutonium samples has continued during this reporting period with limited success. Several problems have been encountered, primarily electrical noise, which has limited resolutions to 4 keV (FWHM) at 60 keV. This has to be improved to between 2 and 3 keV (FWHM) at 60 keV before this phase of the program can be continued. The resolution of our present detector-dewar, electronics system is limited because of the following reasons: (1) The noise level of our present pre-amplifier is approximately a factor of two too high because the input transistor, a Field Effect Transistor, has to be replaced. (2) Moisture condenses and collects at the electrical connectors inside the detector sample chamber of the dewar. (3) The solid state detector, itself, does not meet specifications. These problems are being worked on.

EBWR DEMONSTRATION PROGRAM

Irradiation Testing of EBWR Prototype Fuel Rods

Three capsules, the last of a group of 32, are still under irradiation in the MTR and have attained a maximum burnup of 25,100 MWd/tonne of fuel (6.23×10^{20} fissions/cm³). The maximum goal burnup is 27,500 MWd/tonne of fuel. The double-clad capsules (see table below) contain short lengths of EBWR fuel rods. The Zircaloy-clad rods (1.07 cm OD) were made by the vibrational compaction technique and utilized pneumatically impacted UO₂ - 1.5 wt% PuO₂ fuel. The following capsules were charged into the MTR in February 1964, and have operated at an estimated maximum linear power of 535 W/cm (16.3 kw/ft):

<u>EBWR UO₂ - 1.5 wt% PuO₂ Capsule Tests</u>			
<u>Capsule No.</u>	<u>Fuel Bulk Density</u>	<u>Estimated Current Burnup</u>	
<u>GEH-14-</u>	<u>(% of theo.)</u>	<u>MWd/tonne of fuel</u>	<u>fissions/cm³</u>
523	84	23,600	5.88×10^{20}
524	84	25,100	6.23×10^{20}
529	84	21,400	5.33×10^{20}

Thirty-three production-run EBWR rods, 1.07 cm OD by 148 cm long (includes a plenum, 14.6 cm long), are presently in reactors. Irradiation Fuel Element No. 6501, a 21-rod bundle, in the PRTR will continue when the reactor resumes operation. Present burnup on Fuel Element No. 6501 is 2690 MWd/tonne of fuel (0.7×10^{20} fissions/cm³, and goal burnup is 10,000 MWd/tonne of fuel. Rods can be removed and replaced in the bundle. The other 12 rods are being tested elsewhere in 3-rod cluster form. Cluster goal burnups to 27,500 MWd/tonne of fuel are planned. A total of 58 - 64 full-size rods are to be irradiation tested, and, of these, 25 have been irradiated and discharged.

REACTOR PHYSICS

D₂O Moderated Systems

Correlation of Theoretical and Experimental Lattice Parameters

An attempt is being made to theoretically predict the lattice parameters for a UO₂ fueled - D₂O moderated and cooled 19-rod cluster, which will correlate the experimental values. Results of previous studies^(1,2) in correlating the thermal utilization, f , for the 8-inch lattice, showed a 3% discrepancy between theory and experiment. The analytical (theoretical) results for these studies were obtained assuming Zircaloy cladding and process tube. The experiment, however, was performed using aluminum for the clad and the process tube. A subsequent calculation whereby the aluminum replaced the Zircaloy resulted in a value of f which compares favorably with the measured value.

The scope of the study was extended to include a 7-inch and 9-inch lattice and to compute values of k_{∞} to compare with experimental values. The comparison of preliminary calculated values of f and k_{∞} to experiment are shown in the following table. The theoretical results were obtained from calculations using the THERMOS and HRG codes. The theoretical and experimental values of f and $\bar{\eta}$ are in reasonably good agreement, whereas a 3% discrepancy in k_{∞} results. This discrepancy is apparently resulting from the computation of the product $p\epsilon$. The Bell correction was utilized in determining the mean chord length \bar{l} , which is used in the spatial self-shielding correction in the HRG code. Other means of obtaining this factor are currently being investigated along with their effects on k_{∞} .

Photoneutron Effects

Calculations have continued to determine the effectiveness of gamma rays in producing photoneutrons in deuterium using transport theory methods. Calculations have been completed for various 19-rod clusters at room temperature in the PRTR.

Results show that a uranium-carbide (UC) cluster which is light-water cooled and heavy-water moderated is 25.82% as effective in producing gamma rays in deuterium as is a point source. A Pu-Al cluster which is heavy-water cooled and moderated is 7.20% as effective in producing gamma rays in deuterium as is a point source. These values are compared to 28.06% or 17.58% which was reported previously for a 2 wt% PuO₂ - UO₂ cluster with heavy or light water coolant, respectively.

- (1) J. R. Worden, W. L. Purcell, and R. C. Liikala, "Modifications to the Computer Code, THERMOS, and Comparative Studies on Scattering Kernels," Physics Research Quarterly Report July, August, September 1965, BNWL-193, October 15, 1965.
- (2) J. R. Worden, W. L. Purcell, and R. C. Liikala, "Sensitivity of Thermal Reactor Parameters to Scattering Model," Physics Research Quarterly Report, January, February, March, 1966, BNWL-284, April 15, 1966.

COMPARISON OF THEORETICAL AND EXPERIMENTAL VALUES OF f
AND k_∞ FOR A UO₂ FUELED-D₂O MODERATED AND COOLED 19 ROD CLUSTER

Lattice Spacing (in.)	f		k _∞		$\bar{\eta}$	
	<u>Theoretical</u>	<u>Experimental</u>	<u>Theoretical</u>	<u>Experimental</u>	<u>Theoretical</u>	<u>Experimental</u>
7.0	0.908	0.901	0.974	1.005	1.310	1.31±0.024
8.0	0.931	0.900	1.023	1.052	1.315	1.31±0.024
9.0	0.901	0.897	1.054	1.088	1.315	1.31±0.024

Previous Study^{1,2}
Latest Study

Batch Core Experiment in the PRTR

Fuel loading and critical testing have begun for the Batch Core Experiment in the PRTR. Measurements have been made of fuel worths, boron worths, moderator level coefficients, and some void coefficients in the range of 6 to 55 fuel clusters and boron concentrations from 0 to 25 wppm B^{10} . Analysis of these results is in progress. There is qualitative agreement between the measurements and previous predictions.

Axial flux traverses have been made in the PRTR using bare gold foils. The results of counting have been analyzed using the computer code FDCRLP and then fitted to cosine distributions using the computer code GLEX. The cosine fits are very good at the center of the fuel, with slight deviations at the ends due to reflector effects. The peak-to-average flux ratios obtained from these traverses are given in the following table:

<u>No. of Fuel Elements</u>	<u>Boron-10 Concentration</u>	<u>Moderator Level</u>	<u>Peak-Average Flux</u>	
			<u>Measured</u>	<u>Calculated</u>
9	0 wppm	98.5 in.	1.26	1.25
12	3.5	99.75	1.27	1.26
16	6.9	94.55	1.32	1.29
23	10.1	95.15	1.32	1.30
31	14.2	96.7	1.31	1.31
55	14.2	72.2	1.86	1.78

Cell traverses using lutetium foils are being made.

A paper summarizing the analytical and experimental results of the Batch Core Experiment conducted in the PRCF has been accepted by the American Nuclear Society for presentation at the November meeting.

Additional calculations for the FERTF have been made at the request of the Fuels Development Section of the Materials Department. These calculations determined the power generation rate in the FERTF with a borated stainless steel basket and UO_2 fuel rods, as a function of U^{235} enrichment in the fuel.

Determination of boron concentration in D_2O moderator solutions has continued in the Thermal Test Reactor (TTR). All samples taken from the PRCF during the Batch Core critical experiments have been evaluated for boron concentration by reactivity measurements in the TTR. Measurements have begun on samples taken from the PRTR during critical tests.

H₂O Moderated Systems

Critical Experiments with $PuO_2 - UO_2$ Fuel Rods

Critical experiments have continued in the PRCF using H_2O moderator and 1/2-inch diameter, 2 wt% $PuO_2 - UO_2$ fuel rods containing plutonium which has 24 wt% Pu^{240} . The lattice pitch is 0.85 inch. The temperature coefficient of reactivity has been measured over the temperature range 22°C to 45°C. Dysprosium-aluminum pins have been activated to determine spatial distributions of thermal flux in several different unit cells; the cells contained a fuel rod, a teflon rod (to simulate a void), a cadmium sleeve, or H_2O . Reactor noise experiments have been performed to measure the quantity β/λ .

Calculations have been performed using the series of computer codes THERMOS, HRG, and HFN to obtain analytical results which can be compared with the results of the critical experiments which involve fuel elements containing various concentrations of Pu^{240} . The calculated critical mass is 3.3% high, and the calculated effective multiplication factor is 0.45% (4.5 milli-k) low for the loading containing 24 wt% Pu^{240} . For a loading of fuel rods which contain 8 wt% Pu^{240} , the calculated critical mass is 2.2% low, and the calculated effective multiplication factor is 0.40% (4.0 milli-k) high. For both loadings, calculated radial distributions of thermal copper activation are in good agreement with measured distributions and calculated worths of peripheral fuel rods agree to within 5% with measured worths.

Graphite Moderated Systems

PCTR Experiments on LX $\text{PuO}_2 - \text{UO}_2$ in a Single Rod Geometry

A series of k_{∞} measurements are being made for square graphite lattices containing 0.5-inch diameter fuel rods at spacings of 2.0 inches, 4.0 inches, and 5.0 inches. The fuel contains 0.9 wt% $\text{PuO}_2 - \text{UO}_2$. The plutonium has a Pu^{240} content of 7.3 wt%, and the uranium is depleted to 0.23 wt% U^{235} .

The experimental phase of the 4.0-inch lattice is in progress now. A 64-cell square array has been loaded into the PCTR, and reactivity measurements have been made using the central four cells as the test cell. The unpoisoned lattice has been flux matched to give a neutron energy distribution in the test cell that is typical of the distribution in an infinite array of cells. Foil activation measurements have been made in the test cell to determine the relative absorption rates of the cell components.

Reactivity measurements have been made to determine the worth of the central test cell, the worth of copper on the boundary of the test cell, and the worth of copper in the cavity created by removal of the test cell. Flux measurements have been made on the surface of the cavity and in the copper. The flux and reactivity data will be used to evaluate a recently developed technique for measurements in an unpoisoned lattice. The reactivity data also yields a preliminary estimate of the mass of copper which will be required at the cell boundary to reduce the neutron multiplication to unity. The next step will be to complete the standard experiment to determine the correct mass of copper.

PCTR PuO_2 Particle Size Studies

Reactor experiments are planned to study the reactivity effect of lumping PuO_2 in various sized particles. Fuel rods are being fabricated which will contain 2 wt% PuO_2 in $\text{PuO}_2 - \text{UO}_2$. Two isotopic concentrations of Pu^{240} will be studied, and the concentration of U^{235} will be that of natural uranium. The PuO_2 particles will be oblate spheroids with major to minor axis ratio less than 1.5 and will cover a size range of 0 micron (solid solution) to 700 microns in diameter.

The experiments will be conducted with both graphite and light water moderator. The graphite phase of the study will be coordinated with the 4.0-inch single rod $\text{PuO}_2 - \text{UO}_2$ lattice which is in the reactor now. Initial

design of a water tank for the experiment in the PCTR test cavity has been completed, and drawings are being prepared for its fabrication.

The first delivery of fuel rods is in preparation and should be received next month.

Neutron Physics

Slow-Neutron Scattering

Work has continued on the analysis of scattering law data for H₂O at 20° and 95°C previously obtained with the triple-axis spectrometer. Reduction of data to scattering law format is nearly complete. The identification of measurements which were invalid due to systematic errors caused by subtle order effects is in progress. A formal report is being prepared on these results.

Data reduction has continued on scattering law data taken on H₂O, D₂O, and ice using the rotating-crystal spectrometer. Several inconsistencies in the results obtained from overlapping experiments have been identified and are being investigated. Attempts to fit the observed scattering law results with assumed phonon frequency distributions have been started using the LEAP/ADDELT calculational programs.

The first draft of a paper describing a method of high-resolution monochromatization of slow neutrons has been completed. Subsequently, it has been realized that certain crystallographic principles may be used to show that an appreciable fraction of the "forbidden" reflections which are vital to the success of the method are in fact strictly forbidden by crystal symmetry. These points are now being developed for inclusion in the paper.

Fast-Neutron Cross Sections

A draft of an article which compares the experimental neutron total cross section results on deuterium with theoretical predictions has been completed.

Work has continued on the processing of previously obtained total cross-section results for publication. The work of combining the results of individual runs is essentially complete. Detailed examination of these results to remove input errors and inadequate corrections for systematic effects is in progress.

Cross Section Evaluation

Work has continued on the evaluation of nuclear data on a dozen isotopes for the AEC Evaluated Nuclear Data File/B. In the course of this work it has been determined that the BNW results of Foster and Glasgow on the n-p total cross sections are represented quite accurately by the semi-phenomenological predictions of Gammel (Fast Neutron Physics, J. B. Marion and J. L. Fowler, Editors, Part II, pp. 2221-2222, 1963). On the other hand, the BNW results on the n-d total cross section obtained with the same experimental technique as used for the n-p measurements and the same sample that was used in the precision measurements at Livermore show significant areas of disagreement with the Livermore and some other measurements. These discrepancies are still being studied.

A recent publication from Harwell (AERE-R5166) makes a drastic revision in the value of α_0 (2200 m/sec) for Pu^{241} derived from controlled transmutation measurements in a reactor spectrum. The presently reported value of α_0 is 0.356 ± 0.017 . The original Harwell value of 0.388 ± 0.023 was the only input value in the least-squares adjustment of Westcott, et al, which resulted in a recommended value of 0.379 ± 0.021 . It is apparent that a revised adjustment using the new value would result in a much lower output value for α_0 .

Code Development*

BNW Master Library

Updating of the BNW Master Library continued with the following isotopes receiving extensive modifications:

1. U^{236} was updated by using the resonance parameters contained in BNL-325, Sup. 2, Vol. 3. The cross section data above 1 keV was obtained from the ENDF/A library with the source listed as AWRE 0 30/64. The infinite dilution resonance integral for this version was 310 barns with 0.45 eV cutoff. The recommended value in BNL-325 is 400 barns, but this value could not be obtained with the recommended resonance parameters.
2. Pu^{242} was also updated, but the 2200 m/sec capture cross section was assumed to be 30.0 barns following the measurements of Auchampaugh, et al, at Livermore; Pattenden at Harwell; and Young at Phillips. The resonance parameters were obtained from the values published in AERE-PR/NP 9 and Physical Review Vol. 146, No. 3. The cross sections above 1 keV were assumed to be identical to those of Pu^{240} which is the nearest even plutonium isotope. The resonance integral obtained from the above record was 1175 barns for a 0.45 eV cutoff. The measured integrals average 1280 barns with an error of 60 barns. Several changes will still be made to this isotope from the available fission cross section data. This change should not affect any calculations because of its similarity to Pu^{240} .
3. N^{14} was updated using UNC-5002 as the source. Previous versions of nitrogen also used the same reference but had been updated under the limitation of only 50 points representing differential elastic scattering data. The current record has 69 such points with improved structure in the resonance region.
4. C^{12} was updated with more differential scattering data. The source of cross sections was KFK-120. Differential scattering coefficients were obtained from UNC-5002. Accuracy for the total cross section of carbon in the resonance region is significantly improved.
5. In the updated version of Pu^{240} the resonance region has several new parameters for fission widths, and the new record will reflect these changes. The new data was obtained from LA - DC - 9623. The cross sections above 1 keV were obtained from AWRE 91/64. The fission cross sections in this energy region need to be re-updated to reflect the

*Partially funded by O2.

"PETREL" data which is much higher than the Aldermaston record in the energy region of 1 keV to 100 keV. The Aldermaston record drops to 0.001 barn fission where the Los Alamos data remain approximately 0.1 barn.

The valley at 10 eV has an experimental measurement for sigma total of approximately 32 barns, and the single level parameters have always estimated a value of approximately 10 barns. To account for the vast difference, a very large potential scattering term was assumed as recommended by S. Pearlstein at BNL.

Pu Cross Sections Update

The last major effort of updating the resonance and thermal energy cross sections for the plutonium isotopes on the BNW Master Library was in 1963. (At that time known as the R.B.U. Basic Library.) New cross-section data for these isotopes have been measured and reported in the interim. Also, new evaluations of the 2200 m/sec constants for the fissile nuclides have been made. In addition, changes have been made to the Master Library to improve the fit of partial cross sections as a function of energy. The new cross section data and descriptions are included now on the BNW Master Library.

The thermal cross sections for Pu²³⁹ and Pu²⁴¹ (below 5.0 eV) are now more accurately described as a function of energy. Also, some "spurious" points have been removed. The comparison of the g values at 20°C shown in the following table along with resonance integrals for infinite dilution reflect the effect of these changes.

The resonance cross sections for Pu²⁴¹ and Pu²⁴² have been updated. New resonance parameters which are used in the Breit-Wigner single level formulation of the cross section are on the library. The comparison of the resonance integrals for infinite dilution as shown in the table reflect these changes.

The thermal cross sections for Pu²⁴² have been updated. The 2200 m/sec values of σ_a and σ_s now on the library are 30.0 and 8.9 barns, respectively. These values are the results of recent measurements of the 2200 m/sec total cross section. These new data yield a slightly different g value than the previous data as shown in the table.

The effects of updated cross sections of plutonium on the theoretical prediction of reactivity and burnup are being investigated.

RBU Code

A comparison of RBU calculation with an HRG calculation showed that RBU had an incorrect formulation of the resonance parameter cross sections. This has been corrected and a test case will be run with RBU.

Another comparison of the RBU Monte Carlo and THERMOS calculation was made for a cell containing a boron rod in water. Ideal gas and scattering cross sections were used in both codes. The average cross section of the boron in the rod agreed to within 0.1%, while the average water cross sections are within 1.2%. There is a 10% disagreement in the ratio of the flux in the water to the flux in the boron rod. RBU had a higher flux in the boron rod. The difference is believed to be caused by the assumption in THERMOS of

g Values At 20° C For Pu²³⁹, Pu²⁴¹, and Pu²⁴²

	g Capture		g Fission	
	Pu ²³⁹	Pu ²⁴¹	Pu ²⁴²	Pu ²⁴¹

Old Data, Prior To Update	1.1504	0.9818	1.0101	1.0571
New Data, Result of Updating	1.1436	1.0481	1.0063	1.0547

Resonance Integral for Infinite Dilution (to 0.5 eV)

	Pu ²⁴²		Pu ²⁴¹		Pu ²³⁹	
	I _∞ ABS. (barns)	I _∞ ABS.	I _∞ FISS.	I _∞ FISS.	I _∞ ABS.	I _∞ FISS.

Old Data, Prior to Update	1044	671	575	546	325	
New Data, Result of Updating	1144	678	514	520	331	

2200 m/sec Values For Pu²⁴²

	σ _{ABS.} (barns)	σ _s (barns)
--	---------------------------	------------------------

Old Data, Prior to Update	19	7.9
New Data, Result of Updating	30	8.9

isotropic scattering in the laboratory system. A similar system using the Nelkin Model for water showed a 5% change in the flux ratio when a correction for anisotropic scattering was made. The change should be larger for an ideal gas so it is believed that the RBU Monte Carlo calculation is probably correct. PROGRAM S will be used for this problem with P1 scattering to try and get a more accurate number for comparison with RBU.

FUEL CYCLE ANALYSIS

Fast Reactor Economics

Preliminary analysis of the Allis-Chalmers fast reactor calculations indicates that plutonium from thermal reactors is a better fuel (per gram fissile) than the plutonium produced in a fast reactor blanket. Based on U^{235} at \$12/g, plutonium from a fast reactor blanket is worth \$17 to \$18 per gram fissile and plutonium from thermal reactors, \$19 to \$20 per gram fissile. Recycled plutonium is worth slightly more than that from the first cycle plutonium discharge. Further calculations will be required to determine how much of this is due to the higher value of Pu^{241} relative to Pu^{239} and how much is due to the "free" fertility of Pu^{240} . If Pu^{242} detracts from the value of plutonium (that is, has a negative value as in thermal reactors), it is masked by the increased value of Pu^{240} or Pu^{241} . As a rough measure of the breeding potential of various fueling schemes, the data in the accompanying table are presented.

Four-Group ALTHAEA Chain

The remaining bugs seem to have been eliminated from the 7090 (four-group) chain, and the QUICK and PLOTTER codes are functioning properly.

ALLIS-CHALMERS FAST REACTOR STUDY

<u>Core</u>	<u>Blanket</u>	<u>Net Change in Fissile Inventory, kg/Mwe-yr</u>
Enriched UO_2	Depleted UO_2	-0.33
Depleted UO_2 , Blanket PuO_2 (1)	Depleted UO_2	+0.06
Depleted UO_2 , PWR PuO_2 (2)	Depleted UO_2	+0.11
Depleted UO_2 , Recycle PuO_2 (3)	Depleted UO_2	+0.12
Depleted UO_2 , PWR PuO_2 (2)	Depleted U Metal	+0.20

(1) Blanket plutonium compositions 96% Pu^{239} , 4% Pu^{240} .

(2) PWR plutonium compositions 58.5% Pu^{239} , 23% Pu^{240} , 14% Pu^{241} , 4.5% Pu^{242} .

(3) Recycle plutonium compositions 47% Pu^{239} , 23% Pu^{240} , 17% Pu^{241} , 13% Pu^{242} .

REACTOR ENGINEERING DEVELOPMENT

BWR and PWR with PuO₂ Fuel Study

The computer code REPP, a thermal and hydraulic core sizing routine for light-water moderated reactor power plants, was completed. The present problem is linking REPP into the chain of nodes used by the Advanced Concepts and Fuel Analysis Section so that a complete analysis of BWR and PWR may be accomplished.

REPP uses a fourth order polynomial to determine fuel temperatures at ten various locations along a fuel rod. This adds some flexibility in fuel design, such as annular fuel pins, and contributes to an easy method of integration of the heat transfer equation for cylinders. Three sub-routines were written to provide an exact solution to the polynomial and the proper root is selected as the fuel temperature.

Reactor Components Development

FERTF Support Work

The test, to evaluate the charging and discharging forces of the new FERTF fuel element basket, was completed.

The test consisted of bowing the pressure tube in small increments and charging and discharging the basket at each step, measuring the force for each operation. The tube was bowed with a single point load at the center of the tube with the tube restrained at the top of the top shield and bottom of the bottom shield.

The basket has an outside diameter of 3.150" to 3.171", and the pressure tube has an inside diameter of 3.254" to 3.258" in the vicinity used for this test. The pressure tube was bowed 0.250" at the midpoint before there was any detectable friction when inserting or removing the shell. When the bow was increased to 0.325", the fuel element shell, with 26 pounds added (to simulate the weight of the fuel), would not slide down the tube under its own weight. From the test results it is indicated that a 0.330" bow is the absolute maximum to be tolerated, if the tube dimensions are similar to those described above.

Detailed data on the test were forwarded to Fuel Element Design and Evaluation Unit.

Rupture Loop Particulate Removal Study

Detailed design is complete for entire system and all necessary auxiliary equipment is on order. Separator fabrication has been delayed by HAMTC strike and offsite fabrication is now planned.

Scope design of the loop to test the FERTF axial flow separator was completed. The loop will be a recirculating type with the pump suction and separator discharge connected to an atmospheric pressure storage tank. The tank is sized and baffled such that particle carry-over will be minimum.

Instrumentation to measure flow and pressure drop is included in the loop.

MATERIALS DEVELOPMENT

PRTR Pressure Tube Evaluation

The PRTR reactor safeguards program includes an experimental and analytical evaluation of the failure behavior of the pressure tubes and a study of the effect of reactor environment on these properties.

Tube 5696 was selected for destructive examination because of its exposure and because there was evidence of superficial damage to the inside of the top of the tapered portion of the pressure tube.

Zirconium hydride analysis of a specimen obtained near the damaged area revealed 27 ppm. This low concentration would indicate the mark on the tube has not acted as a site for accelerated hydriding.

Investigation of the effect of temperature on the response of strain gage circuits mounted on the OD and ID of a PRTR tube specimen indicated apparent strains of about 400 micro-strain and 100 micro-strain, respectively, at a temperature of about 175°F (80°C). This experiment is the third of three required for determination of the anisotropic elastic constants of a PRTR tube specimen.

PRTR Activity Monitoring

Monitoring the PRTR moderator system activity in the water during the recent critical tests has shown a marked increase in the Co⁶⁰ concentration. The Co⁶⁰ concentration was 0.08×10^{-3} $\mu\text{Ci/ml}$ before boric acid addition. After one week of boric acid additions totaling 7 ppm boron, the Co⁶⁰ concentration was 1.7×10^{-3} $\mu\text{Ci/ml}$. As the boron concentration was increased to 14 ppm boron and 24 ppm boron, the Co⁶⁰ concentration was 2.9×10^{-3} $\mu\text{Ci/ml}$ and 4.1×10^{-3} $\mu\text{Ci/ml}$, respectively. Total α and β counts were obtained for the first and second week after boric acid addition. Both α counts were negligible. The β counts were more than 90% accounted for by the Co⁶⁰ emission. It appears that the boric acid is replacing Co⁶⁰ deposited in the moderator system and causing the Co⁶⁰ to go into solution. The lack of normal system purification during this period may have contributed to the Co⁶⁰ buildup observed. The operation of cleanup ion exchanger at the conclusion of the critical tests should decrease the Co⁶⁰ concentration. The absorption of activity on reactor component surfaces will be the subject of later studies.

Chemical Shim Studies

The procedure for total solids analysis of borated PRTR moderator water is being investigated. The total solids analysis is utilized in detecting off-standard water quality and the presence of corrosion products in the moderator system. The addition of 150 ppm boric acid to the moderator system has made the total solids analysis temperature dependent. When borated water is evaporated to dryness at 120°C in a vacuum drying oven, the boric acid is removed, but when evaporated to dryness at 105°C, the boric acid is only partially removed. The tests in progress will determine the lower temperature limit to assure complete removal of the boric acid. The total solids analysis will then measure the material other than boric acid present in the water sample.

Ceramic Fuel Dissolution Studies

Ceramic fuel dissolution work during the past month has been centered on (a) determining PuO_2 dissolution rates, (b) familiarization work with liquid ammonia solvents, and (c) determining corrosion effects in concentrated acid solvents.

Following the experimental results obtained in June which showed that the dissolution rates for PuO_2 sintered at 1650°C were much lower than those obtained with PuO_2 fired at 900°C efforts were made to find more effective procedures. Emphasis has been placed on using more concentrated H_3PO_4 at higher temperatures. Phosphoric acid of about 99% concentration produced by heating 85% H_3PO_4 at 210°C for one hour gave higher dissolution rates. Use of this acid at 200°C resulted in a dissolution rate for sintered PuO_2 of $0.165 \text{ gm/cm}^2/\text{hr}$. Inhibition with 6 gm/liter $\text{Fe}(\text{NO}_3)_3 \cdot 9 \text{ H}_2\text{O}$ reduced stainless steel corrosion by a factor of ten to 0.12 mil/hr but also lowered the dissolution rate to $0.024 \text{ gm/cm}^2/\text{hr}$. The latter was still more than four times as effective as the uninhibited 85% H_3PO_4 at 155°C .

Liquid ammonia familiarization work was begun during August with the prime objective being the use of sodium metal-ammonia solutions to reduce ceramic fuel materials. Emphasis has been placed on learning safe handling techniques. During this familiarization work rusted steel specimens and magnetite have been exposed to sodium metal-ammonia solution to obtain qualitative information on their behavior in a highly basic reducing environment. Atmospheric steel corrosion products are reduced. The rust color rapidly changes to black. Subsequent exposure to air leads to the reformation of the reddish brown Fe_2O_3 . Treatment of magnetite under pressure at 100°C results in some Fe_3O_4 reduction. The primary reaction appears to be the formation of sodium amide. The latter reaction will seriously affect the feasibility of this process unless the formation kinetics for sodium amide can be changed.

Corrosion studies have been directed toward determining general and nonuniform effects in concentrated acid solvents. Average corrosion losses under quiescent conditions for Inconel-600 and AISI 446 stainless steel in 155°C concentrated sulfuric acid were 0.033 and 0.039 mil, respectively, in seven days. Exposure of these alloys to a 90 vol% concentrated H_2SO_4 - 5 vol% concentrated HNO_3 - 5 vol% concentrated H_3PO_4 solution at 140°C for seven days resulted in corrosion losses of 0.03 mil and 0.007 mil. A seven-day test of an Inconel-600 - carbon steel galvanic couple in 155°C concentrated sulfuric acid resulted in an accelerated attack on the carbon steel; about 70% of the carbon steel specimen was dissolved. Only minor corrosion losses were found on Inconel-600 - AISI 304 stainless couples after seven days in 155°C concentrated sulfuric acid and 140°C 90 vol% concentrated H_2SO_4 - 5 vol% concentrated HNO_3 - 5 vol% concentrated H_3PO_4 solutions.

TEST REACTOR OPERATION

Operating Experience

The batch core critical tests were completed in August. Work directed toward the start of power operation included the following:

1. The process tubes in position 1053 and 1550 were reconnected to the primary system. These tubes were left empty of primary coolant during the critical tests.
2. Due to the critical test program, the primary system was drained twice in August. The primary system drain and refill were accomplished without difficulty.
3. The primary activity on the core blanket system was directed toward eliminating air in-leakage. The seals were replaced on the core blanket blower. The 35 lines from the penetrations in the bottom primary shield have been returned to service. The sample lines from the process tube expansion bellows are being returned to service at month-end. The silica gel in drying tower No. 1 was replaced, eliminating the flow restriction present in that tower.
4. The cartridges for the moderator side leg filter were replaced for the third time in August. The activity being removed by the filter is predominately cobalt⁶⁰ with some fission products included.
5. The boron shim system was completed. The flow control system was connected to BIX-5 and checked for proper operation. BIX-5 was deuterized, and the moderator cleanup ion exchange unit was saturated with boron.

Indicated helium loss for the month was 114,000 scf. Heavy water loss for July and August was 1239 pounds.

Maintenance Experience

The major accomplishments in August were the completion of the reflector conversion to light water and the completion of the boron shim system.

Improvement Work Status

Work Completed

Diesel Well Pump - Remote Start
 Emergency Visual Alarms
 Containment Valve Addition (Helium)
 Integration of Neutron Probe and Flux Recorder

Work Partially Completed

New Instrument Power Supply
 Traveling Flux Wire Probes
 Reactor Hall Crane Work Platform
 Effluent Monitor System Calibration Modifications
 Instrumented Fuel Element Installation
 Relocate IX-4
 Helium Compressor Compensating Pump
 RL Annex Ventilation Enclosure
 Second Moderator Temperature Probe

Design Work Completed

Helium Supply to Core Blanket
 D₂O Addition to Primary from Outside C.V.
 Rupture Loop Bypass for In-Reactor Section

Design Work Partially Completed

Analysis of HX-1 and Primary Pump Supports
Improvement of pH Monitor

Process Engineering and Reactor Physics

The critical test results were generally as expected. Nine elements were required for the initial critical loading as compared with seven elements in the PRCF. This difference is probably due mainly to the increased absorptions in various stainless steel assemblies in the calandria in the shroud tubes and in the primary coolant (~96.4% D₂O). The annular gas gaps within the shroud tubes also contributed to the reactivity loss. About 21ppm B¹⁰ were required to balance the excess reactivity of the 55-element core, as compared with a predicted 25 ppm B¹⁰. Most of this difference can be attributed to the increased absorptions mentioned earlier.

Measurements of the reactivity change due to loss of coolant for the entire 55-element core showed a loss of reactivity with loss of coolant, measured ~9 milli-k, as compared with a predicted 5 - 8 milli-k.

Several of the Archive samples of borated moderator have been tested in TTR, with excellent results.

All of the scheduled power test descriptions have been prepared and issued, with the exception of the Oscillator Test which is routing for approvals.

Two single-rod THERMOS calculations were carried out on 5 wt% PuO₂ - ThO₂ fuel rods for the Fuel Element Design and Analysis Unit.

Moderator water quality has remained satisfactory throughout PRTR critical testing, even though cleanup has been very limited in order to maintain the boron concentrations needed for testing. Laboratory analyses indicate a conductivity generally below 1 micromho/cm and a pH in the range 5.5 to 7.5.

PRTR Test 12⁴ (Fission Gas Pressure Measurement in HPD Fuel Elements During Irradiation) has been issued, and the two instrumented fuel elements have been charged in the reactor.

Document BNWL-CC-740 was issued to report the results of the In-Reactor Monitoring of Zircaloy-2 PRTR Pressure Tubes.

Technical Guidance - Project CBB-001 - Increased Power Level

Boron shim system construction (Phase II) is complete (except for the deferred installation of the boron analyzer).

The chemical shim cleanup ion exchanger piping was tested and filled with moderator D₂O. The system was placed into service, with the exception of the ion-exchanger, and checked for operability with flow through all valves and flow measuring devices.

The injection pump will be replaced when the new one is received early in September.

Scheduled Phase I items are complete.

Technical Guidance - Project BCP-007 - PRTR Waste Handling

This project is to provide improved waste handling capability and control of reactor systems during accident situations. Design of the 14 items is 95% complete. All engineered equipment items are on order, and some valves have been received. No progress on construction because of the strike.

Technical Guidance - Project BCP-013 - PRTR Contamination and Waste Control

This project is to provide improved contamination and waste control during accident situations at PRTR. (Formerly BCP-007 Phase II) The work includes a new "C" Cell sump pump, charcoal filters for vent units, manhole #3 monitor, sump level indicators, air sampling station, remote D₂O transfer and a pumpout fitting at manhole #2. The project is requested to be Battelle-managed. The project proposal, calling for eight items for PRTR at a cost of \$65,000, has been approved by Battelle and is awaiting approval of the AEC review board.

Technical Guidance - Project CAH-119 - PRTR Storage Basin Addition and Experimental Facilities Modifications

This project is to provide a storage basin addition and equipment for experimental work and additional storage space. The building portion of the project is essentially complete with minor exceptions and additions remaining.

AMF has been instructed to proceed with the underwater equipment contract and to supply galvanized carbon steel or stainless steel for immersed parts and to comply with other contract requirements.

Technical Guidance - Project AEC-193 - Fire Protection Improvements

This project is to provide sprinkler protection in the 309 Building in all areas except the control room and containment vessel. Detailed design for detectors, alarms, and sprinkler risers is being done by Vitro.

Title II comment drawings of underground lines, sprinkler risers, and sprinkler system scope were received and comments returned during the month. Design and construction of the actual sprinkler system is to be done by a sprinkler system contractor.

Reactor Safeguards

A description of the plans for PRTR approach-to-power tests and initial power operation was forwarded to the AEC in further support of our request for approval to start the tests.

Additional information relative to the PRTR batch core experiment was compiled and transmitted to the AEC in response to questions received from the Division of Reactor Licensing. This information should enable Division of Reactor Licensing to complete the review of document BNWL-CC-345, "PRTR Final Safeguards Analysis, Supplement 8, Batch Core Experiment," and lead to AEC approval to resume PRTR power operation.

NUCLEAR SAFETYCONTAINMENT SYSTEMS EXPERIMENT (J. M. Batch)Experimental Facilities

Construction activity remained at a standstill due to the continuation of the strike against Battelle-Northwest. Notification was received from the vendor of a change in the shipping date of the reactor simulator vessel from September 9 to October 24. Design and fabrication estimates were obtained for a 1000 cfm air cleaning system for the containment vessel. The system would allow the use of commercial sizes of particle and charcoal filter modules plus condensers, demisters, and scrubbers. Scope drawings were prepared to obtain cost estimates on possible modifications of the high temperature heating loop to allow blowdown of the reactor simulator vessel through the loop piping and then into the containment vessel, and also to provide a pressurizer vessel and circulating pump to increase the experimental capabilities of the system.

Aerosol Studies

Studies of the behavior of aerosols were continued using the stainless steel aerosol tank in the Aerosol Development Laboratory. Run 67 involved release of elemental iodine in a dry air atmosphere and had the primary objective of examining the effect of air velocity on airborne concentration versus time. Because of an unexpectedly short airborne half-time, the iodine existed mainly in nonreactive chemical forms during the period of air speed variation, and any airborne concentration changes due to air speed were obscured.

Runs 68 and 69 involved injection of stable xenon labeled with 5.3 day Xe^{133} to test mixing effects and sampling equipment for xenon in air and in steam-air atmospheres. Data from sample points at 0.3 and 0.9 vessel radius are being fitted to theoretical curves representing solutions of the diffusion equations to obtain a measure of molecular plus eddy diffusivities. Bulk motion of the xenon in the vessel far overshadowed the molecular diffusivity of about $0.1 \text{ cm}^2/\text{sec}$ for xenon in air. The observed total diffusivity is estimated to be in the order of $1.0 \text{ cm}^2/\text{sec}$. Generally similar results were obtained in Run 69 with a steam-air atmosphere at 80°C , but the results have not yet been analyzed. Run 70 released hydrogen iodide (HI) into a steam-air atmosphere. Results are not available.

The penetration of xenon through the CSE backup traps for the aerosol sampling system was measured for air flow rates of 0.85 and 12.0 liters/min. The penetration is less than 2% for a 1-hour period at 12 liters/min for a trap containing 110 grams of activated coconut charcoal at -77°C .

The retention of xenon on the charcoal paper and charcoal bed of Maypack samplers was observed during Runs 68 and 69. There was no retention by the charcoal paper; however, the charcoal bed retained about 9% of the incident xenon during a 5-min sample period with air at 26°C . The corresponding retention with a steam-air sample at 81°C was about 1%.

The feasibility of collecting xenon tracer gas leakage as an independent check of the leakage calculated from pressure-volume-temperature measurements was determined. The xenon storage system had a known leaky fitting. The leak was bagged with plastic and sweep air was drawn through the bag and xenon collected in a trap. The collected xenon tracer was counted and the leakage rate determined from the known specific activity of the stored gas. The leakage rate calculated from P-V-T measurements was 72 cm³/hr, and from xenon counting, 67 cm³/hr.

Aerosol Generation

Both rapid and slow release rates of aerosol components into the containment vessel are being planned. Test runs were completed of rapid release methods in which up to 100 grams of elemental iodine were released in less than 10 minutes. For the slow releases, the goal is to release iodine at a uniform rate of about 330 mg/min for a release duration of 300 min. Uniform release rates were obtained for periods of 100 min; sweep gas flow rate and generation temperature are being varied to achieve the desired release rates.

A scintillation crystal detector system was set up to count the 80 Kev gamma rays from Xe¹³³ in the charcoal-filled stainless steel xenon traps.

Blowdown Tests

Nine blowdown tests were conducted on the SM-2 vessel with 250°F and 200 psig water and 8-inch rupture discs. A pressure transducer was installed in the top of the vessel to monitor the vapor phase pressure. Oscilloscope traces of the pressure transducers were triggered successfully by a technique using a wire cemented to the upstream rupture disc. Data from these traces have not been completely analyzed yet.

In several tests the blowdown was initiated by increasing the pressure between the two rupture discs instead of releasing pressure.

Decontamination

Containment system decontamination efforts during August have been centered on determining the effectiveness of vapor phase cleaning procedures on painted surfaces. Low efficiencies were obtained with steam suspended solutions of H₃PO₄-HBr and alkaline permanganate followed by HNO₃. Iodine decontamination factors were two or less. The alkaline permanganate-HNO₃ process also led to blistering of the painted surfaces.

CSE Instrumentation

A Norwood 0 - 500 psi strain gage pressure transducer has been calibrated and installed on the SM-2 vessel to measure vapor pressure during blowdown tests.

Tests were conducted on electrodes that were proposed for use as conductivity probes to measure the liquid level in CSE. The Auburn model WCC-1138-K Alumina insulated electrode failed after four hours exposure to 3000 psi and 649°F temperature. Inspection of the failed electrode indicated that the Alumina insulator had cracked along the skirt on the low pressure (ambient)

side. Also, the electrode to Alumina sealing compound was eroded or dissolved in the same area. The Auburn model F-140 Alumina insulated electrode has since been tested in the same environment over a period of 800 hours without failure. Resistance of the electrode from the tip to the base when completely submerged in water was found to be 43K ohms.

The Namak Inc., high-speed thermocouple probes have been received and are being evaluated for accuracy in the Standards Laboratory. The pressure vessels will require modifications to permit the use of these thermocouples.

PRESSURE VESSEL CRACK MONITORING (J. C. Spanner)

Detection of Metal Overstress by Acoustic Emission

A report (BNWL-CC-763), summarizing progress in developing a system to monitor crack growth in reactor pressure piping by sensing acoustic emission, was prepared and issued in accordance with a distribution list furnished by the AEC-DRDT program monitor. This report covers the period March thru June 1966.

Work has been initiated to develop a conceptual design of the prototype monitoring instrumentation system for full scale application to pressure piping surveillance by acoustic emission. The objective is to define a complete instrument system to receive data from multiple transducers, analyze the data for significant content, and present this information in a directly usable form. It must also either directly identify the signal source location or provide the information necessary to calculate source location.

A bonding material capable of withstanding long service at high temperature is needed for transducer mounting. Several epoxy cements are being tested to determine their long term reliability at elevated temperature (600 - 650°F). To date, one epoxy material (W. T. Bean Type H) has withstood two weeks of exposure at 600°F satisfactorily.

A series of tests is in progress to study acoustic emission from crack formation and growth in double cantilever beam specimens. The objective is to substantiate earlier indications of emission patterns characterizing crack formation and growth. Specimens of various thicknesses fabricated from 304-L stainless steel and A212 carbon steel are being used. So far, the same general pattern as before has generated from crack formation. In addition, however, it has been found that increased amplification of the signals obtained from a high sensitivity accelerometer shows that considerable acoustic emission signals are generated by extension of a preformed crack. Earlier tests at lower gains showed strong signals during crack formation but very little activity during crack growth. The combination of a high sensitivity transducer with additional moderate amplification appears advantageous from the standpoint of signal to noise ratio as compared to a lower sensitivity transducer with high ($10^5 - 10^6$) amplification.

An improved self-aligning electrostatic transducer is being developed for detection of acoustic emission. The transducer housing units have been redesigned and prototypes are being fabricated onsite. This transducer will feature an electrostatic shield, low capacity, and a spring loaded, self-aligning hot electrode and should be capable of operating at temperatures to 1000°F or higher with little change in efficiency as a function of temperature.

A special low noise, charge sensitive preamplifier has been fabricated for use with the electrostatic transducer in an effort to alleviate the problem of low sensitivity. Initial evaluation of this preamp indicates that gains of up to 3000 can be obtained through a frequency range of 100 Hz to 2 MHz. This amplifier can also be used to advantage with other types of transducers.

REACTOR SAFETY ANALYSIS AND EVALUATION (R. G. Wheeler)

Subsize Vessel Failure Analysis

Two subsize A-212-B test vessels, 18 inches long, were obtained from the ETR reactor after an exposure of two reactor cycles in the M3 position. A longitudinal slot, 1.0-inch long, 0.06-inch wide, and 0.2-inch through the 0.25-inch wall thickness, was machined in the tubing samples. One test was made at 56°C, the other at 72°C. The specimen at 56°C failed by full length cleavage when the hoop stress reached 60,500 psi. The specimen at 72°C failed in a partially ductile manner at a hoop stress of 71,000 psi. Thus, the nil ductility transition temperature is approximately 73°C for A-212-B pressure vessel steel after two ETR reactor cycles or an approximate total flux of 5×10^{18} nvt ($E > 1$ Mev).

The acoustic emission listening technique was applied to these tests to study the emission patterns. The tests were recorded and are now being played-back for analysis.

COLUMBIA RIVER SEDIMENTATION STUDIES (J. M. Nielsen)

Special sampling of water, suspended sediment, and bottom sediment in the Columbia River, continued during the prolonged shutdown of all reactors, will also be extended to include the period of their reactivation. These samples should provide unique data for determining the release and uptake of several radionuclides by river sediments.

WASTE SOLIDIFICATION CONDENSATE TREATMENT (G. J. Alkire)

Experiments on the two-step scavenging treatment of glass melter condensates were continued. A selection of the optimum concentration of ammonium phosphotungstate (AWP) was based upon the premise that a decontamination factor of 20 for Cs would permit storage of the treated supernate in asphalt without deleterious radiolysis effects. An AWP concentration of 0.005 M was selected for further use.

In the mixed hydrous oxide step, 0.05 M Mn^{+2} was added to the AWP supernate, and precipitation was effected at pH 10. This concentration was selected on the basis of previous work.

For these concentrations the two-step procedure was investigated for optimum mixing and quiescent times. A statistical analysis showed that AWP samples which were mixed vigorously for one hour and then centrifuged gave results comparable to samples which were mixed and/or quiescent for longer periods. For the mixed hydrous oxide step only 5-minute mixing was required prior to centrifugation.

The statistical analysis also revealed the following:

1. In the AWP step only Cs removal was highly reproducible, i.e., $97.6 \pm 0.6\%$. Ru, Ce, and Zr removals varied to a much greater extent, i.e., $18.1 \pm 5.0\%$, $29.7 \pm 7.6\%$, $0.8 \pm 1.8\%$, respectively.
2. In the AWP step only Zr removal appeared to be appreciably affected by longer contact times; however, the additional removal was very slight so that longer time periods involved were not warranted.
3. In the mixed hydrous oxide step Ce and Zr removals were highly reproducible as expected, i.e., $98.7 \pm 0.5\%$ and $97.1 \pm 0.9\%$, respectively. This is attributed to the colloidal nature of these radionuclides at pH 10. On the other hand Cs removals were quite variable ($67.8 \pm 12.0\%$), as observed in previous studies. Once again, Ru removals were fairly variable, being $65.3 \pm 7.2\%$.
4. Over-all removals for the two steps were very good statistically for Ce, Cs, and Zr, i.e., $99.0 \pm 0.4\%$, $99.2 \pm 0.4\%$, and $97.1 \pm 0.9\%$, respectively. Ru variation was still fairly large, but better than for either step alone, i.e., $76.5 \pm 4.2\%$.

Future work will be directed toward determining whether the K ion can be substituted for NH_4 ion in the AWP precipitation and maintain satisfactory Cs removals.

FISSION PRODUCT AEROSOL CONTAINMENT

Removal of Organic Iodide with Hydrazine (L. C. Schwendiman)

The efficiency of sprays containing hydrazine for removing airborne methyl iodide was determined for three hydrazine concentrations. An initial aerosol temperature of $75 - 80^\circ\text{C}$ was used. Four liters of the hydrazine solution was recirculated through the spray nozzle for a period of 60 minutes in two experiments and 90 minutes in a third. The following table shows the removal efficiencies obtained.

SPRAY REMOVAL EFFICIENCY FOR CH_3I

<u>Run</u>	<u>Spray Composition, wt%</u>	<u>Run Duration, min.</u>	<u>% CH_3I Removal</u>
SC-18	10 N_2H_4 , 5 NH_4OH	60	88
SC-19	20 N_2H_4 , 5 NH_4OH	60	93
SC-20	5 N_2H_4 , 5 NH_4OH	90	77

In Run SC-20 the change in concentration with time was measured by sampling the gas phase every 15 minutes. The decrease in concentration of methyl iodide was exponential with time, exhibiting the characteristics of a first order reaction with a half-life of 50 minutes. A large excess of hydrazine was present; hence, the reaction rate was controlled by the concentration of methyl iodide as was anticipated. To reduce the methyl iodide to 1% of the original concentration would have required about 5 hours of spraying with the 5 wt% hydrazine - 5 wt% ammonia.

The fraction of methyl iodide removed in a given time for a given hydrazine concentration was not significantly different at 80°C than at room temperature. This observation is somewhat unexpected; however, it must be remembered that although the starting temperature was 75 - 80°C, the final temperature was about 50°C in these experiments.

Physical Chemistry of Hydrazine-Methyl Iodide Reaction (L. L. Burger)

The study of reactions in the heterogeneous system, hydrazine, water, methyl iodide, and sodium hydroxide, continued with the objectives of determining the rate controlling step and characterizing the reaction mechanisms.

Some experiments were performed to measure the temperature dependence of the rate of methyl iodide removal from the gas phase over solutions of hydrazine. Results are shown in the following table.

VARIATION OF REACTION HALF-LIFE FOR 0.0504N NaOH SOLUTION AND SURFACE AREA OF 5.65 cm² AS A FUNCTION OF WEIGHT PER CENT HYDRAZINE AND TEMPERATURE

<u>Wt%</u> <u>Hydrazine</u>	<u>Temperature,</u> <u>°C</u>	<u>Half-Life,</u> <u>min.</u>
50	50.1	6.7
50	29.7	7.3
17.5	50.1	24.5
17.5	29.7	42

These results showed a rather small temperature dependence for the reaction over 50 wt% hydrazine solutions. A more significant increase in rate with temperature was shown for the 17.5 wt% hydrazine solution.

The possibility of increasing transfer rates to the liquid surface by adding ethanol to the hydrazine was investigated in a single experiment. No significant change in rate of removal of CH₃I was noted when 35 wt% hydrazine, 0.05N NaOH were used. Other organic compounds will be considered which are more surface-active than ethanol for this purpose.

The gas phase reaction between hydrazine and methyl iodide in the absence of an aqueous hydrazine surface was investigated. In the earlier experiments a liquid surface was available which could act to remove some of the products or to provide a phase in which reaction could proceed more rapidly than in the gas phase. The rate of removal of methyl iodide from the gas phase was measured in a vessel in which only gaseous methyl iodide and hydrazine were allowed to react. The initial partial pressure of hydrazine was about 12 mm, and the partial pressure of methyl iodide about 0.004 mm of Hg. The methyl iodide decreased 11% in 73 minutes. In comparable gas concentrations over hydrazine solutions, the methyl iodide is removed with a half-time of about 7 minutes. This experiment emphasizes the importance of the liquid-gas phase reaction.

A study of the reaction of methyl iodide and hydrazine in alkaline aqueous solutions was started. Initial experiments using methyl iodide tagged with radioiodine suggest that acetone present in the tagged methyl

iodide influences the rate of reaction. Previous experiments had indicated that the aqueous phase reaction was first order with respect to hydrazine. The results shown in the following table show that the acetone apparently causes the reaction rate to be much less sensitive to hydrazine concentration.

SUMMARY OF THE REACTION BETWEEN METHYL IODIDE AND
HYDRAZINE IN AQUEOUS SOLUTION AT ca. 22°C

(N ₂ H ₄)		(NaOH)	(C ₃ H ₆ O)	(CH ₃ I) Initial Approximate	T _{1/2}
M	wt%	M	M	M	min.
5.2	16.7	0.08	0.085	Not determined	0.4
0.47	1.5	0.050	0.112	3.4 x 10 ⁻⁷	4
0.235	0.75	0.050	0.112	3.4 x 10 ⁻⁷	4
0.235	0.75	0.050	0.224	6.8 x 10 ⁻⁷	8.7
0.12	0.38	0.050	0.224	6.8 x 10 ⁻⁷	8.8

These are preliminary data and further investigations will be undertaken. Acetone is commonly present in tagged methyl iodide as received; hence, any influence on the reaction rate should be determined to assure valid laboratory results.

DISPOSAL OF REACTOR OFF-GAS INTO SOIL SYSTEMS (W. A. Haney)

Before beginning computer solution of gas injection problems involving confining layers, a rational approach to faster solution has been sought. It was found by numerical experimentation that using one acceleration factor (over-relaxation factor) throughout the problem is probably better than allowing the factor to change. The best approach appears to be: (1) determine the best factor with a coarse grid; (2) refine the grid and determine the best factor for the smaller grid size; (3) extrapolate a curve of acceleration factor vs. grid size to the final desired grid size for solution of the problem; and (4) choose the factor. This approach appears to save considerable solution time over methods used in the past.

The seismic exploration program performed for IDO-AEC at NRTS was completed, and results were transmitted to the Waste Management Branch. The area surveyed, about 1000 ft south of the LOFT site, is that chosen for preliminary gas injection tests and for the actual reactor off-gas injection several years in the future. The shallow-refraction survey covered an area of about 1 mi² on a 600-ft grid. Depths of the basalt from ground surface varied between 8 and 60 ft. Generally, good quality records were obtained from the shooting.

RADIOACTIVE RESIDUE PROCESS DEVELOPMENT (A. M. Platt - G. J. Alkire)

High Level Wastes

The final report on the proposed experimental and operational plan for the waste solidification and evaluation program was reviewed with particular emphasis on the experimental designs for laboratory and plant scale "hot" runs.

Work was continued on a response surface study of the effect of various additives on the closure temperature and drip temperature in the waste solidification process. Special cubic response surfaces were selected, and the contours are being mapped for graphical presentation. Reports on both the phosphorous-boron-silicon system are being prepared.

Waste Solidification Engineering Prototypes (WSEP)

An exploratory rising-level glass run with a modified, simulated PW-1 feed performed in the WSEP equipment in B-Cell was aborted because of corrosion failure of the 310 stainless steel pot. Relatively uniform corrosion rates within the pot of 100 to 200 mils/day were experienced at the 950°C temperature used. Corrosion failure of the 304-L stainless steel thermo-couple well occurred at an even greater rate than with 310 stainless steel. Laboratory data have confirmed the attack of 304-L stainless steel but have indicated attack of 310 stainless steel 1 to 2 orders of magnitude lower than that experienced. The utility of the double-containment feature of the prototype pot furnace was demonstrated by the containment of the 30 liters of molten waste that leaked from the failed pot without damage to any equipment. Successful demonstration of separate addition of modified feed and liquid glass-making additive to the pot was accomplished. Self-cleaning of the total off-gas line and pot neck by controlled reflux techniques was demonstrated.

The film feeding technique made possible the predicted 30 liters/hour feed rate achieved into the 12-inch-diameter pot.

Testing of the modified ultrasonic station for pot wall thickness measurements is nearing completion, and the unit is working satisfactorily. Testing of the gamma scanner system, the pot decontamination and storage systems are well under way. Final clean-up of remotability testing of WSEP in-cell equipment is nearly done.

Installation of the WSEP phosphate glass equipment in the Engineering Development Laboratory 102 is complete and is ready for the forthcoming design verification tests.

The addition of 55 liters/hour of water to a hot (900°C) pot furnace susceptor as an emergency cooling technique was demonstrated to be safe.

The operation of the G.E.-412 computer was reasonably satisfactory during the recent WSE pot calcination cold run. While there was only one failure of the machine itself during the four-day run, the data reduction and data presentation programs are still in need of refinement. Areas of improvement include the calculation of tank depletion rates, furnace power input, and the establishment of reasonable upper and lower limit alarm values. The one failure of the machine apparently stemmed from an electrical power surge experienced about 3:45 a.m., August 9, the transient causing the machine to branch to a nonexistent core location, where it stopped.

Since the next most probable run that will be made with the WSE facility will be a spray calciner run, the 412 computer has been reprogrammed accordingly with a previously prepared program. An initial check proved the spray calcination data logging program to be operable, but, again, considerable refinement is indicated in the same areas as was apparent in the pot calcination program.

Process Chemistry

Effects of Aluminum on Waste Melt Characteristics

An investigation of the effects of varying aluminum concentrations in wastes during spray solidifier and BNL phosphate glass processing is in progress. The aluminum concentration in radioactive wastes which will be processed in WSEP will be somewhat higher than in the PW-1 and PW-2 compositions on which flowsheet development was based. Much higher aluminum concentrations which are of long-term interest are included in the study.

Amounts of aluminum expected to be present in the WSEP radioactive waste solutions did not significantly affect the melting point or slump point of spray solidifier product. The slump point of BNL phosphate glass product was increased and flowsheet modification would be required to accommodate the higher aluminum concentration.

Corrosion studies have not defined a cause for the failure of the 310 stainless steel receiver pot used during the recent ORNL rising liquid glass run RLG-B. Corrosion rates at 950°C for 310 coupons were about 100 mils/mo in melt prepared from feed solutions used in the run and 4 - 10 mils/mo in a sample of product from the run. A specimen of steel taken from the RLG-B pot and exposed to molten RLG-B product at 950°C corroded at about 14 mils/mo.

Platinum - 0.5 rhodium wire specimens (as received and after cold working) were exposed to four waste melt compositions for 215 hours at 1200°C. Melt composition parameters were sulfate, phosphate, and lithium concentrations. The exposed wires show no intergranular attack. Jodele (2. Metallkde, 27, 271 [1935]) has reported that Pt-P alloys containing >0.003 wt% P are brittle at 850°C due to the formation of a brittle fusible eutectic. To see if the brittle phase can be formed under reducing conditions in a phosphate melt, a length of Pt - 0.5 Rh wire has been exposed at 1200°C for 190 hours to a phosphate melt containing one wt% carbon. A pull test at 850°C will be made on the wire.

Product Evaluation

Melts representing products from the current flowsheets for processing PW-1 and PW-2 by the BNL phosphate glass, ORNL rising level glass, and PNL spray solidifier processes were prepared in the quenched and annealed forms. X-ray diffraction patterns of the solid products were obtained. The phosphate glass products, even when annealed, were almost completely amorphous. The microcrystalline ORNL and PNL process products had very complex diffraction patterns with marked pattern differences between quenched and annealed forms.

CUSTOMER

ASSISTANCE TO GENERAL ATOMIC

Fuels Development (W. L. Hampson, Jr.)

PuO₂ - Graphite Compacts

Twelve rods containing PuO₂ - graphite compacts for critical tests are being prepared. These rods consist of six pairs with three different PuO₂ concentrations and two separate isotopic (Pu²⁴⁰) compositions. Four sets of

compacts were prepared using improved blending and sampling techniques. Difficulty in obtaining leak-free final closures has been encountered. Pin holes and cracks occurred in the weld of the 6061 Al components, using 4043 filler metal. With the exception of welding, process development is complete, and the remaining sets of compacts are being prepared.

U. S. NAVAL RESEARCH LABORATORY

Calculation of the Fast-Neutron Spectra and Damaging Rates at the OMRE and Yankee Pressure-Vessel Positions (R. E. Dahl)

Spectral analyses have been completed at the pressure-vessel position of the Organic Moderated Reactor Experiment (OMRE) and the Yankee Reactor. The purpose of the analyses is to provide a basis for correlating damage from in-core experiments on pressure-vessel steels to reactor pressure vessels. These calculations were made to assist the U. S. Naval Research Laboratory (USNRL) in the pressure-vessel surveillance program.

The neutron spectra were calculated at the reactor midplane and extended out through the pressure vessel of each reactor. The spectral analysis was made using a multi-energy, multi-region, one-dimensional transport-theory code, with the reactors represented by cylindrical geometry. The spectra were calculated using 21 energy groups with fine group structure in the fast-neutron range, $E > 0.18$ MeV.

Results of the calculations indicate that the fast-neutron spectrum at the OMRE pressure vessel is similar although somewhat "softer" than the spectrum calculated at the upper grid plate (reported in the July 1966 monthly report). This is to be expected because the neutrons must pass through several inches of iron thermal shields and organic moderator before reaching the pressure vessel, whereas only moderator separates the upper grid plate from the reactor core. The ratio of the integrated flux above 1 MeV to the integrated flux above 0.18 MeV at the grid plate is 0.62; at the pressure vessel the ratio is 0.55.

The fast-flux ratio $[\phi(E > 1.0 \text{ MeV})/\phi(E > 0.18 \text{ MeV})]$ calculated at the inner edge of the pressure vessel of the light-water-moderated Yankee Reactor is 0.54.

The spectral-averaged cross section for iron based on $E > 1$ MeV has been calculated for the OMRE grid plate, OMRE pressure vessel, and the Yankee pressure vessel. The values are 157, 140, and 169 mb, respectively. In a fission spectrum, the value is 121 mb. Thus, if a fission spectrum is assumed for the above reactor positions, the flux will be over-estimated by 30% at the OMRE upper grid plate, 16% at the OMRE pressure vessel, and 40% at the Yankee pressure vessel.

Irradiation damage to steel test specimens that have been irradiated in in-core positions of the Low Intensity Test Reactor (LITR) can be correlated directly to pressure-vessel positions (SMLA pressure vessel, for example) if the neutron exposures are normalized to the integral flux above 0.5 MeV. The following table is a comparison of damage indices between diverse spectra based on the integrated flux above 1.0 MeV and 0.5 MeV.

Reactor	Damage Index* (K_i/K_j)	
	$E_L = 1.0$ MeV	$E_L = 0.5$ MeV
LITR-18	0.85	0.94
OMRE-Upper Grid Plate	0.85	1.03
OMRE-Pressure Vessel Position	0.89	1.03
Yankee-Pressure Vessel Position	0.91	1.03
BGR-W44	1.07	1.02
SM-1A Pressure Vessel	1.0	1.0

*Damage Index is the ratio K_i/K_j where

K = displacements per cm^3 per sec per integral flux
above E_L and the j reactor position is the SM-1A
pressure vessel.

The damage indices between diverse spectra based on $\phi(E > 0.5 \text{ MeV})$ vary only 9%; whereas, if the damage indices were based on $\phi(E > 1 \text{ MeV})$, the variation would be approximately 22%.

DISTRIBUTIONNumber of Copies

1	<u>AEC-AECL, Chalk River, Canada</u> M. N. Hudson
3	<u>AEC Division of Technical Information Extension</u>
1	<u>Aerojet-Nucleonics</u> P. O. Box 77 San Ramon, California G. W. Titus
1	<u>Aeroprojects, Inc.</u> W. B. Tarpley
1	<u>Air Force Materials Laboratory</u> Wright-Patterson AFB S. W. Bradstreet
1	<u>Allis Chalmers Manufacturing Co.</u> Virginia D. Rose
1	<u>Ames Laboratory</u> F. H. Spedding
3	<u>Argonne National Laboratory</u> R. M. Adams C. E. Stevenson R. C. Vogel
1	<u>Armour Research Foundation</u> W. Loewe
1	<u>Atomic Energy Commission, Division of Compliance</u> Region IV, P.O. Box 15266, Denver J. W. Flora
53	<u>Atomic Energy Commission, Washington</u> Advisory Committee on Reactor Safeguards R. F. Fraley (17) Division of Compliance L. Kornblith, Jr. Division of Licensing and Regulation (7) Division of Production F. P. Baranowski (3)

Division of Reactor Development and Technology

R. A. Brodsky (1)
 Col. K. Cooper (1)
 A. Giambusso (1)
 J. E. Robb (1)
 S. A. Szawlewcz (1)
 M. Shaw (16)
 G. W. Wensch (1)

Division of Research

G. A. Kolstad (1)

Office of Assistant General Counsel for Patents

R. A. Anderson (1)

Space Electrical Propulsion Office

Col. G. K. Dicker (1)

- 1 Atomic Power Development Associates, Inc.
 W. H. Jens
- 3 Atomics International
 A. A. Jarrett (2)
 H. Pearlman
- 2 Babcock and Wilcox Company
 Lynchburg, Virginia
 H. S. Allen
 R. A. Webb
- 1 Battelle Memorial Institute
 D. L. Morrison
- 1 Bechtel Corporation
 R. F. Griffin
- 4 Brookhaven National Laboratory
 A. E. Castleman
 Elizabeth J. Edwards
 C. J. Raseman
 D. G. Schweitzer
- 1 Canoga Park Area Office
 R. W. Richards
- 2 Carolinas-Virginia Nuclear Power Associates
 H. T. Babb
- 1 Chicago Operations Office
 Argonne, Illinois
 D. M. Gardiner
- 1 Columbia University, New York
 J. E. Casterline

- 1 Combustion Engineering
P. O. Box 500
Windsor, Connecticut
W. P. Chernock
- 1 Dow Chemical Company, Rocky Flats
J. R. Seed
- 8 DUN
P. A. Carlson
J. R. Carrell
D. R. Hogle (Atomics International)
C. G. Lewis
W. M. Mathis
H. G. Spencer
J. R. Spink
W. K. Woods
- 1 Ebasco Services, Inc.
T. A. Flynn, Jr.
- 4 E. I. duPont de Nemours and Co., Aiken
- 5 General Atomic Division
D. B. Coburn
E. Creutz
A. J. Goodjohn
S. L. Koutz
D. V. Ragone
- 1 General Electric Company, Cincinnati
S. Naymark, NMPO
- 2 General Electric Company, Pleasanton
L. P. Bupp
E. A. Evans
- 8 General Electric Company, Richland
W. J. Dowis
R. E. Dunn
G. C. Fullmer
G. L. Hammons
M. Lewis
J. S. McMahon
J. W. Nickalous
J. W. Riches
- 5 General Electric Company, San Jose
K. P. Cohen
E. R. Kilsby
R. B. Richards
C. H. Robbins
E. L. Zebroski

- 2 General Electric Company, Schenectady
 W. M. Cashin, KAPL
 J. L. Michaelson, Advanced Technology Lab., Bldg. 5
- 6 Idaho Operations Office
 Dr. Quincy Baird, Nuclear Technology Div. (3)
 J. F. Kaufman
 D. S. King
 D. E. Williams
- 2 IIT Research Institute
 10 West 35th Street
 Chicago, Illinois
 W. J. McGonnagle
 T. A. Zaker
- 3 Isochem, Inc.
 H. H. Hopkins
 H. P. Shaw
 R. E. Tomlinson
- 1 Los Alamos Scientific Laboratory
 H. F. Redman
- 1 Massachusetts Institute of Technology
 Manson Benedict
- 1 National Bureau of Standards
 C. Muehlhause
- 10 National Reactor Testing Station (INC)
 G. Bright (2)
 D. R. de Boisblanc
 E. O. Millis
 W. E. Nyer (2)
 F. Schroeder (2)
 T. R. Wilson (2)
- 2 New York Operations Office
 A. J. Rizzo
 C. Stahie
- 1 Nuclear Development Corporation of America
 W. A. Loeb
- 1 Nuclear Materials and Equipment Corporation
 C. S. Caldwell
- 2 Oak Ridge Operations Office
 D. F. Cope
 W. J. Larkin

4 Richland Operations Office
 P. M. Midkiff
 C. L. Robinson
 R. K. Sharp (2)

1 San Francisco Operations Office
 Lt. Col. J. B. Radcliffe, Jr.

1 Sargent and Lundy
 W. A. Chittenden

7 Union Carbide Corporation (ORNL)
 F. L. Culler
 W. B. Cottrell
 J. H. Frye
 R. W. McClung
 O. Sisman
 D. B. Trauger (2)
 M. S. Wechsler

1 United Nuclear Corporation
 C. Graves

1 University of California
 V. E. Schrock

1 University of Minnesota
 H. Isbin

1 University of Texas
 G. W. Watt

4 Westinghouse Electric Corporation
 R. H. Fillnow
 E. J. Kreh
 R. G. McGrath
 R. A. Wieseemann

83 Battelle-Northwest
 F. W. Albaugh
 G. J. Alkire
 R. J. Anicetti
 J. M. Atwood
 J. A. Ayres
 J. M. Batch
 A. L. Bement
 C. A. Bennett
 T. K. Bierlein
 J. G. Bradley
 S. H. Bush
 J. J. Cadwell
 E. D. Clayton
 T. B. Correy

R. E. Dahl
F. G. Dawson
L. J. Defferding
D. R. de Halas
R. F. Dickerson
R. L. Dillon
K. Drumheller
E. A. Eschbach
P. L. Farnsworth
S. L. Fawcett
J. R. Fishbaugher
J. C. Fox
E. P. Galbraith
S. M. Gill
S. Goldsmith
L. A. Hartcorn
H. Harty
R. E. Heineman
R. J. Hennig
H. L. Henry
P. L. Hofmann
E. R. Irish
L. W. Lane
D. D. Lanning
H. V. Larson
G. A. Last
R. D. Leggett
B. R. Leonard
C. W. Lindenmeier
W. W. Little
J. E. Minor
T. C. Nelson
C. E. Newton
R. E. Nightingale
H. M. Parker
R. S. Paul
L. T. Pedersen
A. M. Platt
W. D. Richmond
W. E. Roake
G. J. Rogers
C. A. Rohrmann
L. C. Schmid
L. C. Schwendiman - C. E. Linderoth
W. A. Snyder (5)
W. G. Spear
A. J. Stevens
R. W. Stewart
G. L. Tingey
C. R. Tipton, Jr.
L. D. Turner
C. M. Unruh

E. E. Voiland
F. W. Van Wormer
M. T. Walling
R. G. Wheeler
O. J. Wick
R. D. Widrig
F. W. Woodfield
D. C. Worlton
H. H. Yoshikawa
Technical Information Files (2)
Technical Publications (2)

